Fall 2019

Macromolecular Engineering of Biomass Polymers and Stimuli-Responsive Materials Towards Enhanced Thermomechanical Properties

Meghan E. Lamm

MACROMOLECULAR ENGINEERING OF BIOMASS POLYMERS AND STIMULI-RESPONSIVE MATERIALS TOWARDS ENHANCED THERMOMECHANICAL PROPERTIES

by

Meghan E. Lamm

Bachelor of Arts
Illinois Wesleyan University, 2015

Submitted in Partial Fulfillment of the Requirements

For the Degree of Doctor of Philosophy in

Chemistry

College of Arts and Sciences

University of South Carolina

2019

Accepted by:

Chuanbing Tang, Major Professor

Brian Benicewicz, Committee Member

Thomas Makris, Committee Member

John Regalbuto, Committee Member

Cheryl L. Addy, Vice Provost and Dean of the Graduate School

DEDICATION

I dedicate this to my family for all their love and support, especially my parents and husband. Throughout this experience you have provided encouragement to push me towards this success and I am forever grateful. I also dedicate this to my grandparents, Janet and Stephen, for helping me realize from a young age that I was ambitious, smart and could be successful at anything I wanted to try and achieve.

ACKNOWLEDGEMENTS

First, I would like to express my sincerest gratitude to my advisor, Dr. Chuanbing Tang. I appreciate him giving me the opportunity to work in his research group and mentor me during the last few years. Throughout graduate school he has supported my research, helped me grow into a scientist, and given me endless guidance about both lab and life. He is an extremely talent polymer scientist with a true passion and I have learned so much from him.

Second, I would like to thank Dr. Brian Benicewicz, Dr. Thomas Makris and Dr. John Regalbuto for not only serving as my committee members, but also providing me with ideas and support for my research, as well as this dissertation. I also want to express my appreciation to Dr. Zhongkai Wang for mentoring me and continually supporting my research projects through collaborations with his group at Anhui Agricultural University. I would also like to thank Dr. Liang Yuan for also mentoring me, and Dr. Mitra Ganewatta and Dr. Md Anisur Rahman for their assistance in lab. I also thank Tianyu Zhu, Xinzhou Zhang, and Leman Kurnaz for their great friendship. Furthermore, I would like to thank Ayi Eta for being such an easy undergraduate to mentor. I appreciate all our conversations and am glad to have you as a friend now. Last of all, I would also like to thank all my department friends and colleagues, especially the members of Dr. Tang's research group; Dr. Yali Qiao, Dr. Xiaodong Ying, Dr. Yuzhi Xu, Dr. Jifu Wang, Dr. Peng Yang, Dr. Hui Li, Dr. Shichao Xu, Dr. Ye Sha, Dr. Shaobo Tan, Dr. Ying Lin, Dr. Yufeng Ma, Dr. Puyou

Jia, Dr. Jeffery Hayat, Dr. Paras Pageni, Dr. Ping Li, Bill Floyd, Nathan Trenor, Md Pabel Kabir, Yujin Cha, Ryan Miskin, Lin Fu, Moumita Sharmin Jui, JiHyeon Hwang, Jingya Nan, Haijiao Kang, Ayi Eta, Samuel Hankinson; and my Horizon 1 floor mates; Dr. Amrita Sarkar, Dr. Julia Pribyl, Laura Murdock, and many others. It is a great pleasure to work with all of you and learn from you. Thank you for all your help, support, and suggestions. Most importantly, I also would like to thank Dr. Kayla Lantz, whom became one of my best friends. I appreciate all the shopping and meals spent decompressing from lab and I hope I am lucky enough to keep you as a life-long friend.

Furthermore, I would like to thank my family. My sisters and parents have been there for this entire process. I appreciate the texts of support during successes and phone calls on really bad days. My parents especially have been my go-to resource for all questions. I would not be here without them. I am also immensely grateful that they supported me (financially) through undergraduate, even after three major changes, allowing me to find my passion for chemistry.

Most importantly, I would like to again thank my husband, Dr. Benjamin Lamm. I am forever grateful for the love, and encouragement that you have provided. Having you by my side throughout graduate school has given me tremendous drive and strength. I am beyond proud of *my* Dr. Lamm. We have created the cutest little Ohana.

Finally, I would like to thank funding support from the University of South Carolina, EPScOR, National Science Foundation, and the United Soybean Board. I would also like to thank DuPont for providing us with Plenish® high oleic soybean oil.

ABSTRACT

Commodity polymers are used in every aspect of daily life, and most of these polymeric materials are synthesized using petroleum-derived sources. There are direct environmental consequences to this petroleum dependence including greenhouse gas emissions and climate change. Biomass-based polymers show promise for the mitigation on negative environmental impact, in comparison with petroleum-derived counterparts. However, some biopolymers suffer from low chain entanglement due to bulky or long side chain structures, resulting in poor mechanical properties. In this dissertation work, macromolecular engineering is used to design biomass-derived polymers featuring a variety of structures and functionalities. Additionally, biopolymer properties (including thermomechanical enhancement) and applications such as polymer coatings and stimuli-responsive materials are discussed.

The first part of this dissertation focuses on strategies to overcome poor chain entanglement. Through macromolecular engineering, resultant polymer microstructure can be controlled to produce biomass-based polymers with industrially competitive thermomechanical properties. Specifically, supramolecular interactions are introduced to facilitate chain entanglement of polymers from biomass, which exhibit impressive enhancement of mechanical properties. In Chapter 2,, hydrogen-bonding (H-bonding) is used to enhance interactions between two complementary polymers. One polymer contains pendant acid groups as H-bonding donors that interact with H-bonding acceptor polymers

such as poly(4-vinylpyridine). The blending results in well-entangled polymer chains that can dissipate stress and provide enhancement in tensile strength and toughness. While in Chapter 3, metal-ligand coordination is used to promote entanglements within plant oil-derived copolymers. Metal-ligand coordination imparts unique and promising properties on these materials. The stimuli-responsive properties of both materials are also discussed.

The second part of this dissertation focuses on applications of biomass-based polymeric materials. In Chapter 4, focus switches to the development of an industrially relevant free-radical emulsion polymerization approach. A series of copolymers are synthesized featuring a plant oil-derived methacrylate copolymerized with styrene, methyl methacrylate, and butyl acrylate. Finally, a simple oxidative crosslinking strategy is used to enhance mechanical properties and provide strong, tough materials for potential coating applications.

In Chapter 5, epoxy resin nanocomposites are featured for their use as potential shape memory materials. Soybean-oil derived polymers are polymerized onto cellulose nanocrystals (CNCs) using a grafting-from SI-ATRP strategy with subsequent crosslinking using amine-catalyzed anhydride-epoxy curing. The strength of resulting epoxy resins provided an optimal permanent network allowing for good shape recovery, while the tunable glass transition temperature allowed for ease in shape fixity.

Finally, in Chapter 6, the summary and conclusions are given. Additionally, novel strategies for future work in overcoming poor entanglement for other biomass-derived polymers are presented.

TABLE OF CONTENTS

LIST OF TABLES

LIST OF FIGURES

LIST OF SYMBOLS

M_n Number average molecular weight

$Đ$ Dispersity

M_e Chain entanglement molecular weight

T_g Glass transition temperature

T_m Melting temperature

T_{d5} Temperature at 5% weight loss

T_{d10} Temperature at 10% weight loss

LIST OF ABBREVIATIONS

AA ..... acrylic acid

AIBN ..... 2,2'-Azobis(2-methylpropionitrile)

ATRP ..... Atom transfer radical polymerization

BA ..... butyl acrylate

CEA ..... 2-carboxyethyl acrylate

CNC ..... Cellulose nanocrystals

DCM ..... Dichloromethane

DLS ..... Dynamic Light Scattering

DMA ..... Dynamic mechanical analysis

DMF ..... *N*,*N*-Dimethylformamide

DSC ..... Differential scanning calorimetry

GPC ..... Gel permeation chromatography

FTIR ..... Fourier-transform infrared spectroscopy

MAA ..... methacrylic acid

MMA ..... methyl methacrylate

NMR ..... Nuclear magnetic resonance spectroscopy

P4VP .....poly(4-vinyl pyridine)

RAFT ..... Reversible addition−fragmentation chain-transfer

SAXS .....Small-Angle X-ray Scattering

SBMA .....soybean methacrylate

SBOH .....soybean amide alcohol

SI-ATRP..... Surface Initiated-Atom Transfer Radical Polymerization

SMP..... Shape memory polymer

TGA .....Thermal gravitational analysis

THF ..... Tetrahydrofuran

4VP.....4-vinyl pyridine

XPS ..... X-ray Photoelectron Spectroscopy

CHAPTER 1

GENERAL INTRODUCTION

1.1 Sustainable Polymers from Biomass

For far too long society has been dependent on fossil fuels for energy and the production of commodity products. The processes related to these applications release greenhouse gases into the atmosphere, including carbon dioxide. Unfortunately, after centuries of this behavior, the planet is suffering the effects in the form of global climate change, droughts, loss of habitats, and ocean acidification. In an effort to help mitigate further pollution, researchers have turned to biomass as an alternative source for polymer materials.[1, 2]

Biomass is organic material sourced from agriculture and forestry products, which is used as fuel or industrial raw materials. Traditionally, biomass utilizes materials not consumed as food. There are two main categories of biomass: natural polymers and molecular biomass.[3]

Natural polymers are polymers (repeat units of a single monomer) produced biologically. The presence of covalent bonding between monomer units prevents simple depolymerization, making it more difficult to break these down into small molecules. Cellulose, a homogenous polymer from plant cell walls comprised of repeat β-(1-4) linked *D*-glucose units, which include pendant hydroxyl groups allowing for formation of strong hydrogen-bonding and potential modification, making it an ideal filler in many polymer matrixes (**Figure 1.1a**).[4-7] Lignin, another polymer arising from plant cell walls, features a heterogeneous polyphenolic structure (**Figure 1.1b**). Due to its hydrophobic structure and irregular surface, it can be difficult to functionalize. Recent work has focused on depolymerization of lignin into phenolic monomers for use in a wide variety of polymer materials.[8-11]

Alternatively, molecular biomass comprises a wide array of molecular compounds, some of which can be utilized as monomers. Molecular biomass can be classified into four categories, based upon the composition of hydrogen, carbon, and oxygen: (1) oxygen-rich molecular biomass, which contains a C/O ratio that is less than 5.0, such as lactic acid and furans; (2) hydrocarbon-rich molecular biomass, which contains a C/O ratio greater than 5.0, such as plant oils, fatty acids and rosin acids; (3) hydrocarbon molecular biomass, which contains no oxygen, such as isoprene, butylene and ethylene; and (4) non-hydrocarbon molecular biomass, which contains no hydrogen, such as carbon dioxide and carbon monoxide.[3, 12]

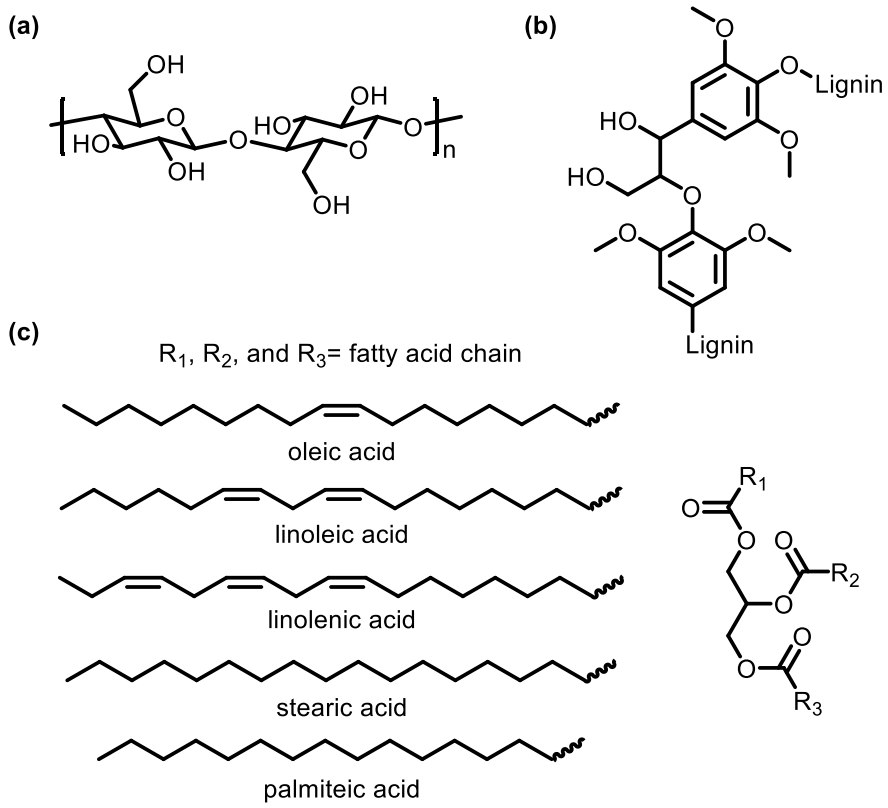

Figure 1.1. Representative structures of natural polymers: (a) cellulose and (b) lignin, and molecular biomass: (c) plant oils, featuring the fatty acids present in soybean oil.

1.2 Plant Oil Polymers

Due to their low cost, wide availability, and ease of functionality, plant oils are a promising molecular biomass source for production of polymer materials. Plant oils have a unique structure featuring a glycerin backbone and three fatty acid chains (**Figure 1.1c**).[13, 14] These fatty acids can vary depending on the plant oil source, and contain structures featuring a variety of functional groups. In this work, high oleic soybean oil (HOSO), which contains a higher content of oleic acid (>70%) than commodity soybean oil (<25%), is utilized. This also means it contains a very low percentage of polyunsaturated fatty acids (<10%) compared to its commodity counterpart (>50%). The presence of polyunsaturated fatty acids can result in radical formation during reactions, potentially leading to unwanted side-reactions and byproducts. Better control is achieved for subsequent reactions, including prevention of crosslinking during polymerization, by using HOSO.

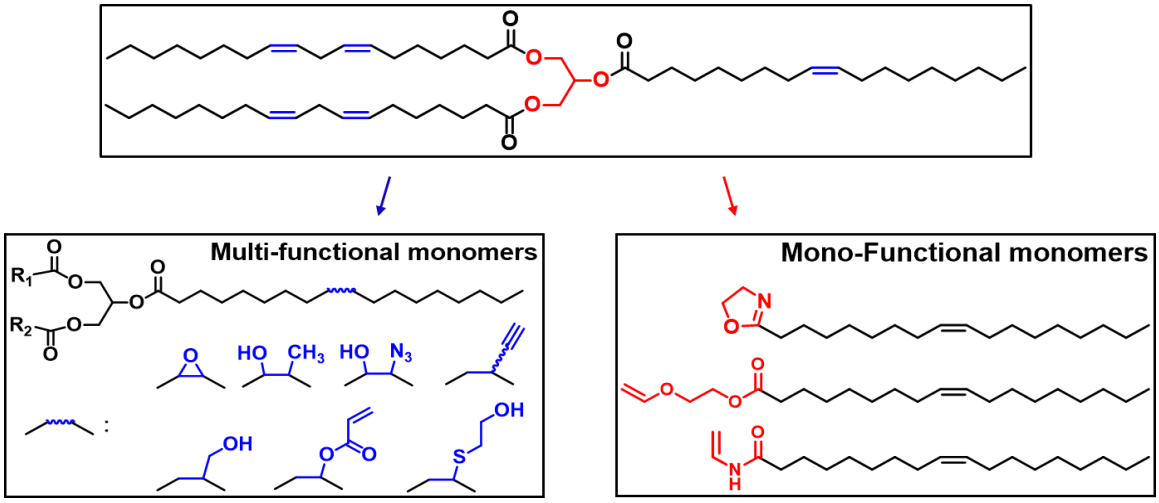

Figure 1.2. The synthesis of thermoset and thermoplastic polymers from plant oils using two different strategies towards mono- and multi-functional monomers.

Due to the structure containing two different functional groups, plant oils can be used to synthesize polymers using two different approaches (**Figure 1.2**). Firstly, the alkene groups located on the fatty acid side chains can be functionalized with a wide array of additional functional groups. The resulting monomers are multi-functional due the presence of multiple polymerizable groups on each molecule. When polymerized, the materials synthesized are thermosets. Thermosets contain chemical crosslinks, which prevent reprocessing, but provide better properties (high strength, chemical resistance).[15-18] Secondly, functionalization can occur at the glycerin backbone where esters can undergo a variety of reactions including cleavage and transesterification. The resulting monomers are mono-functional and only contain one polymerizable group. Mono-functional monomers are used to synthesize thermoplastics, which remain reprocessable. Our group has worked to synthesize a library of plant oil monomers using a simple transesterification strategy.[19, 20] Resultant polymers contain tunable thermal properties, but are only able to achieve soft, mechanically inferior properties compared to commercial polymers.

1.3 Macromolecular Engineering

The topologies or compositions of polymers have a direct effect on behavior and properties; as a result, developing the ability to control these parameters has been a hallmark of polymer science in recent years. Current advances in polymerization techniques and post-polymerization modification have allowed for an explosion in macromolecular engineering capabilities.[21-23] Macromolecular engineering strategies aim to control materials on the macromolecular level, directing resultant chain architectures, topologies, and functionalities (**Figure 1.3**).[24-26] Through careful selection of monomers and methods, there is also control of monomer distribution throughout a polymer chain,

which can affect interaction between monomers and the overall microstructure of the material. There is also control over the shape of a polymer chain and the location and types of functionalities present, unlocking the door for high-order structured materials.

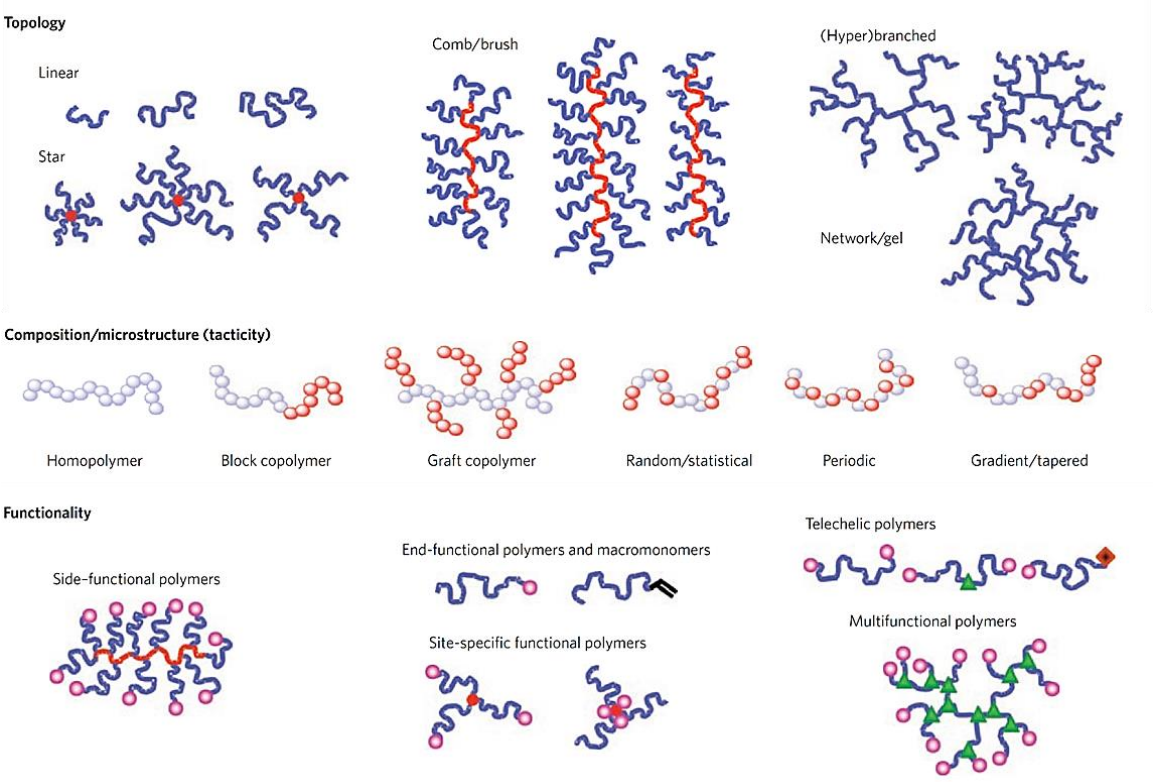

Figure 1.3. Macromolecular engineering aspects, including topology, composition, and functionality. (reprinted by permission from Springer: Nature Chemistry, ref [26])

One useful application includes the use of pendant functionalities on block copolymers to synthesize polymer micelles for drug delivery applications.[27, 28] Some strategies utilized in macromolecular engineering include controlled radical polymerization and chain-end functionality, e.g. click-reactions, where chemistry can be introduced and exploited to achieve specific topology and functionality.[29-33] These new synthetic strategies are especially useful for synthesizing reactive chain ends to achieve grafted and comb/brush

morphologies. Overall, the control achieved on the macromolecular scale provides a toolbox to synthesize polymers with unique, tunable properties.

1.4 Polymerization Techniques

Atom Transfer Radical Polymerization (ATRP)

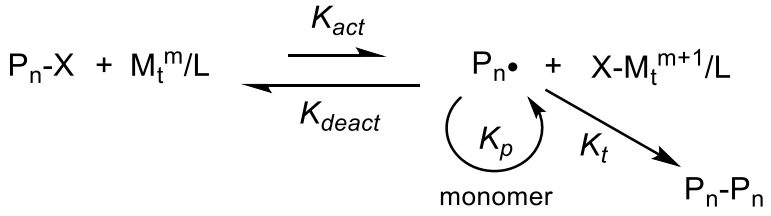

Figure 1.4. A schematic illustration of the ATRP mechanism.

First introduced by Krzysztof Matyjaszewski and Mitsuo Sawamoto in 1995, this polymerization technique has become one of the most popular and versatile living-polymerization methods.[34, 35] The theory of this method involves the activation and deactivation of radical species using copper(I) bromide and an alkyl bromide as mediators (**Figure 1.4**). When activated, copper(I) bromide is oxidized to copper(II), creating an active radical species capable of undergoing monomer addition or polymerization at a constant rate (*kp*). However, the equilibrium is strongly shifted towards the reverse reaction to form the dormant species (*kact* << *kdeact*), so the favored reaction, deactivation, reforms copper(I) bromide and a dormant polymer chain with pendant bromine group. The favored dormant species helps prevent side reactions such as chain transfer and termination (*kt*).[36, 37]

The success of this method has led to the development of a variety of related methods including polymerizations controlled by light or utilizing different metal species.[38-43] Due

to the good polymerization control and low dispersity, ATRP is used to synthesize many functional materials with specific chain architectures such as triblock copolymers and stars, as well as grafted structures from macromonomers including grafted combs and nanocomposites using a variety of grafting strategies.[21, 29]

Reversible Addition Fragmentation Transfer Polymerization (RAFT)

First discover in 1998 by the Commonwealth Scientific and Industrial Research Organization (CSIRO), this living radical polymerization method utilizes a unique initiator to control the rate of radical formation and thus polymerization.[44] The unique structure of RAFT agents is responsible for its behavior. The R-group is reactive enough to fragment and re-initiate the polymerization, but also help stabilize the growing radical formed. Alternatively, the Z-group helps control the stability of the C=S bond, assisting in fragmentation and polymer growth periods. Additionally, there are different types of RAFT agents available, including dithioesters, trithioesters, thiocarbamates, and xanthates.[45-47] The R- and Z- groups within a RAFT agent can also be changed to help stabilize and control the polymerization. By controlling the overall structure of the RAFT agent, polymerization control can be tailored for a range of monomers.

There are five steps involved in RAFT polymerization (**Figure 1.5**). After initiation, a growing polymer chain transfers its radical onto the RAFT agent. Due to the structure, the RAFT agent can fragment and transfer this radical to a subsequent growing polymer chain, allowing for monomer addition. Further steps involve repetition of this transfer, fragmentation, and polymer growth. Due to the low population of radical species, termination and other undesired side-reactions are minimized.[48, 49]

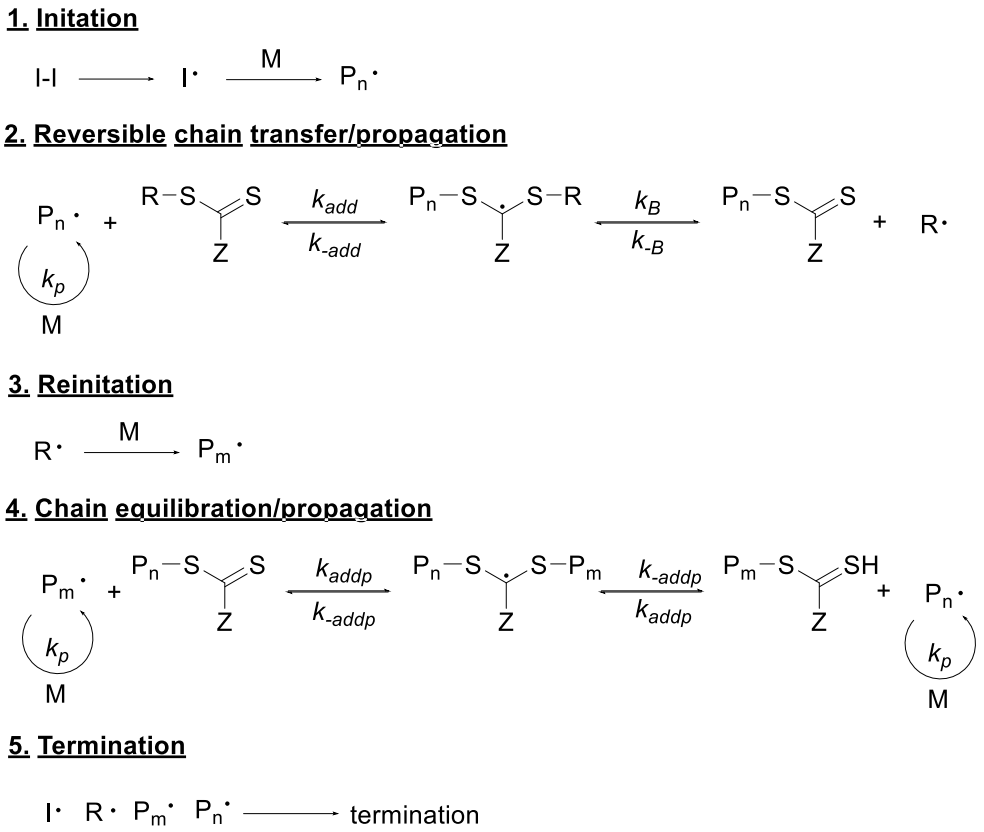

Figure 1.5. A schematic illustration of the RAFT polymerization mechanism.

As with other living radical polymerization methods, polymers synthesized from RAFT feature predictable molecular weights (*Mn*) and low dispersity. The chain-ends and macromolecular architecture can also be controlled to adapt materials towards desired applications.[48, 50] Due to the lack of metal in this polymerization, polymers synthesized from RAFT are very promising for biomaterials.[51]

Emulsion Polymerization

This method of polymerization utilizes an emulsion, typically between an oil and water phase. A surfactant, an amphiphilic molecule featuring a hydrophilic head and hydrophobic tail, is usually necessary to stabilize these two phases.[52] The oil droplets consist of

immiscible monomers coated in a layer of surfactant, which results in the formation of micelles. There are a few emulsion polymerization processes, which differ in how the emulsion is formed and maintained. A batch process starts with all materials; water, monomer, surfactant, and initiator; present in the reactor. The mixture is agitated to form an emulsion and heated to form radicals, thus initiating polymerization. This method is the easiest, but can result in coagulation and runaway exothermic reactions. Alternatively, a semi-batch process begins with water and a small portion of the surfactant and monomer mixture. The solution is heated and initiator added to begin polymerization. The residual mixture of surfactant and monomer is added slowly over a set time interval, usually concurrently with additional initiator. Despite the longer reaction time and addition set-up, this process is easier to control (exothermic reactions) and results in more homogenous polymers. The last method that is commonly utilized is a continuous process; however, this is primarily used only in industry for synthetic rubbers.[53]

The mechanism of emulsion polymerization first described by Smith and Ewart is complex, but it can be broken down into three key intervals.[54-58] Firstly, monomer is dispersed in water using a surfactant. The surfactant concentration needs to be above the critical micelle concentration to allow for the creation of micelles in water. Additionally, the surfactant serves to form and stabilize the smaller, growing polymer micelles present in the next steps. This mixture is emulsified using agitation (high-speed stirring or ultra-sonication) to create large, surfactant-stabilized monomer droplets. An initiator is added, decomposes to radicals, and disperses into the smaller monomer micelles. Initiators need to be water-soluble to be able to transfer easily throughout the medium. In the micelles, polymerization begins, and monomer concentration quickly drops (Smith-Ewart Interval

1). During polymerization, micelles containing growing polymer chains are continuously consuming smaller monomer micelles and droplets, resulting in a steady rate of polymerization (Smith-Ewart Interval 2, **Figure 1.6a**). Steady polymerization continues until no free monomer is present in the system (Smith-Ewart Interval 3). At this point, additional initiator can be added to push towards complete monomer consumption within the polymer particles. Once complete, the resultant latex is used directly for many applications. Alternatively, microemulsions can be used to synthesize polymer latexes. This method differs from standard emulsion polymerization kinetically and is significantly more complex.[59]

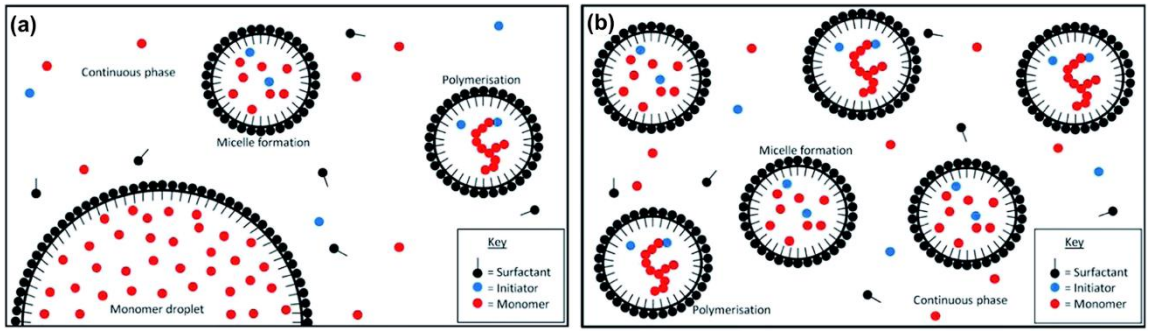

Figure 1.6. A schematic illustration of the mechanism for (a) emulsion polymerization and (b) microemulsion polymerization. (reproduced with permission from ref [58] published by The Royal Society of Chemistry)

Emulsion polymerization is used industrially to synthesize many different polymers due to its high polymerization rates and good control, partially due to good heat transfer from water throughout the reaction. Additionally, the lack of organic solvent and ease of processing make them optimal for many applications such as coatings and adhesives, many of which are utilizing sustainable monomer alternatives.[60-66]

1.5 Stimuli-Responsive Polymers

Stimuli-responsive polymers are a class of high-performance smart polymeric materials. In these materials, a response occurs after introduction of stimuli, which can include changes in shape, permeability, conductivity, color, transparency, and state of matter.[67-69] The stimuli that produce these responses can be broken down into three categories: physical, chemical, or biological (**Figure 1.7**). Due to the wide array of potential stimuli and response combinations, these materials can be used in such applications as biomedicine, separations technology, and agriculture. Some stimuli are more useful in certain applications, such as utilizing biological stimuli for biomaterials. For example, polymers can be designed to change shape in the presence of certain enzymes or proteins to mimic a natural response or prevent a potentially harmful mutation within the body.[70, 71] Depending on the desired applications, these stimuli can also be used in combination to create dual- and multi-responsive polymeric materials.

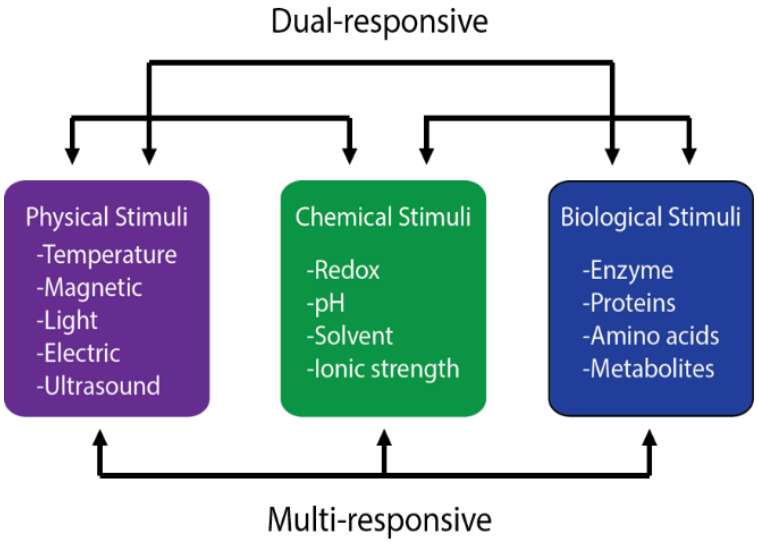

Figure 1.7. An illustration of the types of stimuli-response and their corresponding stimuli.

Shape Memory Polymers

Shape memory polymers (SMPs) are a type of stimuli-responsive material that can change shape upon exposure to an external stimuli.[72, 73] As discussed, these stimuli can include temperature, pH, light, or a combination of stimuli to create multi-responsive SMPs, which can transform into more than one shape successively.

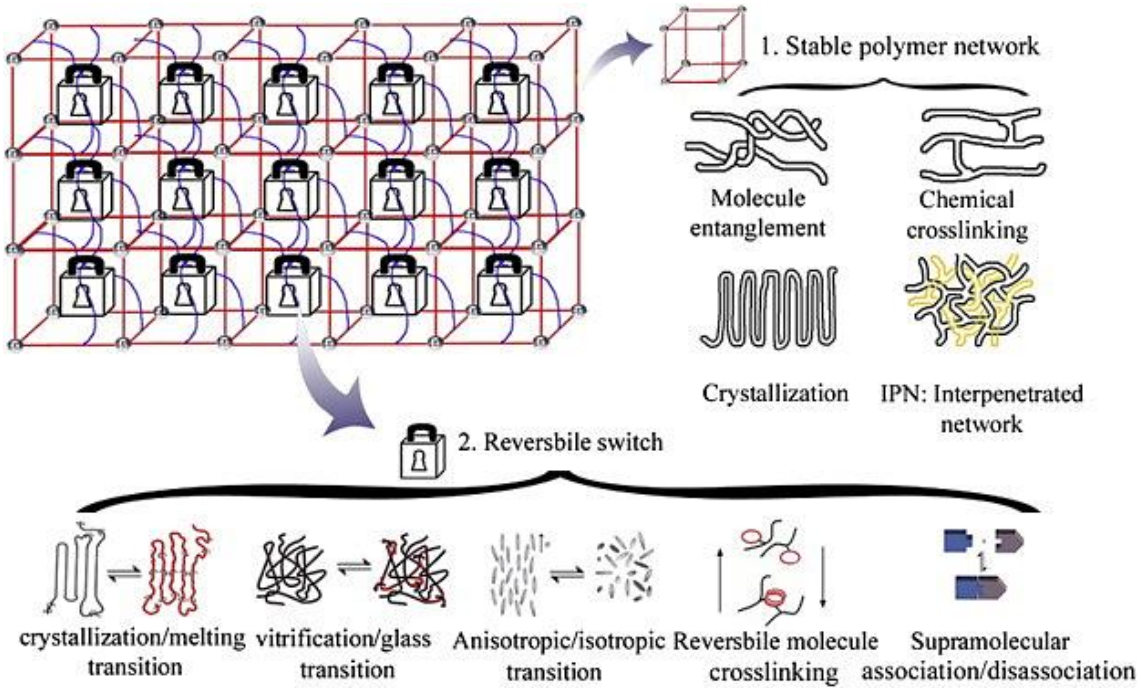

Figure 1.8. The two networks present in a shape memory polymer (SMP): the permanent network (stable polymer network) and the temporary network (reversible switch). (reprinted from ref [74] with permission from Elsevier)

In order to respond to stimuli, the microstructure of SMPs usually need to involve two separate networks, a permanent network and a temporary network (**Figure 1.8**).[74] The permanent network is a stable network that serves to maintain the original, permanent shape of the polymeric material, support fixation of the temporary shape, and assist in quick recovery to the permanent shape. In order to achieve this, the permanent network typically

features chemical crosslinking but can also utilize strong supramolecular interactions.[75, 76] Alternatively, the temporary network utilizes switchable chemistry. This can include dynamic bonds, including reversible covalent bonding such as Diels Alder reactions, or thermal transitions, such as glass transition temperature (*Tg*) or crystallization. The dynamic chemistry needs to respond to the stimuli quickly and efficiently in order for SMPs to undergo shape recovery. Dynamic mechanical analysis (DMA) can be utilized to quantify shape-memory properties, such as the shape fixity and shape recovery, of SMPs.

Self-Healing Polymers

Self-healing polymers are materials that have a natural ability to heal damage without the need for outside intervention.[77, 78] Over time, many polymeric materials degrade as a result of fatigue and wear, all of which can be expedited under certain working conditions. In some applications though, it can be difficult to replace these materials. When cracks and damage initially begin to form within polymeric materials, self-healing properties can be useful to stop the propagation of these defects and prevent complete mechanical failure.

The two categories of self-healing polymers are defined as intrinsic (reversible) and extrinsic (irreversible).[79-81] Intrinsic self-healing polymers utilize chemistry present within the polymer itself, such as supramolecular interactions. This chemistry is reversible, allowing a material to heal repeatedly. Alternatively, extrinsic self-healing utilizes additional catalysts and additives, which serve to initiate a reaction (e.g. polymerization or crosslinking) that heals the material. As there is a limited amount of additional components present, and as the resultant healing often involves formation of chemical bonds, the self-healing in these materials is irreversible and can only occur once.

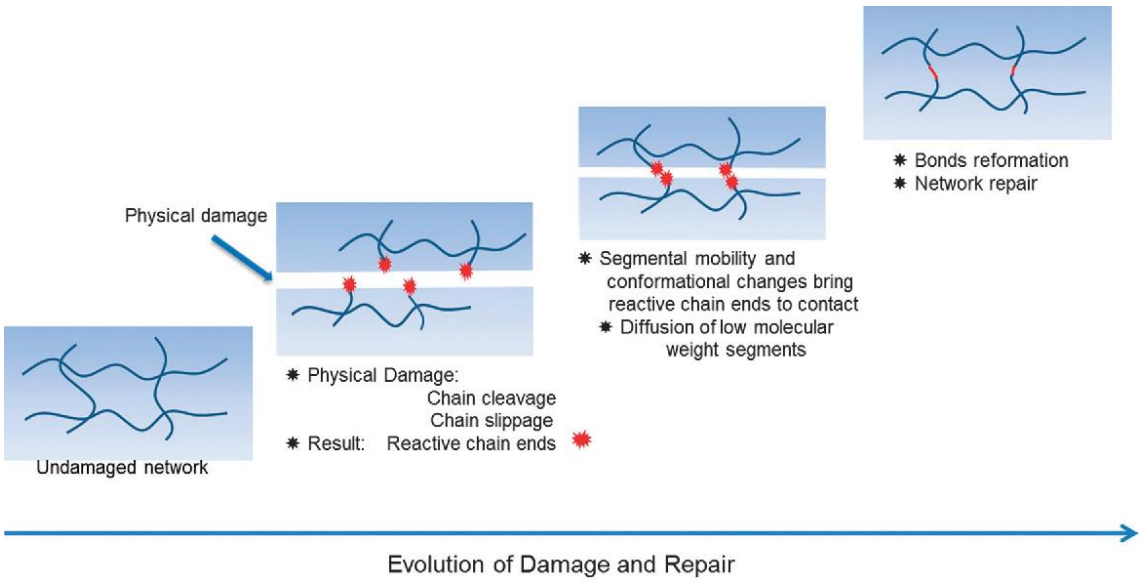

Figure 1.9. An illustration of the mechanism for intrinsic self-healing polymers. (reproduced with permission from ref [78] published by The Royal Society of Chemistry)

The mechanism involved in self-healing is simple (**Figure 1.9**). Firstly, the materials are physically damaged (cut, torn, cracked) which results in a loss of network integrity (chain cleavage or slippage within the polymer network). This is the same for both intrinsic and extrinsic systems. Next, in intrinsic systems, mobility within the polymer allows for chain movement, diffusing reactive chain ends throughout the network. These reactive chain ends are responsible for undergoing the reformation of the intrinsic network (supramolecular: hydrogen bonding, Diels-Alder, *etc*.). For extrinsic systems, the original physical damage serves to rupture or release the chemicals responsible for the subsequent crosslinking reactions. In either case, network integrity is reestablished and the original physical damage can no longer be detected. A variety of characterization techniques can be used to quantify the damage and study the healing process. Most involve two parts: determination of the presence of visual damage using microscopy techniques (scanning electron microscopy (SEM), optical microscopy, and atomic force microscopy (AFM));

and determining if network integrity was lost, which results in a loss of thermomechanical properties that is easily detected by tensile testing or DMA.

1.6 Research Objectives

The major objective of my dissertation was to utilize macromolecular engineering to control biomass-derived polymers. Despite their environmental advantages, many bioplastics and elastomers from sustainable resources suffer from poor thermal and mechanical properties. By controlling the structure and topology of these polymers, through macromolecular engineering, polymeric materials with detailed microstructures and predictable properties can be achieved.

Firstly, supramolecular interactions including hydrogen-bonding and metal-ligand coordination are used to introduce "crosslinking junctions" and mimic chain entanglement. The obtained materials also display stimuli-responsive properties including self-healing and shape-memory. Extensive studies were performed on both systems to elucidate the direct effect of the introduced physical bonding on microstructures and resultant properties.

The second half of this dissertation focuses on developing an industrially feasible route towards plant oil-derived materials. One such application, polymer coatings, would benefit greatly from a direct replacement of petroleum-derived components with biomass alternatives due to its large-scale usage. For this project, emulsion polymerization was used to synthesize copolymers, which could be crosslinked through a facile strategy and directly cast as acrylic polymer coatings. The second application, epoxy resin nanocomposites, is another widely used material that has already benefited greatly from incorporation of biomass-derived components. By incorporating fillers, enhanced thermal and mechanical properties are achievable. Additionally, the presence of different polymer networks (arising

from the epoxy crosslinks and grafted polymers) imparts shape-memory properties in these polymeric materials.

1.7 References

1. Dodds, D. R.; Gross, R. A. Chemistry. Chemicals from Biomass. *Science* **2007,** 318, 1250-1251.

2. Ragauskas, A. J.; Williams, C. K.; Davison, B. H.; Britovsek, G.; Cairney, J.; Eckert, C. A.; Frederick, W. J., Jr.; Hallett, J. P.; Leak, D. J.; Liotta, C. L.; Mielenz, J. R.; Murphy, R.; Templer, R.; Tschaplinski, T. The Path Forward for Biofuels and Biomaterials. *Science* **2006,** 311, 484-489.

3. Yao, K. J.; Tang, C. B. Controlled Polymerization of Next-Generation Renewable Monomers and Beyond. *Macromolecules* **2013,** 46, 1689-1712.

4. Hasani, M.; Cranston, E. D.; Westman, G.; Gray, D. G. Cationic Surface Functionalization of Cellulose Nanocrystals. *Soft Matter* **2008,** 4, 2238-2244.

5. Roy, D.; Semsarilar, M.; Guthrie, J. T.; Perrier, S. Cellulose Modification by Polymer Grafting: A Review. *Chem. Soc. Rev.* **2009,** 38, 2046-2064.

6. Mariano, M.; El Kissi, N.; Dufresne, A. Cellulose Nanocrystals and Related Nanocomposites: Review of Some Properties and Challenges. *J. Polym. Sci., Part B: Polym. Phys.* **2014,** 52, 791-806.

7. Wohlhauser, S.; Delepierre, G.; Labet, M.; Morandi, G.; Thielemans, W.; Weder, C.; Zoppe, J. O. Grafting Polymers from Cellulose Nanocrystals: Synthesis, Properties, and Applications. *Macromolecules* **2018,** 51, 6157-6189.

8. Sun, Z.; Fridrich, B.; de Santi, A.; Elangovan, S.; Barta, K. Bright Side of Lignin Depolymerization: Toward New Platform Chemicals. *Chem. Rev.* **2018,** 118, 614-678.

9. Isikgor, F. H.; Becer, C. R. Lignocellulosic Biomass: A Sustainable Platform for the Production of Bio-Based Chemicals and Polymers. *Polym. Chem.* **2015,** 6, 4497-4559.

10. Chung, H.; Washburn, N. R. Chemistry of Lignin-Based Materials. *Green Mater.* **2013,** 1, 137-160.

11. Kai, D.; Tan, M. J.; Chee, P. L.; Chua, Y. K.; Yap, Y. L.; Loh, X. J. Towards Lignin-Based Functional Materials in a Sustainable World. *Green Chem.* **2016,** 18, 1175-1200.

12. Wang, Z.; Yuan, L.; Tang, C. Sustainable Elastomers from Renewable Biomass. *Acc. Chem. Res.* **2017,** 50, 1762-1773.

13. Biermann, U.; Bornscheuer, U.; Meier, M. A.; Metzger, J. O.; Schafer, H. J. Oils and Fats as Renewable Raw Materials in Chemistry. *Angew. Chem. Int. Ed.* **2011,** 50, 3854-3871.

14. Meier, M. A. R.; Metzger, J. O.; Schubert, U. S. Plant Oil Renewable Resources as Green Alternatives in Polymer Science. *Chem. Soc. Rev.* **2007,** 36, 1788-1802.

15. Wang, Z.; Yuan, L.; Ganewatta, M. S.; Lamm, M. E.; Rahman, M. A.; Wang, J.; Liu, S.; Tang, C. Plant Oil-Derived Epoxy Polymers toward Sustainable Biobased Thermosets. *Macromol. Rapid Commun.* **2017,** 38, 1700009.

16. Xu, S. C.; Lamm, M. E.; Rahman, M. A.; Zhang, X. Z.; Zhu, T. Y.; Zhao, Z. D.; Tang, C. B. Renewable Atom-Efficient Polyesters and Thermosetting Resins Derived from High Oleic Soybean Oil. *Green Chem.* **2018,** 20, 1106-1113.

17. Jian, X.-Y.; An, X.-P.; Li, Y.-D.; Chen, J.-H.; Wang, M.; Zeng, J.-B. All Plant Oil Derived Epoxy Thermosets with Excellent Comprehensive Properties. *Macromolecules* **2017,** 50, 5729-5738.

18. Luo, Q.; Liu, M.; Xu, Y.; Ionescu, M.; Petrović, Z. S. Thermosetting Allyl Resins Derived from Soybean Oil. *Macromolecules* **2011,** 44, 7149-7157.

19. Yuan, L.; Wang, Z. K.; Trenor, N. M.; Tang, C. B. Amidation of Triglycerides by Amino Alcohols and Their Impact on Plant Oil-Derived Polymers. *Polym. Chem.* **2016,** 7, 2790-2798.

20. Yuan, L.; Wang, Z. K.; Trenor, N. M.; Tang, C. B. Robust Amidation Transformation of Plant Oils into Fatty Derivatives for Sustainable Monomers and Polymers. *Macromolecules* **2015,** 48, 1320-1328.

21. Ran, J.; Wu, L.; Zhang, Z.; Xu, T. Atom Transfer Radical Polymerization (ATRP): A Versatile and Forceful Tool for Functional Membranes. *Prog. Polym. Sci.* **2014,** 39, 124-144.

22. Matyjaszewski, K.; Tsarevsky, N. V. Macromolecular Engineering by Atom Transfer Radical Polymerization. *J. Am. Chem. Soc.* **2014,** 136, 6513-6533.

23. Lutz, J.-F.; Schlaad, H. Modular Chemical Tools for Advanced Macromolecular Engineering. *Polymer* **2008,** 49, 817-824.

24. Matyjaszewski, K. Macromolecular Engineering: From Rational Design through Precise Macromolecular Synthesis and Processing to Targeted Macroscopic Material Properties. *Prog. Polym. Sci.* **2005,** 30, 858-875.

25. Polymeropoulos, G.; Zapsas, G.; Ntetsikas, K.; Bilalis, P.; Gnanou, Y.; Hadjichristidis, N. 50th Anniversary Perspective: Polymers with Complex Architectures. *Macromolecules* **2017,** 50, 1253-1290.

26. Matyjaszewski, K.; Tsarevsky, N. V. Nanostructured Functional Materials Prepared by Atom Transfer Radical Polymerization. *Nat. Chem.* **2009,** 1, 276-288.

27. Jin, Q.; Liu, G.; Ji, J. Micelles and Reverse Micelles with a Photo and Thermo Double-Responsive Block Copolymer. *J. Polym. Sci., Part A: Polym. Chem.* **2010,** 48, 2855-2861.

28. Pollino, J. M.; Weck, M. Non-Covalent Side-Chain Polymers: Design Principles, Functionalization Strategies, and Perspectives. *Chem. Soc. Rev.* **2005,** 34, 193-207.

29. Coessens, V.; Pintauer, T.; Matyjaszewski, K. Functional Polymers by Atom Transfer Radical Polymerization. *Prog. Polym. Sci.* **2001,** 26, 337-377.

30. Mattson, K. M.; Pester, C. W.; Gutekunst, W. R.; Hsueh, A. T.; Discekici, E. H.; Luo, Y.; Schmidt, B. V. K. J.; McGrath, A. J.; Clark, P. G.; Hawker, C. J. Metal-Free Removal of Polymer Chain Ends Using Light. *Macromolecules* **2016,** 49, 8162-8166.

31. Martens, S.; Holloway, J. O.; Du Prez, F. E. Click and Click-Inspired Chemistry for the Design of Sequence-Controlled Polymers. *Macromol. Rapid Commun.* **2017,** 38.

32. Kempe, K.; Krieg, A.; Becer, C. R.; Schubert, U. S. “Clicking” on/with Polymers: A Rapidly Expanding Field for the Straightforward Preparation of Novel Macromolecular Architectures. *Chem. Soc. Rev.* **2012,** 41, 176-191.

33. Lowe, A. B. Thiol-Ene “Click” Reactions and Recent Applications in Polymer and Materials Synthesis. *Polym. Chem.* **2010,** 1, 17-36.

34. Wang, J.-S.; Matyjaszewski, K. Controlled/"Living" Radical Polymerization. Halogen Atom Transfer Radical Polymerization Promoted by a Cu(I)/Cu(II) Redox Process. *Macromolecules* **1995,** 28, 7901-7910.

35. Kato, M.; Kamigaito, M.; Sawamoto, M.; Higashimura, T. Polymerization of Methyl Methacrylate with the Carbon Tetrachloride/Dichlorotris-(Triphenylphosphine)Ruthenium(II)/Methylaluminum Bis(2,6-Di-Tert-Butylphenoxide) Initiating System: Possibility of Living Radical Polymerization. *Macromolecules* **1995,** 28, 1721-1723.

36. Matyjaszewski, K.; Xia, J. Atom Transfer Radical Polymerization. *Chem. Rev.* **2001,** 101, 2921-2990.

37. Matyjaszewski, K. Atom Transfer Radical Polymerization (ATRP): Current Status and Future Perspectives. *Macromolecules* **2012,** 45, 4015-4039.

38. Treat, N. J.; Sprafke, H.; Kramer, J. W.; Clark, P. G.; Barton, B. E.; Read de Alaniz, J.; Fors, B. P.; Hawker, C. J. Metal-Free Atom Transfer Radical Polymerization. *J. Am. Chem. Soc.* **2014,** 136, 16096-101.

39. Huang, Z.; Gu, Y.; Liu, X.; Zhang, L.; Cheng, Z.; Zhu, X. Metal-Free Atom Transfer Radical Polymerization of Methyl Methacrylate with ppm Level of Organic Photocatalyst. *Macromol. Rapid Commun.* **2016,** 10.1002/marc.201600461.

40. Dadashi-Silab, S.; Pan, X.; Matyjaszewski, K. Photoinduced Iron-Catalyzed Atom Transfer Radical Polymerization with ppm Levels of Iron Catalyst under Blue Light Irradiation. *Macromolecules* **2017,** 50, 7967-7977.

41. Pan, X.; Lamson, M.; Yan, J.; Matyjaszewski, K. Photoinduced Metal-Free Atom Transfer Radical Polymerization of Acrylonitrile. *ACS Macro Lett.* **2015,** 4, 192-196.

42. Pan, X.; Malhotra, N.; Dadashi-Silab, S.; Matyjaszewski, K. A Simplified Fe-Based PhotoATRP Using Only Monomers and Solvent. *Macromol. Rapid Commun.* **2016,** 10.1002/marc.201600651.

43. Tasdelen, M. A.; Ciftci, M.; Yagci, Y. Visible Light-Induced Atom Transfer Radical Polymerization. *Macromol. Chem. Phys.* **2012,** 213, 1391-1396.

44. Chiefari, J.; Chong, Y. K. B.; Frances Ercole; Krstina, J.; Jeffery, J.; Le, T. P. T.; Mayadunne, R. T. A.; Meijs, G. F.; Moad, C. L.; Moad, G.; Rizzardo, E.; Thang, S. H. Living Free-Radical Polymerization by Reversible Addition-Fragmentation Chain Transfer: The RAFT Process. *Macromolecules* **1998,** 31, 5559-5562.

45. Chong, Y. K.; Krstina, J.; Le, T. P. T.; Moad, G.; Postma, A.; Rizzardo, E.; Thang, S. H. Thiocarbonylthio Compounds [Sc(Ph)S−R] in Free Radical Polymerization with Reversible Addition-Fragmentation Chain Transfer (RAFT Polymerization). Role of the Free-Radical Leaving Group (R). *Macromolecules* **2003,** 36, 2256-2272.

46. Barner-Kowollik, C.; Buback, M.; Charleux, B.; Coote, M. L.; Drache, M.; Fukuda, T.; Goto, A.; Klumperman, B.; Lowe, A. B.; Mcleary, J. B.; Moad, G.; Monteiro, M. J.; Sanderson, R. D.; Tonge, M. P.; Vana, P. Mechanism and Kinetics of Dithiobenzoate-Mediated RAFT Polymerization. I. The Current Situation. *J. Polym. Sci., Part A: Polym. Chem.* **2006,** 44, 5809-5831.

47. Keddie, D. J.; Moad, G.; Rizzardo, E.; Thang, S. H. RAFT Agent Design and Synthesis. *Macromolecules* **2012,** 45, 5321-5342.

48. Moad, G.; Chong, Y. K.; Postma, A.; Rizzardo, E.; Thang, S. H. Advances in RAFT Polymerization: The Synthesis of Polymers with Defined End-Groups. *Polymer* **2005,** 46, 8458-8468.

49. Perrier, S. 50th Anniversary Perspective: RAFT Polymerization—A User Guide. *Macromolecules* **2017,** 50, 7433-7447.

50. Keddie, D. J. A Guide to the Synthesis of Block Copolymers Using Reversible-Addition Fragmentation Chain Transfer (RAFT) Polymerization. *Chem. Soc. Rev.* **2014,** 43, 496-505.

51. Boyer, C.; Bulmus, V.; Davis, T. P.; Ladmiral, V.; Liu, J.; Perrier, S. Bioapplications of RAFT Polymerization. *Chem. Rev.* **2009,** 109, 5402-5436.

52. Qun, W.; Shoukuan, F.; Tongyin, Y. Emulsion Polymerization. *Prog. Polym. Sci.* **1994,** 19, 703-753.

53. Eliseeva, V. I.; Ivanchev, S. S.; Kuchanov, S. I.; Lebedev, A. V., *Emulsion Polymerization and Its Applications in Industry*. Springer: USA: New York City, 2012; p 195-213.

54. Chern, C. S. Emulsion Polymerization Mechanisms and Kinetics. *Prog. Polym. Sci.* **2006,** 31, 443-486.

55. Asua, J. M. Emulsion Polymerization: From Fundamental Mechanisms to Process Developments. *J. Polym. Sci. Part A: Polym. Chem.* **2004,** 42, 1025-1041.

56. Smith, W. V.; Ewart, R. H. Kinetics of Emulsion Polymerization. *The Journal of Chemical Physics* **1948,** 16, 592-599.

57. Slomkowski, S.; Alemán José, V.; Gilbert Robert, G.; Hess, M.; Horie, K.; Jones Richard, G.; Kubisa, P.; Meisel, I.; Mormann, W.; Penczek, S.; Stepto Robert, F. T., Terminology of Polymers and Polymerization Processes in Dispersed Systems (IUPAC Recommendations 2011). *Pure Appl. Chem.*, 2011; Vol. 83, p 2229.

58. Bonham, J. A.; Faers, M. A.; van Duijneveldt, J. S. Non-Aqueous Microgel Particles: Synthesis, Properties and Applications. *Soft Matter* **2014,** 10, 9384-9398.

59. Asua, J. M. Challenges for Industrialization of Miniemulsion Polymerization. *Prog. Polym. Sci.* **2014,** 39, 1797-1826.

60. Moreno, M.; Goikoetxea, M.; Barandiaran, M. J. Biobased-Waterborne Homopolymers from Oleic Acid Derivatives. *J. Polym. Sci. Part A: Polym. Chem.* **2012,** 50, 4628-4637.

61. Kingsley, K.; Shevchuk, O.; Demchuk, Z.; Voronov, S.; Voronov, A. The Features of Emulsion Copolymerization for Plant Oil-Based Vinyl Monomers and Styrene. *Ind. Crops Prod.* **2017,** 109, 274-280.

62. Moreno, M.; Goikoetxea, M.; de la Cal, J. C.; Barandiaran, M. J. From Fatty Acid and Lactone Biobased Monomers toward Fully Renewable Polymer Latexes. *J. Polym. Sci., Part A: Polym. Chem.* **2014,** 52, 3543-3549.

63. Bunker, S.; Staller, C.; Willenbacher, N.; Wool, R. Miniemulsion Polymerization of Acrylated Methyl Oleate for Pressure Sensitive Adhesives. *Int. J. Adhes. Adhes.* **2003,** 23, 29-38.

64. Pu, G.; Dubay, M. R.; Zhang, J.; Severtson, S. J.; Houtman, C. J. Polyacrylates with High Biomass Contents for Pressure-Sensitive Adhesives Prepared Via Mini-Emulsion Polymerization. *Ind. Eng. Chem. Res.* **2012,** 51, 12145-12149.

65. Wang, J.; Lu, C.; Liu, Y.; Wang, C.; Chu, F. Preparation and Characterization of Natural Rosin Stabilized Nanoparticles Via Miniemulsion Polymerization and Their Pressure-Sensitive Adhesive Applications. *Ind. Crops Prod.* **2018,** 124, 244-253.

66. Moreno, M.; Miranda, J. I.; Goikoetxea, M.; Barandiaran, M. J. Sustainable Polymer Latexes Based on Linoleic Acid for Coatings Applications. *Prog. Org. Coat.* **2014,** 77, 1709-1714.

67. Liu, F.; Urban, M. W. Recent Advances and Challenges in Designing Stimuli-Responsive Polymers. *Prog. Polym. Sci.* **2010,** 35, 3-23.

68. Wei, M.; Gao, Y.; Li, X.; Serpe, M. J. Stimuli-Responsive Polymers and Their Applications. *Polym. Chem.* **2017,** 8, 127-143.

69. Stuart, M. A. C.; Huck, W. T. S.; Genzer, J.; Müller, M.; Ober, C.; Stamm, M.; Sukhorukov, G. B.; Szleifer, I.; Tsukruk, V. V.; Urban, M.; Winnik, F.; Zauscher, S.; Luzinov, I.; Minko, S. Emerging Applications of Stimuli-Responsive Polymer Materials. *Nat. Mater.* **2010,** 9, 101.

70. Chan, B. Q.; Low, Z. W.; Heng, S. J.; Chan, S. Y.; Owh, C.; Loh, X. J. Recent Advances in Shape Memory Soft Materials for Biomedical Applications. *ACS Appl. Mater. Interfaces* **2016,** 8, 10070-87.

71. Alarcón, C. d. l. H.; Pennadam, S.; Alexander, C. Stimuli Responsive Polymers for Biomedical Applications. *Chem. Soc. Rev.* **2005,** 34, 276-285.

72. Xie, T. Recent Advances in Polymer Shape Memory. *Polymer* **2011,** 52, 4985-5000.

73. Ratna, D.; Karger-Kocsis, J. Recent Advances in Shape Memory Polymers and Composites: A Review. *J. Mater. Sci.* **2008,** 43, 254-269.

74. Meng, H.; Li, G. A Review of Stimuli-Responsive Shape Memory Polymer Composites. *Polymer* **2013,** 54, 2199-2221.

75. Hu, J.; Zhu, Y.; Huang, H.; Lu, J. Recent Advances in Shape–Memory Polymers: Structure, Mechanism, Functionality, Modeling and Applications. *Prog. Polym. Sci.* **2012,** 37, 1720-1763.

76. Jiang, Z. C.; Xiao, Y. Y.; Kang, Y.; Pan, M.; Li, B. J.; Zhang, S. Shape Memory Polymers Based on Supramolecular Interactions. *ACS Appl. Mater. Interfaces* **2017,** 9, 20276-20293.

77. Syrett, J. A.; Becer, C. R.; Haddleton, D. M. Self-Healing and Self-Mendable Polymers. *Polym. Chem.* **2010,** 1, 978-987.

78. Yang, Y.; Urban, M. W. Self-Healing Polymeric Materials. *Chem. Soc. Rev.* **2013,** 42, 7446-7467.

79. Yang, Y.; Ding, X.; Urban, M. W. Chemical and Physical Aspects of Self-Healing Materials. *Prog. Polym. Sci.* **2015,** 49-50, 34-59.

80. Garcia, S. J. Effect of Polymer Architecture on the Intrinsic Self-Healing Character of Polymers. *Eur. Polym. J.* **2014,** 53, 118-125.

81. Hillewaere, X. K. D.; Du Prez, F. E. Fifteen Chemistries for Autonomous External Self-Healing Polymers and Composites. *Prog. Polym. Sci.* **2015,** 49-50, 121-153.

CHAPTER 2

TUNING MECHANICAL PROPERTIES OF BIOBASED POLYMERS BY SUPRAMOLECULAR CHAIN ENTANGLEMENT

Adapted with permission from Lamm, M.E.; Song, L.; Wang, Z.; Rahman, Md. A.; Lamm, B.; Fu, L.; and Tang, C. *Macromolecules*, **2019**, DOI: 10.1021/acs.macromol.9b01828.

2.1 Abstract

A variety of biobased polymers have been derived from diverse natural resources. However, the mechanical properties of some of these polymers are inferior due to low chain entanglement. We report a facile strategy termed "supramolecular chain entanglement" via supramolecular interactions to create physical crosslinking and entanglements for polymers with long pendent fatty chains. The ensuing bioplastics – prepared by mixing copolymers, composed of a plant oil-derived methacrylate with an acid-containing monomer as a hydrogen-bonding donor – and poly(4-vinylpyridine) as a wrapping chain with a hydrogen-bonding acceptor, show tunable mechanical strength and toughness. These polymer blends, consisting of > 90 wt% sustainable sources, show marked improvement in thermomechanical properties compared with the viscoelastic nature of the biobased homopolymer as a direct result of chain wrapping and hydrogen bonding between the carboxylic acid and pyridine groups. Spectroscopic evidence confirmed the hydrogen-bonding interaction within the copolymers, while morphological and thermal characterization was carried out to elucidate microstructures of biobased polymers.

2.2 Introduction

Common commodity polymers, including polypropylene, polyethylene and polystyrene, are heavily dependent on petroleum-based chemicals. Production of fossil-based monomers and polymers aggravates net carbon emission and undesirable climate change. Thus, recent thrusts are aimed at increasing the use of renewable carbon-neutral resources in the manufacture of bioplastics.[1-9] Nevertheless, sustainable polymers face many challenges, including high cost and poor performance, which limit their

competitiveness in the current market. These issues could be mitigated by using common, cheap biomass sources coupled with minimal or highly efficient functionalization.[10-12] For example, plant oils with a global production of nearly 200 million tons are a promising renewable resource for making biobased polymers with additional benefits of low cost and value-added functionality.[1, 13-17]

However, many of these bioplastics have poor mechanical properties, including fragility and low strength. Derived from a variety of biomass, these polymers could possess bulky or long pendent chains, which can result in significantly lower chain entanglement (and therefore high entanglement molecular weight, M_e).[18] M_e is very high for polymers with bulky side groups from biomass such as soybean oil (>200 kDa), rosin acids (>90 kDa), and terpenes (>30 kDa).[19-21] A few strategies have been developed to overcome high M_e: (1) the use of ultrahigh molecular weight polymers;[20] (2) utilization of chain architectures such as block copolymers to allow for stress dissipation;[19, 21-27] and (3) incorporation of physical or dynamic chemical crosslinking to induce chain entanglement.[27-29] Dynamic crosslinking is a viable approaches with the aid of a wide variety of chemistries such as supramolecular interactions and exchangeable bonding. Supramolecular interactions such as hydrogen bonding (H-bonding) have been widely used as dynamic bonds to improve properties of polymers.[30-41]

Herein we report a simple, yet robust "supramolecular chain entanglement" strategy for the creation of physical crosslinking and entanglements to substantially enhance mechanical properties of biomass-derived polymers, as illustrated in **Figure 1**. We present plant oils as a biomass origin to demonstrate the validity of this concept. Specifically, we introduce H-bonding into a polymeric system to induce physical crosslinks. Acidic proton

donors (e.g. carboxylic acids) and basic proton acceptors (e.g. amines and pyridines) are among the most desirable H-bonding pairs due to their high affinity, good precursor solubility, and facile availability.[42, 43] In this work, commercial carboxylic acids such as methacrylic acid (MAA), acrylic acid (AA), and 2-carboxy-ethyl acrylate (CEA) were used as H-bonding donor co-monomers, which were introduced into soybean oil-derived polymers via radical copolymerization. The copolymers were then mixed with poly(4-vinypyridine) (P4VP), an H-bonding acceptor. The H-bonding interactions between pyridine and acid units would create physical crosslinks among bulky biomass-derived polymers and further enable the chains of P4VP to wrap around them.

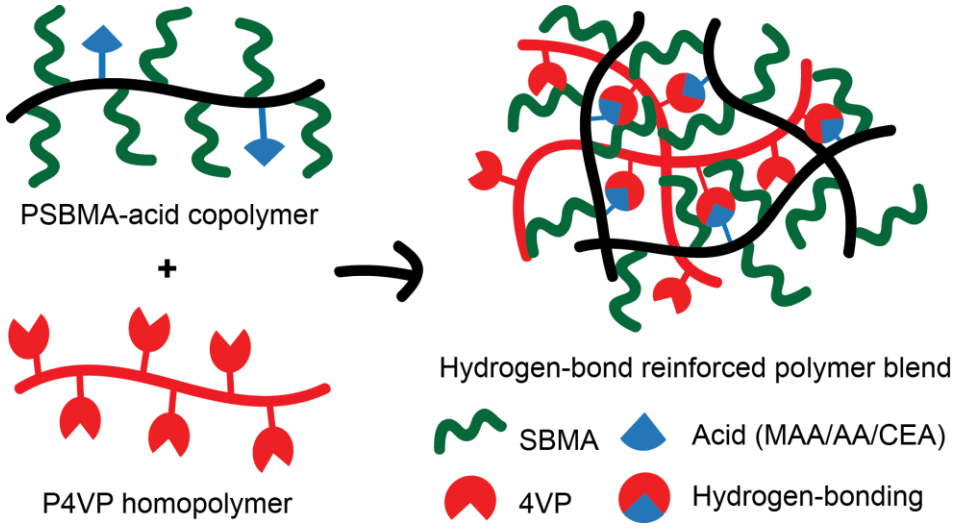

Figure 2.1. Graphical illustration of "supramolecular chain entanglement": P4VP is used as H-bonding acceptors to interact and wrap soybean oil-based copolymers containing H-bonding acidic donors, which produces physical crosslinks toward more efficient chain entanglements.

A few design principles guide the macromolecular compositions: (1) The entangling polymers should be readily processable and have a relative low M_e with functionalities to facilitate the formation of physical crosslinks. P4VP could meet these criteria with its M_e at ~30 kDa.[18] (2) Biomass monomers should be able to copolymerize with other monomers

that are not only low cost and commercially available, but are also able to induce supramolecular interactions with the entangling polymers. Thus, carboxylic acid-based (meth)acrylate monomers would be a good choice. (3) The biomass content should be aimed at sustainability, in other words, the entangling polymers and those for supramolecular interactions should be used at the minimum level.

2.3 Experimental

Materials

Plenish high oleic soybean oil (HOSO) was provided by Pioneer. Azobisisobutyronitrile (AIBN, 98%, Aldrich) was recrystallized from methanol. 4-Vinyl pyridine (Sigma, 96%) was vacuum distilled. Other monomers were run through basic alumina to remove inhibitors. All other reagents were from commercial resources and used as received unless otherwise mentioned. SBMA (soybean methacrylate) and SBMA and PSBMA were synthesized following previously published procedures.[54]

Synthesis of Copolymers (P(SBMA-co-MAA), P(SBMA-co-AA), and P(SBMA-co-CEA))

The following procedure was used for **MAA5**, similar procedures were followed for all other copolymers. SBMA (7 g, 0.017 mol), MAA (0.33 g, 0.0035 mol) and AIBN (35 mg, 0.21 mmol) were placed in a 50 mL round bottom flask and dissolved in toluene (14 mL). The flask was sealed, purged with nitrogen for 15 min, and placed in an 80 ^{o}C oil bath. After 16 h, the polymer was poured into cold methanol. The resulting polymer was precipitated twice into methanol and dried for 24 h in a 50 ^{o}C vacuum oven.

Synthesis of Poly(4-vinylpyridine)

The following procedure was used to synthesize **P4VP-30**. Similar procedure was followed for other molecular weights. 4-Vinylpyridine (6.13 mg, 56.9 mmol) and 4-cyano-4-(thiobenzoylthio)pentanoic acid (42 mg, 0.15 mmol) were placed in a 25 mL Schlenk flask. AIBN (1.23 mg, 0.0075 mmol) was dissolved in THF (0.1 mL) and added to the flask. The flask was sealed and purged of oxygen using three cycles of freeze-pump-thaw. The flask was placed in a 60 ºC oil bath. The polymer was dissolved into hexane and precipitated in diethyl ether three times. The polymer was dried in a 60 ºC oven for 24 h.

Characterization

^{1}H NMR and ^{13}C NMR spectra were recorded on a Varian Mercury 300 spectrometer in deuterated chloroform ($CDCl_3$) with tetramethylsilane (TMS) as an internal reference. Solid state ^{13}C CP-MAS spectra were collected on a Bruker Avance III-HD 500 MHz (^{13}C frequency of 129.79 MHz) spectrometer fitted with a 1.9mm MAS probe. The spectra were collected at ambient temperature with sample rotation rate of 20 kHz. 2 ms contact time with linear ramping on the ^{1}H channel and 62.5kHz field on the ^{13}C channel were used for cross polarization. ^{1}H dipolar decoupling was performed with SPINAL64 modulation and 145kHz field strength. Free induction decays were collected with a 20 msec acquisition time over a 350 ppm spectra width with a relaxation delay of 2s. Molecular weight and molecular weight distribution of polymers were determined by gel permeation chromatography (GPC) equipped with a 2414 RI detector, a 1525 Binary Pump and three Styragel columns. The columns consisted of HR 1, HR 3 and HR 5E with effective molecular weight ranges of 100−5K, 500−30K, and 2K−4M respectively. THF was used as eluent at 35 °C with a flow rate of 1.0 mL/min. The system was calibrated with

polystyrene standards obtained from Polymer Laboratories. GPC samples were prepared by dissolving the sample in THF with a concentration of 3.0 mg/mL and passing through microfilters with a pore size of 0.2 μm. Glass transition temperature (T_g) of polymers was determined using differential scanning calorimetry (DSC) conducted on a DSC 2000 instrument (TA Instruments). Samples were first heated from −70 to +200 °C at a rate of 10 °C/min. After cooling down to −70 °C at the same rate, the data were collected from the second heating and cooling scan. About 10 mg of each sample was used for the DSC test with nitrogen gas at a flow rate of 50 mL/min. Thermogravimetric analysis (TGA) was conducted on a Q5000 TGA system (TA Instruments), ramping from 25 to 600 °C with a rate of 10 °C/min. About 10 mg of sample is used per test. Tensile stress−strain testing was carried out with an Instron 5543A testing instrument with a cross-head speed of 20mm/min. Five replicate samples from different films were used to obtain an average value for each. Error was calculated from standard deviation using data collected from all five replicate samples. Fourier transform infrared spectrometry (FTIR) spectra were taken on a PerkinElmer spectrum 100 FTIR spectrometer. Variable temperature FT-IR (VT-FTIR) experiments were performed on a Bruker Tensor 27 FT-IR spectrophotometer with Eurotherm 2404 temperature controller. Dried polymer films were used for measurement. Dynamic thermomechanical analysis (DMA) was performed by using a Q800 DMA (TA Instruments). The DMA spectra were scanned with a frequency of 1 Hz and a heating rate of 3 ºC/min. Small-angle X-ray scattering (SAXS) experiments were conducted using SAXSLab Ganesha at the South Carolina SAXS Collaborative at the University of South Carolina. A Xenocs GeniX3D microfocus source was used with a copper target to generate a monochromic beam with a 0.154 nm wavelength. The instrument was calibrated using a

silver behenate reference with the first order scattering vector q* = 1.076 nm−1, with q = 4πλ−1 sin θ, where λ is the X - ray wavelength and 2θ is the total scattering angle. A 300 K Pilatus detector (Dectris) was used to collect the two-dimensional (2D) SAXS patterns. Radial integration of 2D patterns reduced the data to 1D profiles. Polymer films were fixed to a mount such that only the sample was measured at the exclusion of any mounting tape. All data were acquired for about 0.5 hour at room temperature with an incident X-ray flux of ∼1.5 M photons per second. Temperature-dependent SAXS measurements were taken using a Linkam Scientific Instrument HFS350X-GI hot stage in a SAXSLab Ganesha. The sample was heated at a rate of 10 °C/min and left to equilibrate for 10 min. Cooling of the sample to room temperature was performed at a rate of 5 °C/min. Microscopy images were taken using a Leica DM750 microscope equipped with a mounted EC3 camera. Self-healing experiments involved damaging films using a standard razor blade to cut films. A new razor blade was used for each experiment.

Mechanical Properties

Films for tensile testing were prepared by dissolving 0.75 g of a copolymer and various amounts of P4VP in 10 mL of chloroform. The solution was sonicated for 5 minutes and poured in a PTFE mold. After the evaporation of solvent over 48 h, the film was put under vacuum for 12 h at room temperature and then 12 h at 60 °C. Dog-bone shaped specimens were cut from the cast film with a length of 20 mm and width of 5.0 mm. The thickness was measure prior to each measurement. Testing occurred at room temperature with the crosshead speed of 20 mm/min.

2.4 Results

Preparation of H-bonded polymer blends

Soybean oil-based copolymers were synthesized using free radical copolymerization of soybean monomers and carboxylic acid monomers (**Scheme 1**). Large-scale synthesis of soybean methacrylate (SBMA) monomer was recently demonstrated.[44] However, the SBMA homopolymer (PSBMA) is a viscoelastic liquid.[45, 46] The addition of a small fraction (≤ 5wt%) of acid-based comonomers successfully transformed the viscoelastic homopolymer to thermoplastic copolymers. This is substantial in terms of the effect of comonomers on mechanical properties.

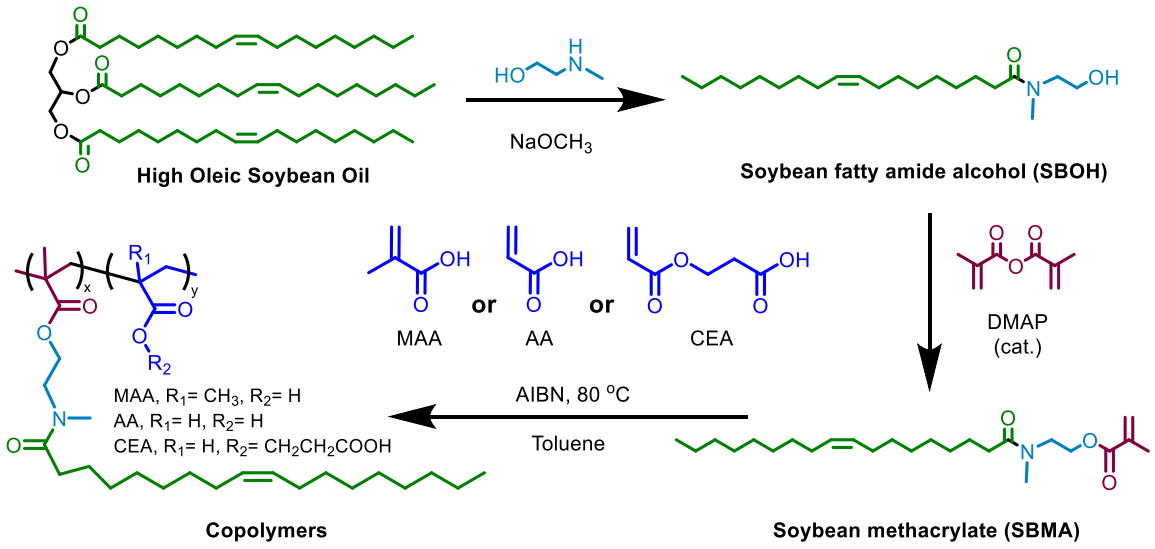

Figure 2.2. Synthesis of soybean oil-based methacrylate monomers from high oleic soybean oil and soybean oil-based copolymers P(SBMA-co-MAA/AA/CEA) via free radical copolymerization.

To examine the effect of acid contents, copolymers of each acid system with two different weight fractions of acid (2 and 5 wt%) were prepared (copolymer named with acid monomer and its weight percentile, **Table 2.1**). First, MAA-containing copolymers

suffer from brittleness, mostly due to the high T_g nature of MAA polymer (PMAA T_g ~230 ^oC). Therefore, a comparative system with a softer AA component was utilized (PAA T_g ~106 ^oC). As both MAA and AA units are much smaller than bulky SBMA, the acid units are likely surrounded by pendant fatty side chains, potentially limiting the formation of H-bonding.[124] Thus, CEA-containing copolymers were synthesized. CEA is a soft acid monomer (PCEA T_g ~30 ^oC), bearing a longer pendant carboxylic group.

Table 2.1. Characterization data of PSBMA homopolymer, P(SBMA-co-MAA) copolymers (MAA2 and MAA5), P(SBMA-co-AA) copolymers (AA2 and AA5), and P(SBMA-co-CEA) copolymers (CEA2 and CEA5).

Sample code	Acid content (wt%)[a]	Acid content (mol%)[a]	T_g (^oC)[b]	M_n (KDa)[c]	$Đ$[c]
PSBMA	0	0	-6	43.4	1.78
MAA2	2	8.8	19	83.5	2.49
MAA5	5	20.0	35	81.3	2.21
AA2	2	10.3	-4	29.4	2.70
AA5	5	22.9	-2	32.9	2.98
CEA2	2	5.5	-6	33.4	2.66
CEA5	5	12.9	-5	32.9	2.64

[a]Weight and molar fractions of MAA, AA, and CEA were calculated based on ^{1}H NMR. [b]T_g values were obtained by DSC (2nd heating cycle). [c]Molecular weight and molecular weight distribution were characterized via GPC.

Table 2.2. Weight and molar fractions of all components in polymer blends containing P4VP and SBMA copolymer (**MAA2**, **MAA5**, **AA2**, **AA5**, **CEA2**, and **CEA5**).

Sample code (wt% in Number)	Weight Fraction (wt %)[a]			Molar Fraction (mol %)[a]		
	Acid	4VP	SBMA	Acid	4VP	SBMA
MAA2-P4VP2[b]	2	2	96	7.2	6.8	86.0
MAA2-P4VP5[b]	2	5	93	7.7	15.7	76.6
MAA5-P4VP2[b]	5	2	93	16.6	7.6	75.8
MAA5-P4VP5[b]	5	5	90	15.1	14.3	70.6
AA2-P4VP2	2	2	96	7.8	6.7	85.5
AA2-P4VP5	2	5	93	8.1	16.3	75.6
AA5-P4VP2	5	2	93	17.1	8.0	74.9
AA5-P4VP5	5	5	90	15.9	15.1	69.0
CEA2-P4VP2	2	2	96	6.8	7.0	86.2
CEA2-P4VP5	2	5	93	7.2	15.4	77.4
CEA5-P4VP2	5	2	93	16.5	7.0	76.5
CEA5-P4VP5	5	5	90	14.1	14.9	71.0

[a]Weight and molar fractions of MAA, AA, and CEA were calculated based on ^{1}H NMR. [b]Same ratios used for all MAA blends, regardless of P4VP M_n.

All copolymers were characterized by ^{1}H NMR. Due to the difference in monomer reactivity, the molecular weight of AA and CEA copolymers is much lower than MAA copolymers. Compared to glass transition temperature (T_g) of **PSBMA** homopolymer (-6 ^{o}C), a significant increase was observed for MAA copolymers, 19 ^{o}C for **MAA2** and 35 ^{o}C for **MAA5**; whereas a minimal change in T_g was observed for AA and CEA copolymers.

The weight and molar fractions of comonomers in the resulting copolymers were calculated based on feed ratios and conversion of comonomers in the crude reaction mixture after polymerization, both confirmed by ^{1}H NMR (**Table 2.1**).

Supramolecular polymer blends were prepared by solution mixing of soybean copolymers and P4VP. P4VP was synthesized using reversible addition fragmentation transfer (RAFT) polymerization, following an established procedure.[48] Three P4VP polymers with different molecular weight were synthesized (M_n = 8, 30, and 60 kDa). All blends used the following naming system: the copolymer name indicating the acid monomer and its weight fraction in number (**MAA2**, **MAA5**, **AA2**, **AA5**, **CEA2**, or **CEA5**) and P4VP following by a number indicating its weight fraction. The number in parenthesis refers to as the molecular weight P4VP. For example, blend **MAA5-P4VP2 (30K)** contains MAA-based copolymer with 5wt% MAA and 2wt% P4VP with M_n = 30kDa. Molar and weight fractions of all components in each polymer blend are shown in **Table 2.2**. In order to maintain high sustainability, all blends contain ≥90wt% of soybean monomer, while the fractions of acid monomer (MAA, AA, or CEA) and 4VP together are ≤10 wt%. All polymer blends formed free-standing films, a remarkable mechanical improvement compared to the tacky PSBMA homopolymer.

As H-bonding is sensitive to temperature, variable temperature FTIR was employed to probe its presence in the blend system for understanding the effect of supramolecular interactions on microstructures.[119, 120, 124, 126] As shown in **Figure 2.3a**, three peaks were tracked: N···H, bonded C=O in amide, and free C=O in amide. At lower temperature, an N···H peak (1608 cm^{-1}) appeared, due to the delocalization of the carbonyl as a result of H-bonding with the pyridine group. This peak decreases in intensity with the increase of

temperature, indicating the weakening of H-bonding. Additionally, tertiary amide groups from the SBMA units also participate the H-bonding. They serve as H-bonding acceptors, in which the carbonyl bond was observed with a shift in its peak position, with a lower peak (1650 cm^{-1}) present at lower temperature, which corresponds to the associated H-bonding amide, and a higher peak (1654 cm^{-1}) present at higher temperature, which corresponds to the dissociated moiety not participating in H-bonding. There is also a correlation between all these peaks which show trends in peak intensity for N···H, free C=O and bonded C=O as a function of temperature (**Figure 2.3b**).

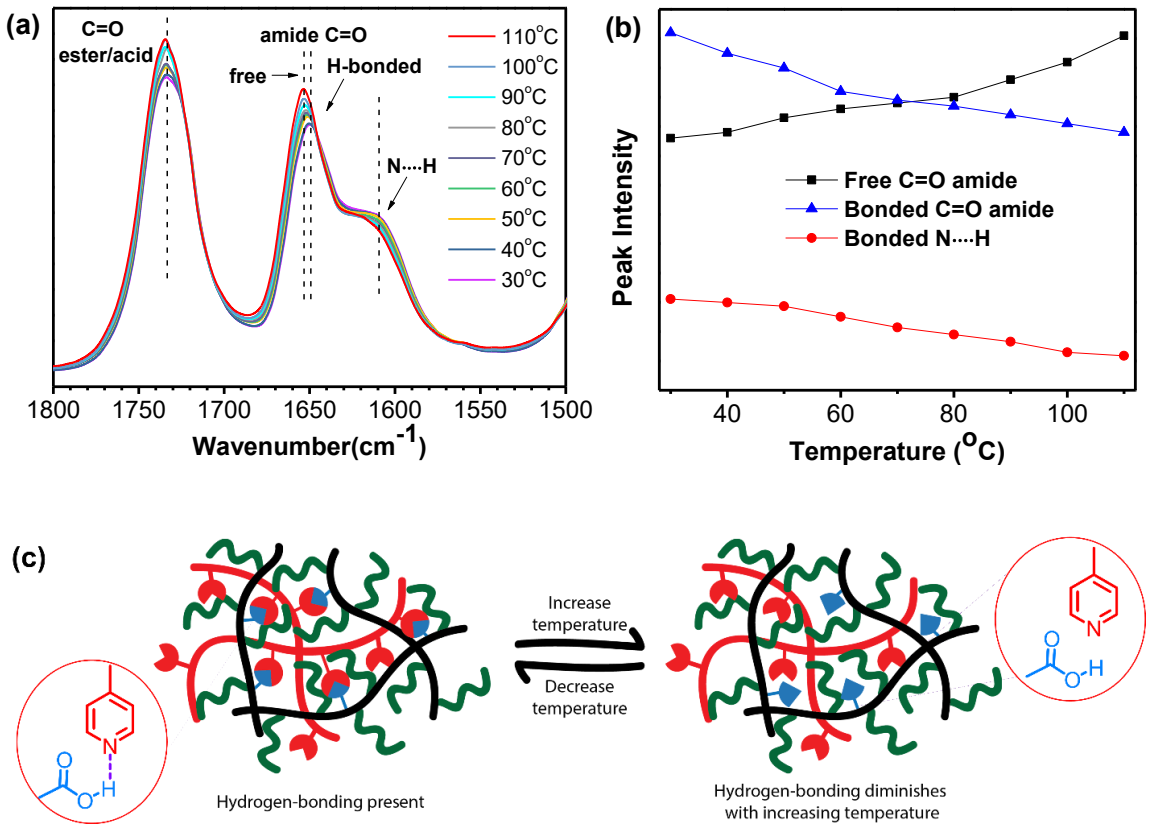

Figure 2.3. (a) Variable temperature FTIR spectra of a representative polymer blend (MAA5-P4VP5 (60K)) at various temperature; (b) Peak intensity of different bonds involving H-bonding as a function of temperature; (c) A proposed microstructure of polymer blends during heating and cooling cycles.

Additional characterization on H-bonding was performed using solid-state ^{13}C CP-MAS NMR. It has been reported that carboxylic acid can undergo dimerization, which can be disrupted by the addition of pyridine due to the formation of stronger hydrogen bonding between acid and pyridine.50 In this work, an MAA copolymer with a higher faction of MAA (molar ratio of SBMA: MAA at 1:1) was synthesized in order to amplify acid peaks from those of aliphatic backbone and side chain. This copolymer was blended with P4VP-60 to give a final molar ratio of SBMA: MAA: 4VP around 1:1:1. Using ^{13}C NMR, the copolymer and blend were compared (**Figure 2.4**). For the copolymer there is a broad peak around 172 ppm, representing the ester and amide carbonyls. An additional smaller peak at 182 ppm corresponds to the acid carbonyl. This peak location is consistent with the dimerization of carboxylic acid as reported in literature. The blend only exhibits one broader peak at 173 ppm, while the peak at 182 ppm completely disappeared. This indicates that the acid is no longer dimerized, most likely due to the new interaction between acid and pyridine. Taken together with FTIR results, it is evident that there is a presence of complex supramolecular interactions within 4VP, SBMA and MAA units through H-bonding.

Further morphological data was obtained using small angle x-ray scattering (SAXS). At room temperature (25 ^{o}C), only one broad peak is present corresponding to a *d*-spacing of 3-3.8 nm (**Figure 2.4**), which is consistent with previously reported ill-defined side-chain packing of pendant fatty chains.[102] The lack of high orders of scattering peaks at low *q* values indicates the absence of phase separation, further suggesting that the polymer blends are mostly miscible.

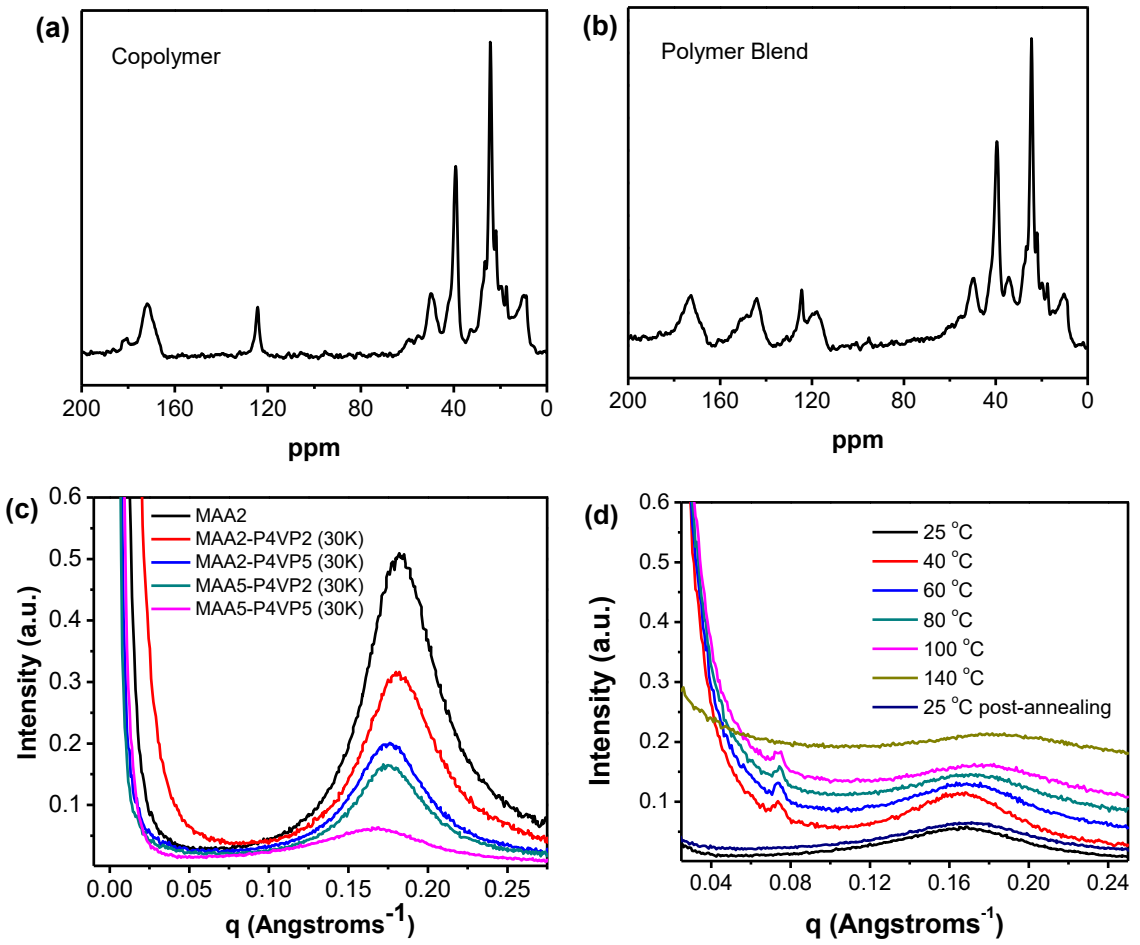

Figure 2.4. (a) ^{13}C solid-state NMR spectra of P(SBMA-*co*-AA) copolymer (1:1 molar ratio of SBMA: MAA) and (b) polymer blend (1:1:1 molar ratio of SBMA: MAA: 4VP); (c) SAXS profiles of copolymer (MAA2) and polymer blends containing P4VP and P(SBMA-co-MAA) copolymers at 25°C; (d) polymer blend MAA5-P4VP5 (60K) at various temperature.

We further carried out SAXS experiments to track phase separation of the blend system at various temperature (**Figure 2.4b**). Once heated from 40 °C to 100 °C, the SAXS profiles show the emergence of a new peak with increasing intensity associated with a larger correlation length (~ 8.5 nm), suggesting that there is an increasing phase separation. It could be explained by the disruption of H-bonding and thus gradual increase of immiscibility. Further heating to 140 °C resulted in the disappearance of the newly formed peak, most likely due to the "order-disorder" transition that is commonly associated with

the change of temperature-dependent Flory-Huggins parameter (it is beyond the scope of this work to make quantitative analysis). However, after cooling to room temperature, the SAXS profile are also identical to the one before heating, mostly likely due to the recovered H-bonding and therefore miscibility.

Based on these results, a proposed microstructure model is illustrated in **Figure 2.1**, where chains of soybean copolymer and P4VP are favorably entangled, facilitated by supramolecular interactions between carboxylic acid groups in the copolymer and pyridine groups in P4VP. The formation of H-bonding based physical networks can dissipate stress from one macromolecule to another, thus potentially changing physical properties over the viscoelastic homopolymers. Varying the compositions of H-bonding moieties and chain flexibility could allow for tailorable bioplastics that have mechanical improvement compared to soybean oil-based homopolymers.

Mechanical properties

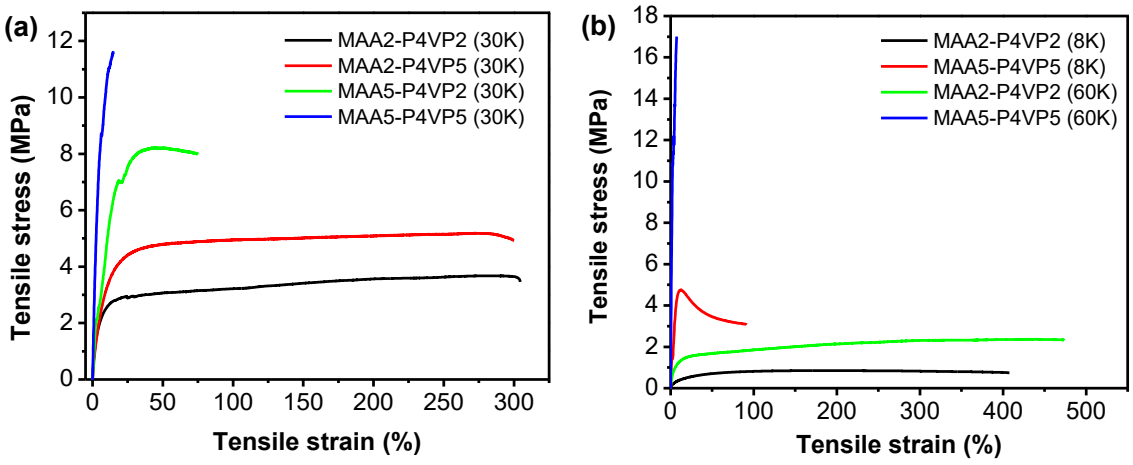

Figure 2.5. Stress-strain curves of polymer blends with variation in compositions: (a) Variation in H-bonding fractions; (b) Variation in molecular weight of P4VP.

A major goal of this work was to demonstrate that supramolecular chain entanglement could be tuned for direct control of mechanical properties. By changing chemical compositions, including the level H-bonding, chain wrapping M_n, and chain flexibility, the direct effect of variations in macromolecular composition on thermomechanical properties can be elucidated.

We first chose P4VP with M_n = 30,000 Da as a model H-bonding acceptor polymer for making polymer blends, as this molecular weight is close to M_e of P4VP. To examine the effect of H-bonding components on mechanical properties of polymer blends, we varied the overall weight ratios of H-bonding monomeric units, which are maintained ≤ 10wt% in order to maximize the sustainable component of soybean (**Table 2.3**, **Figure 2.5a**). Via increasing H-bonding weight fractions from 4% to 10% with MAA : 4VP at 1:1, the tensile strength increased from 3.6 MPa to 11.6 MPa, while the strain at break decreases from 300% to 14%, indicating the dramatic impact of H-bonding on the blends. In addition, a series of dynamic mechanical analysis (DMA) shows that blends with higher H-bonding content (10 wt%) had the highest storage modulus at 25 ^{o}C (**Figure 2.7a**), consistent with the tensile tests. However, with the same total fractions of H-bonding components (**MAA5-P4VP2 (30K)** vs. **MAA2-P4VP5 (30K)**), the more the MAA (**MAA5-P4VP2 (30K)**), the stronger the blend. This could be partially due to the existence of intrinsic H-bonding among carboxylic acid units, while 4VP units do not possess.

Table 2.3. Mechanical properties of H-bonded polymer blends with varied molecular weight of P4VP. All blends use the following naming system: the copolymer name indicating the acid monomer and its weight fraction in number (MAA2 and MAA5) and P4VP following by a number indicating its weight fraction. The number in parenthesis refers to as the molecular weight P4VP.

Sample Code (wt% in Number)	M_n (Da) (P4VP)	T_g (°C)[a]	Stress at Break (MPa)	Strain at Break (%)	Toughness (MJ/m^3)	Storage Modulus at 25°C (MPa)
MAA2-P4VP2	8,000	19	0.7 ± 0.03	408 ± 9	3.2 ± 0.3	8.6
MAA2-P4VP5		22	0.7 ± 0.05	391 ± 14	2.6 ± 0.3	--
MAA5-P4VP2		38	5.1 ± 0.3	18 ± 2	0.6 ± 0.1	--
MAA5-P4VP5		42	3.1 ± 0.2	91 ± 13	3.3 ± 0.1	199
MAA2-P4VP2	30,000	20	3.6 ± 0.05	300 ± 13	10.1 ± 0.3	51
MAA2-P4VP5		23	5.1 ± 0.1	290 ± 9	14.5 ± 0.3	--
MAA5-P4VP2		39	8.0 ± 0.4	75 ± 2	5.3 ± 0.1	--
MAA5-P4VP5		43	11.6 ± 0.3	14 ± 0.5	1.2 ± 0.0	202
MAA2-P4VP2	60,000	20	2.3 ± 0.02	474 ± 22	9.9 ± 0.4	31
MAA2-P4VP5		24	4.7 ± 0.05	267 ± 14	11.1 ± 0.2	--
MAA5-P4VP2		39	12.0 ± 0.4	16 ± 0.5	1.2 ± 0.0	--
MAA5-P4VP5		43	17.0 ± 0.9	7 ± 0.2	0.8 ± 0.0	390

[a] T_g values were obtained via DSC (2nd heating cycle).

We then explored two other P4VP homopolymers with different molecular weight: M_n = 8,000 Da and M_n = 60,000 Da, which are respectively below and above the M_e of P4VP. In the case of M_n << M_e, the blends with both low and high fractions of H-bonding components exhibited very low tensile strength (< 3-5 MPa, **Figure 2.5b**). The storage

modulus of these blends at 25 °C was low for all samples (< 200 MPa, **Figure 2.7a**). However, when the molecular weight of P4VP is significantly higher than its M_e, the blend with the highest H-bonding fraction (**MAA5-P4VP5 (60K)**) became much more rigid. It has an impressive 17MPa of tensile strength. This value is substantial, given the simplicity of processing and easy availability of materials. Additionally, this blend sample also exhibited the highest storage modulus of 390 MPa at 25 °C. Under low fraction of H-bonding components (4 wt%), this blend system with **P4VP-60** did not show much difference with those using low molecular weight P4VP (**MAA2-P4VP2 (8K)** vs. **MAA2-P4VP2 (60K)**). In both cases, only soft and partially elastic bioplastics were obtained. Additionally, DMA tests indicated that all samples underwent complete slippage at high temperature and never reached a rubbery plateau.

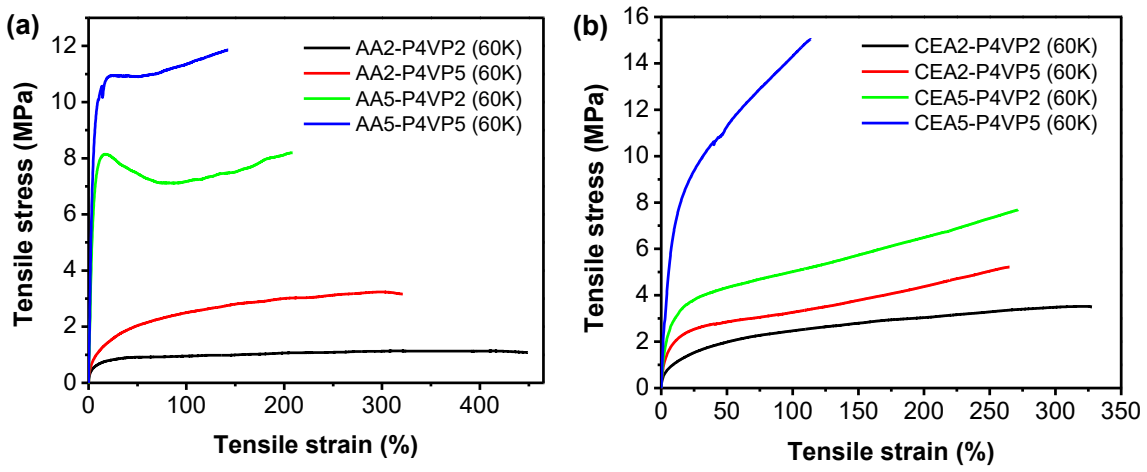

Figure 2.6. Stress-strain curves of polymer blends with variation in acid monomers used as H-bonding donors: (a) AA copolymers; (b) CEA copolymers.

Given the initial investigation, we concluded that the presence of highly entangled P4VP (high M_n) could serve as efficient chain wrapping. We then focused on the use of P4VP with M_n = 60,000 Da for further studies. In next steps, we considered to tune the

compositions of H-bonding donors: the structures of acids. PAA is much more elastic than PMAA. The blends with MAA as H-bonding donors are rigid, but very brittle. We hypothesized that with the introduction of acrylic acid-type donors, it is possible to prepare rigid and tough bioplastics. **Table 2.4** lists mechanical properties of another set of blend systems with AA as co-monomer unit with soybean monomer.

Table 2.4. Mechanical properties of H-bonded polymer blends with varied acid monomers. All blends use the following naming system: the copolymer name indicating the acid monomer and its weight fraction in number (AA2, AA5, CEA2, or CEA5) and P4VP following by a number indicating its weight fraction. The number in parenthesis refers to as the molecular weight P4VP.

Sample Code (wt% in Number)	M_n (Da) (P4VP)	T_g (°C)[a]	Stress at Break (MPa)	Strain at Break (%)	Toughness (MJ/m^3)	Storage Modulus at 25°C (MPa)
AA2-P4VP2	60,000	-2	1.1 ± 0.01	433± 5	4.6 ± 0.4	35
AA2-P4VP5		1	3.2± 0.1	315± 11	8.5 ± 0.2	--
AA5-P4VP2		3	8.2± 0.2	208± 2	14.4 ± 0.2	--
AA5-P4VP5		8	11.9± 0.5	143± 4	15.5 ± 0.1	280
CEA2-P4VP2	60,000	-4	3.5 ± 0.05	328 ± 13	8.9 ± 0.2	95
CEA2-P4VP5		-1	7.7 ± 0.5	272 ± 9	9.6 ± 0.0	--
CEA5-P4VP2		1	10.8 ± 0.3	238 ± 7	14.9 ± 0.0	--
CEA5-P4VP5		5	15.0 ± 0.2	112 ± 3	12.7 ± 0.1	140

[a] T_g values were obtained via DSC (2nd heating cycle).

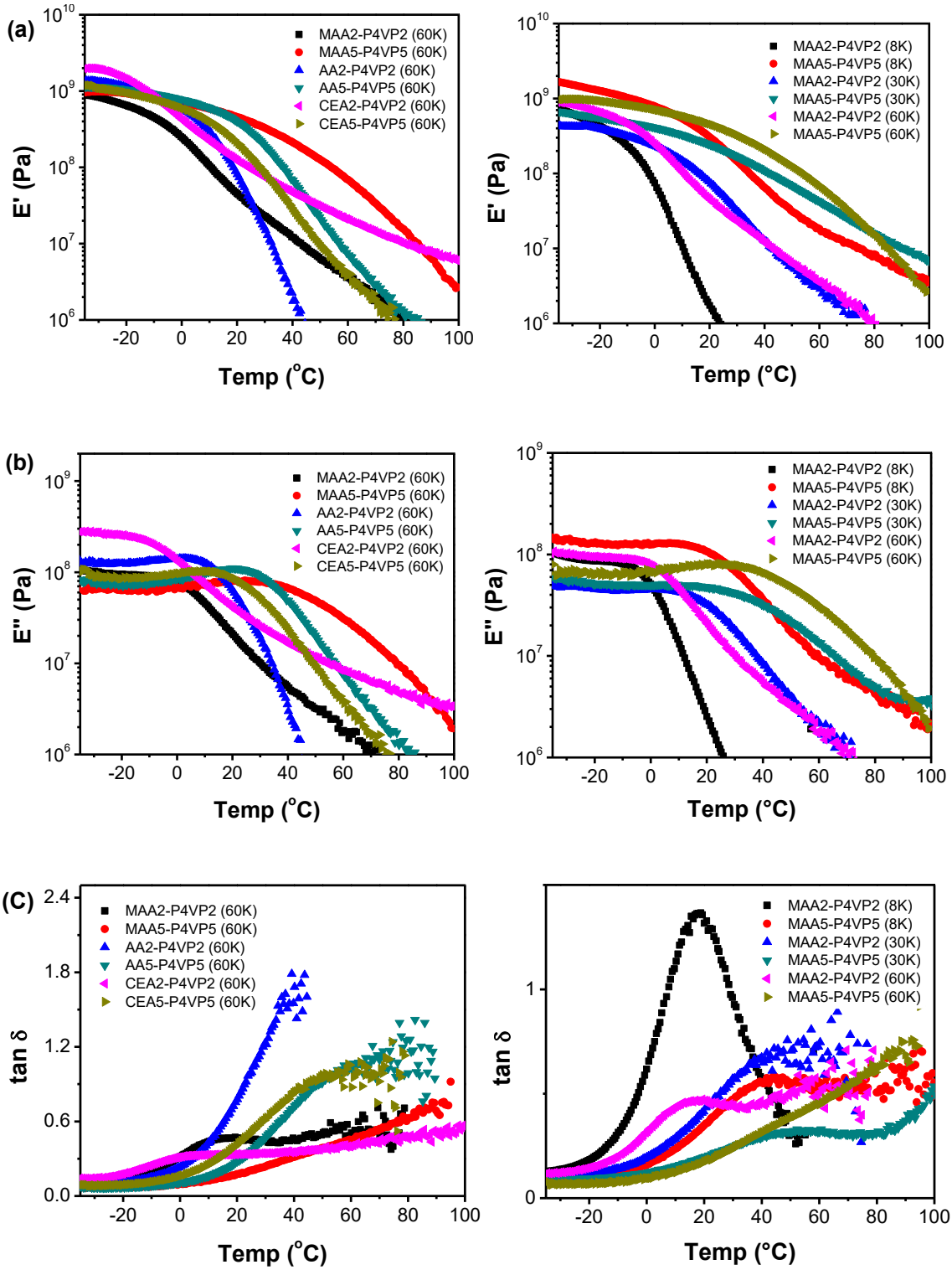

Figure 2.7. DMA curves of polymer blends with various compositions of copolymers and P4VP: (a) storage modulus; (b) loss modulus; (c) tan delta.

According to differential scanning calorimetry (DSC), the T_gs (-2 – 4 ^oC) in new copolymers P(SBMA-*co*-AA) are much lower than those (19 – 35 ^oC) in P(SBMA-*co*-MAA) with acid donors in the range of 2-5wt%. In the blend with P4VP (60K), a low fraction of H-bonding components (i.e. 4wt% in **AA2-P4VP2**), only a soft and elastic polymer was obtained (**Figure 2.6a**). When the fraction increases to 10wt%, the blend has tensile strength and strain-at-break respectively at ~12 MPa and ~140%. In addition, it was observed with almost 20-time increase in toughness compared with an equivalent blend using MAA (15.5 vs. 0.8 MJ/m^3).

Given the long pendant fatty chains on SBMA units, there was a concern whether the small AA units could be deeply surrounded by SBMA, leading to insufficient H-bonding interactions between the acid and pyridine groups.[124] To overcome such steric hindrance, a longer acid monomer, CEA, was used. This copolymer, P(SBMA-*co*-CEA), would be the softest of the three acid systems due to its ductile backbone and a longer, flexible side chain. It turned out that this set of blend systems showed enhanced toughness (**Figure 2.6b**), especially when the fractions of H-bonding components are low. A blend with only 4wt% of CEA and 4VP possesses tensile strength as high as 3.5 MPa, about three times of the AA-based blend system. A similar increase in mechanical properties was observed by DMA for this sample, which has storage modulus of ~100 MPa, the highest among all blends with 4 wt% H-bonding components. For the blend with 10wt% H-bonding components (**CEA5-P4VP5 (60K)**), it displayed as a tough and elastic bioplastic, with tensile strength and strain-at-break respectively at ~15 MPa and ~112%.

Self-Healing Properties

Reversible bonding, including H-bonding, has been utilized extensively in self-healing polymeric systems.[79, 127-129] Due to the presence of supramolecular polymer networks in the blends, self-healing properties were expected. To test the self-healing of these blends, films were placed into an oven at 50 °C, above the T_g of these materials and a temperature at which the H-bonding is in the process of weakening (from SAXS data). Optical microscopy was used to monitor the self-healing. Images were taken directly every hour until full healing was observed (**Figure 2.8**).

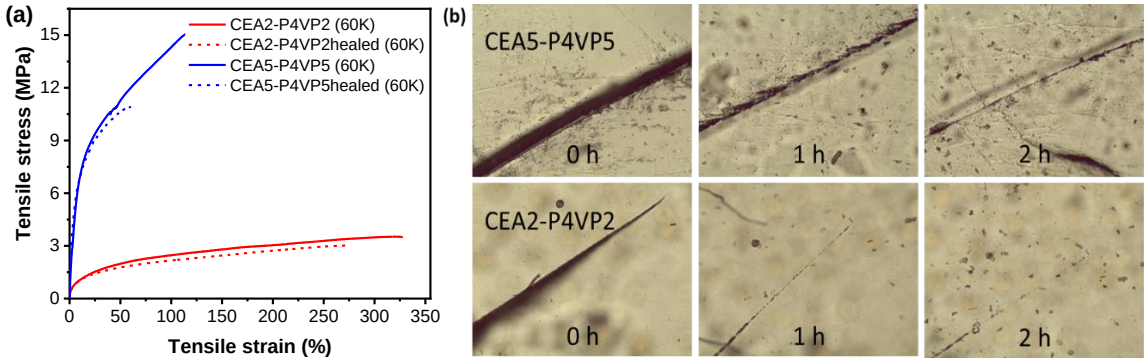

Figure 2.8. Self-healing of polymer blends: (a) Stress-strain curves of polymer blends, CEA2-P4VP2 (60K) and CEA5-P4VP5 (60K), before and after healing; (b) Optical microscopy images of polymer blends heated at 50 °C over 2 hours.

Both CEA-containing copolymers, **CEA2-P4VP2 (60K**) and **CEA5-P4VP5 (60K)**, appeared visually mended almost completely after two hours, though the former self-healed faster due to the low level of H-bonding. Additionally, tensile testing was used to evaluate the recovery of mechanical properties. Overall, both films exhibited a decrease in elasticity and toughness, observed by a decrease in tensile stress and strain at break. When tested, other films from MAA-containing and AA-containing copolymers could not mend

even under higher temperature (80 ^{o}C) and longer time (> 48 h), indicating the critical role of structures of H-bonding donors.

2.5 Discussion

Among various strategies we have developed to improve mechanical properties of biobased polymers, the "supramolecular chain entanglement" strategy is aimed to combine simplicity and robustness. It must consider both economics and sustainability. By varying a few simple structural components in the polymer blends, including carboxylic acids, molecular weight of wrapping polymers, and the level of H-bonding, the physically crosslinked supramolecular microstructures can be well controlled, leading to highly tailorable thermomechanical properties. We believe there are three major compositions that could be tuned towards manipulation of mechanical properties of the polymeric systems in this work, as illustrated in **Figure 2.9**.

*(I) The level of physical crosslinking via H-Bonding (**Figure 2.9a**):*

The goal in designing simple supramolecular H-bonding is to achieve physical crosslinking, which could overcome the poor entanglement of matrix polymers. One could utilize other H-bonding systems with much stronger association such as quadrupole H-bonding. However, the economics must be considered in the design. Additionally, the H-bonding fractions of carboxylic acids and pyridine need to be balanced. The lower fraction leads to soft blends, while the higher composition results in brittle bioplastics. In addition, the biomass component should be maximally used. In the current blend systems, a range of fractions from 4wt% to 10wt% seems to be sufficient to induce various levels of physical crosslinks that significantly enhance chain entanglements compared with simple soybean oil-derived homopolymers.

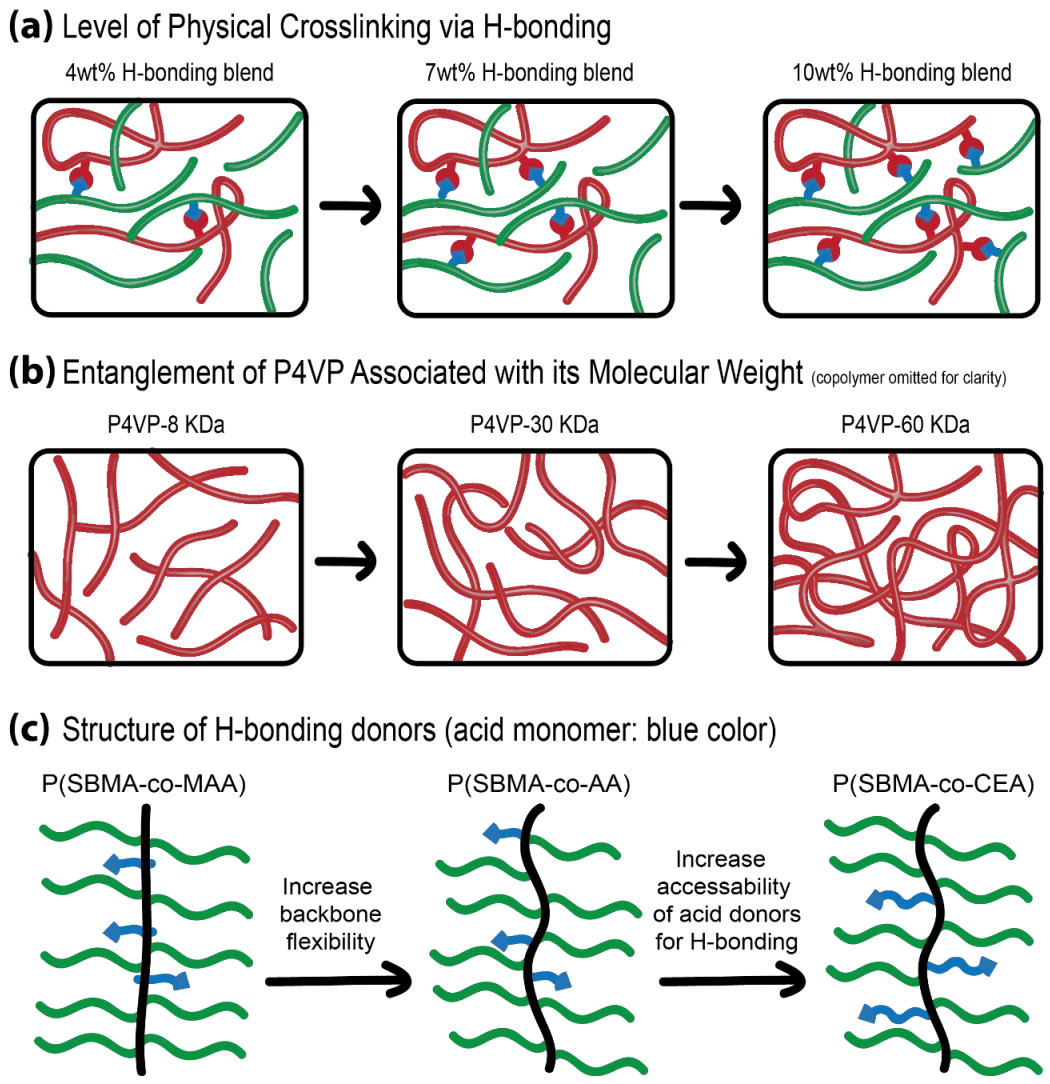

Figure 2.9. Illustration of varying chemical compositions on the molecular interactions of polymer blends: (a) level of physical crosslinking via H-bonding; (b) entanglement by P4VP by changing its molecular weight; (c) structures of H-bonding honors (acid monomers).

*(II) The molecular weight of chain-wrapping polymers (**Figure 2.9b**):*

The chain-wrapping polymer essentially serves as a type of entanglements to wrap around biobased polymers, in addition to physical crosslinking via H-bonding. It is highly preferred that both physical phenomena corroborate with each other. It is believed that P4VP could achieve both roles in this system, providing its inherent entanglement ability

and “chain wrapping” via its pyridine as a H-bonding acceptor. Therefore, the entanglement present inherently in the P4VP portion of this system is important to the mechanical properties of polymer blends. When low molecular weight P4VP (8 KDa) is used, well below its M_e (~30 KDa), the effect of chain wrapping would be minimal. Under this scenario, the possible entanglement of PSMBA polymers could be only assisted by the presence of H-bonding. As a result, mechanical properties are mostly inferior. When the M_n of P4VP is increased to 30 KDa and then 60 KDa, the increasing entanglement of P4VP and therefore chain wrapping enable the ability to dissipate stress in the blends, resulting in mechanical enhancement.

*(III) The chemical structures of H-Bonding donors (**Figure 2.9c**):*

The structures for H-bonding donors not only control the physical crosslinking, but also dictate the chain rigidity. With the use of carboxylic acids, methacrylic comonomer (MAA) significantly increases the rigidity of copolymer, P(SBMA-co-MAA), resulting in fragility of polymer blends. These blends behave like glassy thermoplastics with low strain-at-break. When the copolymer backbone is softened using acrylic comonomer (AA), blends have more flexibility for chain movement and are observed with more rubbery properties (much higher strain at break and thus increased toughness). Lastly, the softest and most ductile copolymer, P(SBMA-co-CEA), contains a soft backbone and a flexible side chain. In addition to having benefits similar to AA copolymer, the flexible side chain would facilitate more efficient H-bonding. Combining all together, CEA-containing blends exhibit higher strength, strain, and toughness under all fractions of H-bonding, compared with MAA and AA counterparts.

2.6 Conclusions

In summary, this work demonstrated a new concept of "supramolecular chain entanglement" that exploits H-bonding and physical entanglement to improve thermomechanical properties of biobased polymers. Simple radical copolymerization was employed for soybean oil-derived fatty monomer and (meth)acylic acid, the latter of which serves as H-bonding donor to interact with a pyridine-based polymer that additionally provides chain wrapping around unentangled fatty polymers. Despite poor chain entanglement of plant oil-based homopolymers, control of macromolecular compositions in these polymer blends was achieved through tuning acid donor structures, molecular weight of chain wrapping polymers and the level of H-bonding. The dual effects of H-bonding and chain wrapping enable a substantial enhancement in mechanical properties of biobased polymers. Given the availability of versatile supramolecular interactions together with the ease of synthesis and atom economics, this strategy could pave a new path to accessing high performance sustainable polymers and materials from renewable resources.

2.7 References

1. Biermann, U.; Bornscheuer, U.; Meier, M. A.; Metzger, J. O.; Schafer, H. J. Oils and Fats as Renewable Raw Materials in Chemistry. *Angew. Chem. Int. Ed.* **2011,** 50, 3854-3871.
2. Raquez, J. M.; Deléglise, M.; Lacrampe, M. F.; Krawczak, P. Thermosetting (Bio)Materials Derived from Renewable Resources: A Critical Review. *Prog. Polym. Sci.* **2010,** 35, 487-509.
3. Schneiderman, D. K.; Hillmyer, M. A. 50th Anniversary Perspective: There Is a Great Future in Sustainable Polymers. *Macromolecules* **2017,** 50, 3733-3750.

4. Wang, Z.; Yuan, L.; Tang, C. Sustainable Elastomers from Renewable Biomass. *Acc. Chem. Res.* **2017,** 50, 1762-1773.

5. Zhu, Y.; Romain, C.; Williams, C. K. Sustainable Polymers from Renewable Resources. *Nature* **2016,** 540, 354-362.

6. Lambert, S.; Wagner, M. Environmental Performance of Bio-Based and Biodegradable Plastics: The Road Ahead. *Chem. Soc. Rev.* **2017,** 46, 6855-6871.

7. Yao, K.; Tang, C. Controlled Polymerization of Next-Generation Renewable Monomers and Beyond. *Macromolecules* **2013,** 46, 1689-1712.

8. Hong, M.; Chen, E. Y. X. Chemically Recyclable Polymers: A Circular Economy Approach to Sustainability. *Green Chem.* **2017,** 19, 3692-3706.

9. Yu, J.; Wang, J.; Wang, C.; Liu, Y.; Xu, Y.; Tang, C.; Chu, F. Uv-Absorbent Lignin-Based Multi-Arm Star Thermoplastic Elastomers. *Macromol. Rapid Commun.* **2015,** 36, 398-404.

10. Gandini, A.; Lacerda, T. M.; Carvalho, A. J.; Trovatti, E. Progress of Polymers from Renewable Resources: Furans, Vegetable Oils, and Polysaccharides. *Chem. Rev.* **2016,** 116, 1637-1669.

11. Isikgor, F. H.; Becer, C. R. Lignocellulosic Biomass: A Sustainable Platform for the Production of Bio-Based Chemicals and Polymers. *Polym. Chem.* **2015,** 6, 4497-4559.

12. Cornille, A.; Auvergne, R.; Figovsky, O.; Boutevin, B.; Caillol, S. A Perspective Approach to Sustainable Routes for Non-Isocyanate Polyurethanes. *Eur. Polym. J.* **2017,** 87, 535-552.

13. Lligadas, G.; Ronda, J. C.; Galià, M.; Cádiz, V. Renewable Polymeric Materials from Vegetable Oils: A Perspective. *Mater. Today* **2013,** 16, 337-343.

14. Miao, S.; Wang, P.; Su, Z.; Zhang, S. Vegetable-Oil-Based Polymers as Future Polymeric Biomaterials. *Acta Biomater.* **2014,** 10, 1692-1704.

15. Montero de Espinosa, L.; Meier, M. A. R. Plant Oils: The Perfect Renewable Resource for Polymer Science?! *Eur. Polym. J.* **2011,** 47, 837-852.

16. Ronda, J. C.; Lligadas, G.; Galià, M.; Cádiz, V. Vegetable Oils as Platform Chemicals for Polymer Synthesis. *Eur. J. Lipid Sci. Technol.* **2011,** 113, 46-58.

17. Desroches, M.; Escouvois, M.; Auvergne, R.; Caillol, S.; Boutevin, B. From Vegetable Oils to Polyurethanes: Synthetic Routes to Polyols and Main Industrial Products. *Polymer Reviews* **2012,** 52, 38-79.

18. Wool, R. P. Polymer Entanglements. *Macromolecules* **1993,** 26, 1564-1569.

19. Ding, W.; Wang, S.; Yao, K.; Ganewatta, M. S.; Tang, C.; Robertson, M. L. Physical Behavior of Triblock Copolymer Thermoplastic Elastomers Containing Sustainable Rosin-Derived Polymethacrylate End Blocks. *ACS Sustainable Chem. Eng.* **2017,** 5, 11470-11480.

20. Ganewatta, M. S.; Ding, W.; Rahman, M. A.; Yuan, L.; Wang, Z.; Hamidi, N.; Robertson, M. L.; Tang, C. Biobased Plastics and Elastomers from Renewable Rosin Via "Living" Ring-Opening Metathesis Polymerization. *Macromolecules* **2016,** 49, 7155-7164.

21. Wang, S.; Kesava, S. V.; Gomez, E. D.; Robertson, M. L. Sustainable Thermoplastic Elastomers Derived from Fatty Acids. *Macromolecules* **2013,** 46, 7202−7212.

22. Rahman, M. A.; Lokupitiya, H. N.; Ganewatta, M. S.; Yuan, L.; Stefik, M.; Tang, C. Designing Block Copolymer Architectures toward Tough Bioplastics from Natural Rosin. *Macromolecules* **2017,** 50, 2069-2077.

23. Wang, Z.; Yuan, L.; Trenor, N. M.; Vlaminck, L.; Billiet, S.; Sarkar, A.; Prez, F. E. D.; Stefik, M.; Tang, C. Sustainable Thermoplastic Elastomers Derived from Plant Oil and Their "Click-Coupling" Via Tad Chemistry. *Green Chem.* **2015,** 17, 3806–3818.

24. Nasiri, M.; Reineke, T. M. Sustainable Glucose-Based Block Copolymers Exhibit Elastomeric and Adhesive Behavior. *Polym. Chem.* **2016,** 7, 5233-5240.

25. Shin, J.; Lee, Y.; Tolman, W. B.; Hillmyer, M. A. Thermoplastic Elastomers Derived from Menthide and Tulipalin A. *Biomacromolecules* **2012,** 13, 3833-3840.

26. Gallagher, J. J.; Hillmyer, M. A.; Reineke, T. M. Acrylic Triblock Copolymers Incorporating Isosorbide for Pressure Sensitive Adhesives. *ACS Sustainable Chem. Eng.* **2016,** 4, 3379-3387.

27. Nasiri, M.; Saxon, D. J.; Reineke, T. M. Enhanced Mechanical and Adhesion Properties in Sustainable Triblock Copolymers Via Non-Covalent Interactions. *Macromolecules* **2018,** 51, 2456-2465.

28. Yuan, L.; Wang, Z.; Ganewatta, M. S.; Rahman, M. A.; Lamm, M. E.; Tang, C. A Biomass Approach to Mendable Bio-Elastomers. *Soft Matter* **2017,** 13, 1306-1313.

29. Song, L.; Wang, Z.; Lamm, M. E.; Yuan, L.; Tang, C. Supramolecular Polymer Nanocomposites Derived from Plant Oils and Cellulose Nanocrystals. *Macromolecules* **2017,** 50, 7475-7483.

30. Brunsveld, L.; Folmer, B. J. B.; Meijer, E. W.; Sijbesma, R. P. Supramolecular Polymers. *Chem. Rev.* **2001,** 101, 4071-4097.

31. Yang, L.; Tan, X.; Wang, Z.; Zhang, X. Supramolecular Polymers: Historical Development, Preparation, Characterization, and Functions. *Chem. Rev.* **2015,** 115, 7196−7239.

32. Pollino, J. M.; Weck, M. Non-Covalent Side-Chain Polymers: Design Principles, Functionalization Strategies, and Perspectives. *Chem. Soc. Rev.* **2005,** 34, 193-207.

33. Zhang, Z. P.; Rong, M. Z.; Zhang, M. Q. Polymer Engineering Based on Reversible Covalent Chemistry: A Promising Innovative Pathway Towards New Materials and New Functionalities. *Prog. Polym. Sci.* **2018,** 80, 39-93.

34. Yang, Y.; Urban, M. W. Self-Healing Polymeric Materials. *Chem. Soc. Rev.* **2013,** 42, 7446-7467.

35. Chen, L. J.; Yang, H. B. Construction of Stimuli-Responsive Functional Materials Via Hierarchical Self-Assembly Involving Coordination Interactions. *Acc. Chem. Res.* **2018,** 51, 2699-2710.

36. Heinzmann, C.; Weder, C.; de Espinosa, L. M. Supramolecular Polymer Adhesives: Advanced Materials Inspired by Nature. *Chem. Soc. Rev.* **2016,** 45, 342-358.

37. Liu, J.; Tan, C. S.; Yu, Z.; Lan, Y.; Abell, C.; Scherman, O. A. Biomimetic Supramolecular Polymer Networks Exhibiting Both Toughness and Self-Recovery. *Adv. Mater*. **2017,** 29, 1604951.

38. Razgoniaev, A. O.; Mikhailov, K. I.; Obrezkov, F. A.; Butaeva, E. V.; Ostrowski, A. D. Supramolecular Elastomers: Switchable Mechanical Properties and Tuning Photohealing with Changes in Supramolecular Interactions. *J. Polym. Sci., Part A: Polym. Chem.* **2018,** 56, 1003-1011.

39. Deng, Y.; Wang, T.; Guo, Y.; Qiu, X.; Qian, Y. Layer-by-Layer Self-Assembled Films of a Lignin-Based Polymer through Hydrogen Bonding. *ACS Sustainable Chem. Eng.* **2015,** 3, 1215-1220.

40. Shimizu, L. S. Perspectives on Main-Chain Hydrogen Bonded Supramolecular Polymers. *Polym. Int.* **2007,** 56, 444-452.

41. Sontjens, S. H. M.; Renken, R. A. E.; Gemert, G. M. L. v.; Engels, T. A. P.; Bosman, A. W.; Janssen, H. M.; Govaert, L. E.; Baaijens, F. P. T. Thermoplastic Elastomers Based on Strong and Well-Defined Hydrogen-Bonding Interactions. *Macromolecules* **2008,** 41, 5703-5708.

42. He, Y.; Zhu, B.; Inoue, Y. Hydrogen Bonds in Polymer Blends. *Prog. Polym. Sci.* **2004,** 29, 1021-1051.

43. Lee, J. Y.; Painter, P. C.; Coleman, M. M. Hydrogen Bonding in Polymer Blends. 4. Blends Involving Polymers Containing Methacrylic Acid and Vinylpyridine Groups. *Macromolecules* **1988,** 21, 954-960.

44. Lamm, M. E.; Li, P.; Hankinson, S.; Zhu, T.; Tang, C. Plant Oil-Derived Copolymers with Remarkable Post-Polymerization Induced Mechanical Enhancement for High Performance Coating Applications. *Polymer* **2019,** 174, 170-177.

45. Yuan, L.; Wang, Z.; Trenor, N. M.; Tang, C. Amidation of Triglycerides by Amino Alcohols and Their Impact on Plant Oil-Derived Polymers. *Polym. Chem.* **2016,** 7, 2790-2798.

46. Yuan, L.; Wang, Z.; Trenor, N. M.; Tang, C. Robust Amidation Transformation of Plant Oils into Fatty Derivatives for Sustainable Monomers and Polymers. *Macromolecules* **2015,** 48, 1320-1328.

47. Coleman, M. M.; Pehlert, G. J.; Painter, P. C. Functional Group Accessibility in Hydrogen Bonded Polymer Blends. *Macromolecules* **1996,** 29, 6820-6831.

48. Convertine, A. J.; Sumerlin, B. S.; Thomas, D. B.; Lowe, A. B.; McCormick, C. L. Synthesis of Block Copolymers of 2- and 4-Vinylpyridine by Raft Polymerization. *Macromolecules* **2003,** 36, 4679-4681.

49. Coleman, M. M.; Painter, P. C. Hydrogen Bonded Polymer Blends. *Prog. Polym. Sci.* **1995,** 20, 1-59.

50. Akbey, Ü.; Graf, R.; Peng, Y. G.; Chu, P. P.; Spiess, H. W. Solid-State Nmr Investigations of Anhydrous Proton-Conducting Acid–Base Poly(Acrylic Acid)–Poly(4-Vinyl Pyridine) Polymer Blend System: A Study of Hydrogen Bonding and Proton Conduction. *J. Polym. Sci., Part B: Polym. Phys.* **2009,** 47, 138-155.

51. Sahu, P.; Bhowmick, A. K. Sustainable Self-Healing Elastomers with Thermoreversible Network Derived from Biomass Via Emulsion Polymerization. *J. Polym. Sci., Part A: Polym. Chem.* **2019,** 57, 738-751.

52. Bossion, A.; Olazabal, I.; Aguirresarobe, R. H.; Marina, S.; Martín, J.; Irusta, L.; Taton, D.; Sardon, H. Synthesis of Self-Healable Waterborne Isocyanate-Free Poly(Hydroxyurethane)-Based Supramolecular Networks by Ionic Interactions. *Polym. Chem.* **2019,** 10, 2723-2733.

53. Comí, M.; Lligadas, G.; Ronda, J. C.; Galià, M.; Cádiz, V. Adaptive Bio-Based Polyurethane Elastomers Engineered by Ionic Hydrogen Bonding Interactions. *Eur. Polym. J.* **2017,** 91, 408-419.

54. Yuan, L.; Wang, Z. K.; Trenor, N. M.; Tang, C. B. Robust Amidation Transformation of Plant Oils into Fatty Derivatives for Sustainable Monomers and Polymers. *Macromolecules* **2015,** 48, 1320-1328.

55. Lamm, M.E.; Song, L.; Wang, Z.; Rahman, Md. A.; Lamm, B.; Fu, L.; and Tang, C. *Macromolecules*, **2019**, DOI: 10.1021/acs.macromol.9b01828.

CHAPTER 3

ENHANCING BIOBASED FATTY ACID-CONTAINING POLYMERS THROUGH METAL-LIGAND COORDINATION

Lamm, M.E.; Song, L.; Wang, Z.; Lamm, B.; Fu, L.; and Tang, C. *Polym. Chem*., **2019**, Accepted Manuscript, DOI: 10.1039/C9PY01479A. Adapted from Ref. 80 with permission from The Royal Society of Chemistry.

3.1 Abstract

Biomass-based polymers show promise for the mitigation of environmental issues associated with petroleum-derived commodity polymers; however, due to poor entanglement, many of these polymers typically lack mechanical strength and toughness. Herein, we report a facile strategy utilizing metal-ligand coordination to create physical crosslinking and entanglements for plant oil-derived polymers. A series of soybean oil-derived copolymers containing a pendant acid group can be easily synthesized using free-radical polymerization. The resulting chain architecture can be controlled through supramolecular interactions to produce bioplastics with enhanced thermomechanical properties. The metal-ligand coordination in this work can be varied by changing the metal lability and the density of metal-ligand bonds, allowing for further control of properties. The final bioplastics remain reprocessable and feature good thermoplastic and stimuli-responsive properties.

3.2 Introduction

Developing renewable sources for the production of sustainable bioplastics has become increasingly important to address some of emerging issues toward a sustainable society.[1-5] However, many biomass-derived polymers face challenges like high cost and inferior performance in comparison to petroleum-sourced equivalents, limiting the competitiveness of "green" polymers on the current industrial market.[6] Plant oils have received great attention as a renewable feedstock for manufacturing polymeric materials due to their low cost and abundance.[7-18] We and others have prepared a variety of plant oil-derived vinyl polymers with diverse properties.[17-20] Several of these polymers exhibit poor thermal and mechanical properties, as observed with some other biomass polymers. Particularly,

polymers containing bulky or long pendant groups have insufficient chain entanglement (in other words, high chain entanglement molecular weight, M_e). (Meth)acrylic polymers derived from structurally bulky biomass have very high M_e, such as soybean oil (>225 kg/mol), rosin acids (>90 kg/mol) and terpenes (>30 kg/mol),[21-23] representing a significant hurdle to achieving desirable mechanical properties. Various strategies have been directed to overcome the low chain entanglements in these polymers by macromolecular engineering on chain topologies and compositions.[4, 21-45]

Dynamic bonding is gaining attention in polymer science for its use as reversible crosslinking.[46-48] For example, many dynamic covalent chemistries, such as transesterification and imine formation, are used to obtain vitrimers.[49-52] However, with a dependence on a limited number of reversible, thermally activated exchangeable bonds, vitrimers can be difficult to develop and apply to wide array of materials. Alternatively, non-covalent dynamic bonding, such as supramolecular interactions, presents a facile strategy for incorporation into polymeric materials.[53, 54] Due to their reversible nature, supramolecular interactions, including hydrogen bonding, pi-pi stacking, and metal-ligand coordination allow for unique tailoring of materials.[29, 30, 55]

Metal-ligand coordination has been widely used in preparing polymeric materials due to the versatility of metal-ligand pairing.[40, 54, 56] Through cleverly designed macromolecular engineering, ligands can be incorporated onto both polymer main and side chains.[57-60] The dynamic interaction of metal-ligand coordination allows for a simple switch between linear thermoplastics and crosslinked counterparts, providing enhancement in thermomechanical properties similar to thermoset materials.[61] Stronger bonding ligands, such as terpyridine, have even been used to synthesize ultra-high molecular weight main chain polymers

through coordination of the polymer end groups.[62] However, most syntheses for these ligands require multiple steps making them less scalable.

The use of commercially available monomers that can serve as ligands is of increasing interest to the polymer community. Monomers that include groups such as pyridines and carboxylates have shown promise.[40, 63] Specifically, bivalent transition metal complexes have gained the attention of researchers due to the diversity and variety of properties in the resulting polymer. The stability of metal-ligand complexes using bivalent metal ions of the first transition series follows the Irving-Williams order: $Mn^{2+} < Fe^{2+} < Co^{2+} < Ni^{2+} < Cu^{2+} > Zn^{2+}$, irrespective of the nature of ligands.[64] This order takes into account the ionic radii, ionic charge, and ligand field stabilization energy (LFSE) for the given metal-ligand pairing.[65, 66] Using a carboxylate bidentate ligand like acetate or propionate, Group II elements, such as calcium, are more labile than the above transition metals and are thus used extensively in soft materials like hydrogels.[56, 67, 68] Comparatively, d-block transition metals are capable of forming stronger interactions (pseudo-covalent in some cases) with ligands.[69, 70]

In this work, metal-ligand coordination is conceptualized to enhance mechanical properties of biobased polymers by introducing dynamic crosslinking thus increasing chain entanglements (**Scheme 1**). Specifically, we introduced soybean oil-derived copolymers with acid groups that can coordinate with metal ions. The metal-ligand coordination can serve as "crosslinking junctions" to dissipate stress and prevent chain slippage, leading to improved mechanical properties such as higher tensile strength and toughness.

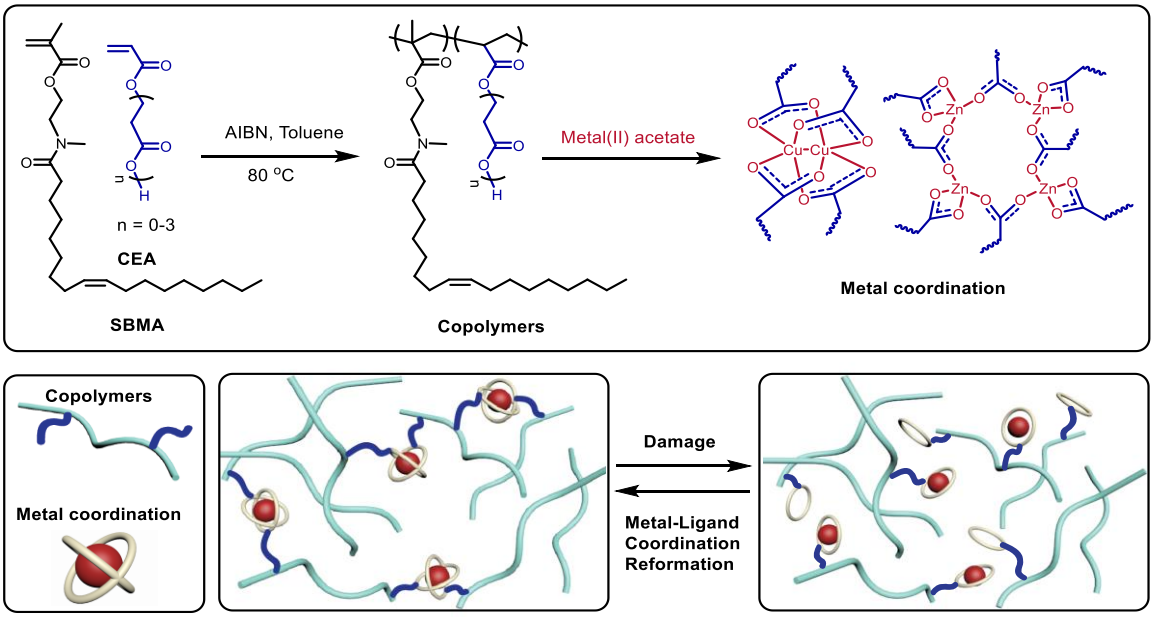

Figure 3.1. Synthesis of soybean oil-based copolymeric materials via metal-ligand coordination. Free-radical copolymerization of soybean methacrylate (SBMA) and 2-carboxy ethyl acrylate (CEA) was followed by coordination with metal ions.

3.3 Experimental

Materials

Plenish high oleic soybean oil (HOSO) was provided by Pioneer. Azobisisobutyronitrile (AIBN, 98%, Sigma Aldrich) was recrystallized from methanol twice prior to use. Soybean methacrylate (SBMA) was synthesized following a previously published procedure.[21] 2-Carboxyethyl acrylate oligomers (anhydrous, CEA), copper(II) acetate monohydrate (ACS reagent, ≥ 98%), and zinc(II) acetate dihydrate (ACS reagent, ≥ 98%) were all purchased from Sigma Aldrich. Monomers were run through basic alumina to remove inhibitors. All other reagents were from commercial sources and used as received unless otherwise mentioned.

Synthesis of SBMA Copolymers

The following procedure was used for synthesizing copolymer **CEA5**; similar procedures were followed for other copolymers containing different fractions of CEA. SBMA (7 g, 0.017 mol), CEA (0.7 g, 0.0049 mol) and AIBN (35 mg, 0.21 mmol) were placed in a 50 mL round bottom flask and dissolved in toluene (14 mL). The flask was sealed, purged with nitrogen for 15 min, and placed in an 80 ^{o}C oil bath. After 16 h, the polymer was poured into cold methanol. The resulting polymer was precipitated twice into methanol and dried for 24 h in a 50 ^{o}C vacuum oven.

Synthesis of Metal-Coordinated Copolymers

Copolymer (PSBMA-*co*-CEA) was dissolved in chloroform. Metal acetate (copper(II) or zinc(II)) was added to the solution. Methanol was added to help dissolve the metal salt. The final solution was sonicated for 5 min, degassed, and poured into a Teflon mold. The solvent was evaporated at room temperature over 72 h, 24 h under vacuum at room temperature, and 24 h under vacuum at 60 ^{o}C.

Characterization

300 MHz ^{1}H NMR spectra were recorded on a Bruker Avance III HD 300 spectrometer using $CDCl_3$ as solvent with tetramethylsilane (TMS) as an internal reference. Molecular weight and molecular weight distribution of polymers were determined by gel permeation chromatography (GPC) on a Waters system equipped with a 515 HPLC pump, a 2410 refractive index detector, and three Styragel columns (HR1, HR3, HR5E in the effective molecular weight range of 100-5000 g/mol, 500-30,000 g/mol, and 5000-500,000 g/mol, respectively) with HPLC-grade tetrahydrofuran (THF) as the eluent at 30 ^{o}C and a flow

rate of 1.0 mL/min. THF and polymer solutions were filtered through microfilters with an average pore size of 0.2 mm. The columns were calibrated against polystyrene standards. GPC samples were prepared by dissolving the sample in THF with a concentration of 5.0 mg/mL and passing through microfilters with an average pore size of 0.2 mm. Glass transition temperature (T_g) of polymers was tested through differential scanning calorimetry (DSC) conducted on a DSC 2000 instrument (TA Instruments). Samples were first heated from -70 to 200 ^{o}C at a rate of 10 ^{o}C/min. After cooling down to -70 ^{o}C at the same rate, the data was collected from the second heating scan. About 8 mg of each sample was used for the DSC test under nitrogen gas at a flow rate of 50 mL/min. Fourier transform infrared spectrometry (FTIR) spectra were taken on a PerkinElmer spectrum 100 FTIR spectrometer. Dried film samples were used for measurements. Microscopy images were taken using a Leica DM750 microscope equipped with a mounted EC3 camera. Self-healing experiments involved damaging films using a standard razor blade to cut films. A new razor blade was used for each experiment. Tensile stress-strain testing was carried out with an Instron 5543 A testing instrument. Films were prepared by casting solution (1.2 g/film) in a Teflon mold as described above. Dog-bone shaped specimens were cut from the cast film with a length of 20 mm and width of 5.0 mm. The thickness was measured prior to each measurement. Testing was done at room temperature with a crosshead speed of 20 mm/min. Five replicate samples were used to obtain an average value for each. Dynamic thermomechanical analysis (DMA) was performed by using a Q800 DMA from TA Instruments. Samples were rectangles with dimensions 12 mm length, 5 mm width, and 0.3 mm thickness. The DMA curves were obtained by scanning at a frequency of 1 Hz and a heating rate of 3 ^{o}C/min from -50 to 120 ^{o}C. Stress relaxation experiments were

conducted on DMA at temperature in the range of 35 to 75 °C. Samples were first heated to the desired temperature and equilibrated for 5 minutes. A strain of 1% was applied and stress was recorded. All the shape memory tests were carried out in a stress-controlled thin film tension mode on a NETZSCH DMA 242 instrument. Shape fixity was determined using equation 1

(1) $$R_f = \frac{\varepsilon_u}{\varepsilon_m} \times 100\%$$

where $\mathcal{E}_m$ is the strain after stretching and fixing for temporary shape, and $\mathcal{E}_u$ is the strain after removal of stress. Shape fixity ratio was calculated using equation 2

(2) $$R_{r1} = \frac{\varepsilon_r}{\varepsilon_u} \times 100\%$$

where $\mathcal{E}_r$ is the strain after recovery from temporary shape.

3.4 Results and Discussion

Preparation of Copolymers with Metal-Ligand Coordination

Both soybean methacrylate monomer (SBMA) and its polymer (PSBMA) have been reported previously.[4, 14, 15, 71] The details of synthesis and characterization are provided in experimental and supporting information. PSBMA is a soft polymer with low glass transition temperature (T_g = –6 °C). In this work, a library of soybean oil-based copolymers was synthesized via free radical copolymerization of SBMA with carboxylic acid-containing comonomers (**Figure 3.1**). Acid comonomers were chosen for promoting the metal-ligand coordination. Instead of simple acrylic acid or methacrylic acid that could be embedded within the long fatty chain of PSBMA, we chose 2-carboxyethyl acrylate (CEA) due to the presence of pendent -$CH_2CH_2CO_2$- moieties that could better facilitate acid group coordination with metal ions. The monomer is a mixture of 2-carboxyethyl acrylate

oligomers with average molecular weight of 170 Da (CH_2=$CHCO_2(CH_2CH_2CO_2)_nH$, n = 0–3).

Table 3.1. Characterization of soybean oil homopolymer and copolymers containing acid monomer CEA.

Polymer code	Wt% CEA[a]	Mole% CEA[a]	M_n (KDa)[b]	$Đ$[b]
PSBMA	0	0	43.4	1.78
CEA2	2	4.7	45.6	2.18
CEA5	5	11.2	32.9	2.64
CEA10	10	21.0	30.6	2.57
CEA20	20	37.4	30.5	2.61

[a]Weight and molar content of CEA were calculated via ^{1}H NMR. [b]Molecular weight (M_n) and molecular weight distribution ($Đ$) were characterized via GPC.

Complete characterization of these copolymers is summarized in **Table 3.1**. Each copolymer is labeled as "CEA" followed with the weight fraction of CEA in the copolymer. All copolymers have molecular weight (M_n) in the range of 30,000-45,000 Da with similar dispersity ($Đ$), regardless of compositions. Copolymers were first dissolved in chloroform and then added with metal salt. Depending on the amount of salt in the solution, the addition of methanol improved solubility (<10% by volume). Resultant metal salt-copolymer solutions displayed an increased viscosity, implying the formation of metal-ligand coordination. After drying, all copolymer films were transparent. It is also worth noting that good miscibility was achieved with no formation of metal ionic clusters, despite incorporating high polarity metal salts in such a non-polar matrix.

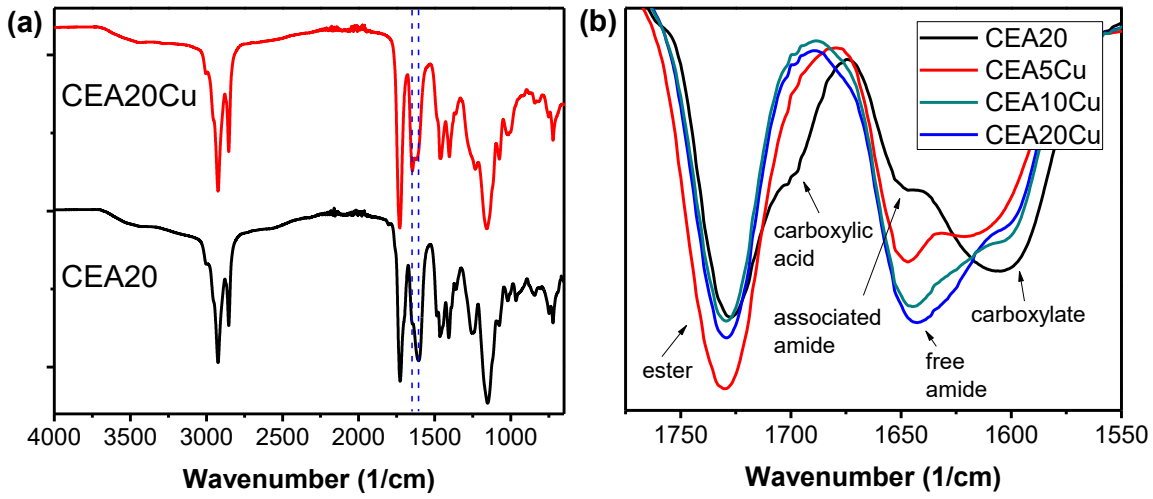

Figure 3.2. FTIR spectra of (a) CEA20 and CEA20Cu; (b) C=O stretching peaks in different functional groups between 1775-1550 cm-1 in samples CEA20, CEA5Cu, CEA10Cu, and CEA20Cu.

Fourier transform infrared (FTIR) spectroscopy was used to track the metal-ligand coordination between salts and copolymers (**Figure 3.2**). When acid groups in a copolymer are coordinated with metal ions, there is only a carboxylate C=O stretching peak present (1604 cm^{-1}), compared with an additional carboxylic acid C=O stretching peak (1699 cm^{-1}) in the copolymers. Additionally, there is a slight shift in the amide C=O stretching peak. In the copolymer, the amide is associated with the acid monomers by hydrogen bonding, with a peak at 1649 cm^{-1}. However, after the metal ion coordinates with acid, these amides are freed, as indicated by the peak shift to 1643 cm^{-1}. Copolymers are referred to by the names in **Table 3.1**. When coordinated with metal, it is labeled with the metal after the copolymer name, i.e. **CEA10Cu** is a copolymer of CEA10 coordinated with copper. Metal-coordinated copolymers contain an optimized metal-to-acid ratio of 1:2, unless otherwise noted.

Thermomechanical Properties

The introduction of metal-ligand coordination in copolymers resulted in a change of thermal properties, e.g. glass transition temperature. Compared with homopolymer **PSBMA**, copolymers with CEA were observed with a small increase in T_g (from -6 to between -5 – 1 ^{o}C). When coordinated with metal ions, a significant increase in T_g was observed (66 ^{o}C and 69 ^{o}C for **CEA20Cu** and **CEA20Zn** respectively).

Tensile test and dynamic mechanical analysis (DMA) were performed to understand the effect of metal-acid coordination on mechanical properties. Firstly, tensile testing was used to investigate the optimized metal-acid ratio for all copolymers with copper and zinc ions (**Figure 3.3a and 3.3b**). The optimal metal-acid ratio was determined as 1:2 for both metals, which led to the best ductility and toughness. It is worth noting that a 1:2 ratio is consistent with the metal-ligand ratios in copper(II) acetate and zinc(II) acetate salts, $Cu_2(CH_3COO)_4$ and $Zn_4(CH_3OO)_8$.[72] Alternatively, adjusting the ratios could be utilized to tailor properties toward either elasticity or stiffness. Increasing metal content resulted in reduction of strain and toughness, but increase in strength and stiffness. For example, an increase from 1:2 to 1:1 in **CEA10Zn** reduced strain from 101.5% to 32% and toughness from 5.95 MJ/m^3 to 3.1 MJ/m^3, but did result in an increase in tensile strength from 7.9 MPa to 10.5 MPa and Young's modulus from 13 MPa to 185 MPa, an over ten times increase (**Figure 3.3b**). Whereas at lower metal ratios, e.g. 1:3, there was a sacrifice in tensile strength with a reduction from 7.9 to 4 MPa that accompanies an increase in elasticity from 101% to 158% for **CEA10Zn**.

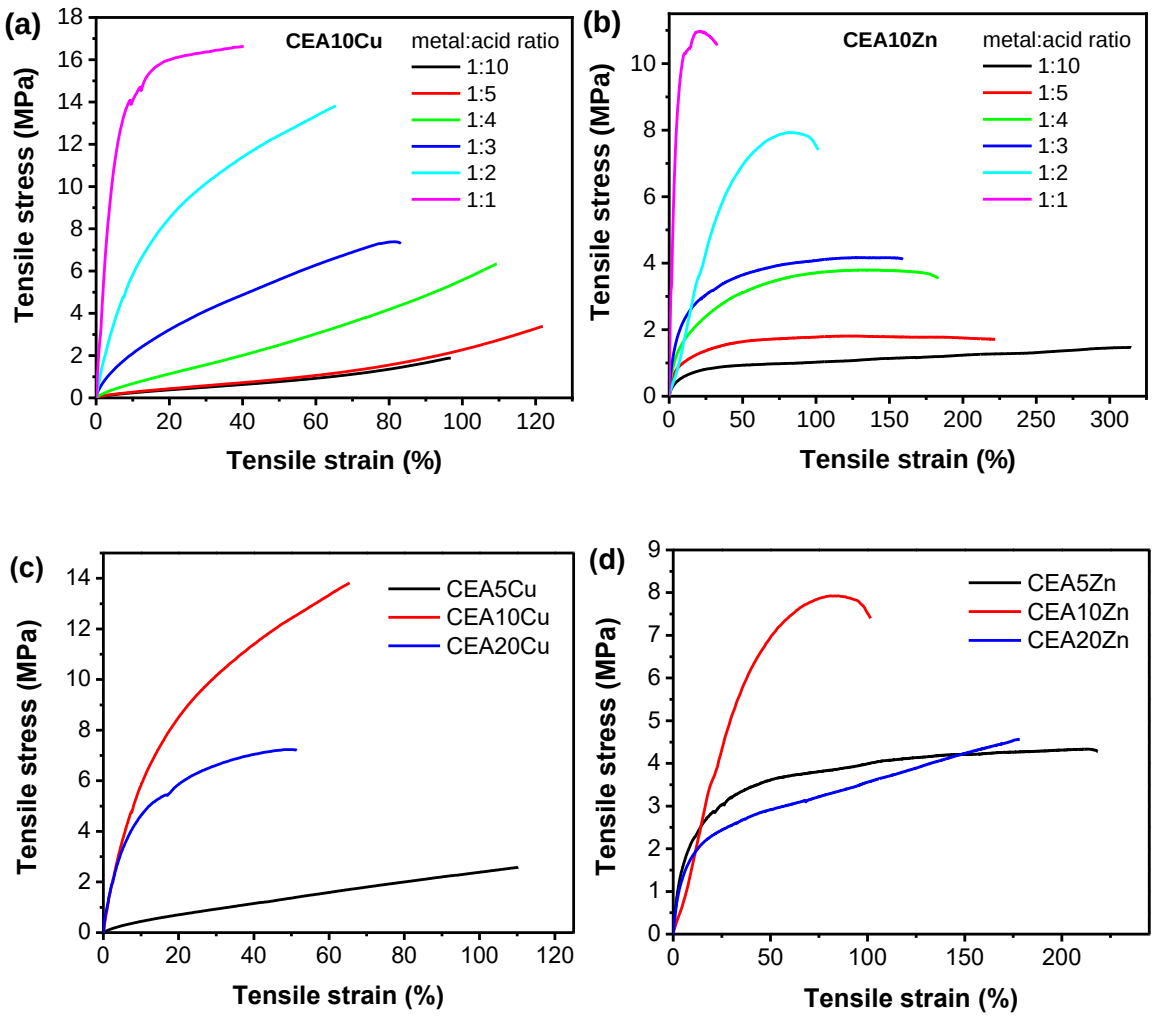

Figure 3.3. Stress-strain curves of metal-ligand coordinated copolymers using various metal-to-ligand ratios in copolymer CEA10 coordinated with (a) copper and (b) with zinc; Copolymers with various contents of acid coordinated with (c) copper and (d) zinc, with a metal-to-ligand ratio of 1:2.

Metal ions play a critical role in dictating properties of copolymers (**Table 3.2**). Copolymers with copper ion were typically stiffer at higher contents of acid. Tensile stress was much higher for copper-coordinated copolymers (13.8 MPa and 7.2 MPa for **CEA10Cu** and **CEA20Cu** respectively), whereas zinc-coordinated copolymers have only about half the values (7.9 MPa and 4.5 MPa for **CEA10Zn** and **CEA20Zn** respectively).

Table 3.2. Mechanical properties from tensile testing of metal-ligand coordinated copolymers with a metal-to-acid ratio of 1:2.

Polymer	Tensile stress (MPa)	Tensile strain (%)	Young's Modulus (MPa)	Toughness (MJ/m^3)
CEA5Cu	4.3 (± 0.1)	217.5 (± 13)	4.4 (± 0.01)	6.17 (± 0.1)
CEA10Cu	13.8 (± 1)	65.4 (± 4)	59.6 (± 0.3)	6.31 (± 0.01)
CEA20Cu	7.2 (± 0.5)	51.3 (± 5)	47.4 (± 0.1)	2.96 (± 0.4)
CEA5Zn	4.3 (± 0.2)	215.7 (± 22)	19.3 (± 0.01)	8.28 (± 0.2)
CEA10Zn	7.9 (± 0.6)	101.5 (± 12)	13.0 (± 0.05)	5.95 (± 0.07)
CEA20Zn	4.5 (± 0.1)	177.6 (± 10)	16.1 (± 0.01)	5.93 (± 0.1)

At lower levels of metal-ligand coordination, zinc coordination resulted in stiffer materials. As shown in **Figure 3.3c** and **3.3d**, copolymers with 5 wt% of acid content, **CEA5Zn** and **CEA5Cu**, have similar tensile stress (~4 MPa) and strain (~215%); however, the zinc sample is significantly stiffer with a Young's modulus of 19.3 MPa, over 4 times that of **CEA5Cu** (4.4 MPa). These differences in properties can be explained by the structure and strength of the coordination systems. Copper(II) acetate forms a smaller complex between two copper groups containing a central Cu-Cu bond, resulting in a stronger pseudo-covalent bond.[72] This system thus interacts better with a higher ligand density, as the final metal-ligand coordination requires a close proximity of ligands to arrange properly. Alternatively, zinc(II) acetate has a very large cage-like structure between four zinc groups.[73] When ligand density is low, as is the case in **CEA5Zn**, zinc ions are able to bridge the gap between propionate-type groups more easily than copper.

Additionally, zinc forms weaker metal-ligand bonds than copper, behaving similarly to traditional supramolecular bonds.[64] Importantly, this difference in bond strength affects both thermomechanical properties and stimuli-responsive behavior of these systems, which is discussed later.

On the other hand, the trend of toughness is difficult to predict. There are two potential issues: (1) the increase of metal-ligand coordination enhances strength, but also simultaneously decreases the strain, which may justify the trend when complexes increase from 5% to 10%; (2) further increase of the fraction of metal-ligand complexes would encounter miscibility challenges, as such increase should have a limit (20% complexes may have such an issue).

DMA was used to further explore the viscoelastic properties of copolymers (**Figure 3.4**). Storage modulus for all films was above 1 MPa at 25 ^{o}C, indicating good mechanical properties would be maintained at room temperature. However, there was storage modulus failure with no rubbery plateau observed for copolymers with the decreased metal-ligand coordination (**CEA5Cu**, **CEA5Zn** and **CEA10Zn**). Samples began to melt as they underwent complete chain slippage, occurring at around 80 ^{o}C for both sets of copolymers. Overall, the metal-ligand coordination imparted copolymers with tough and elastic properties.

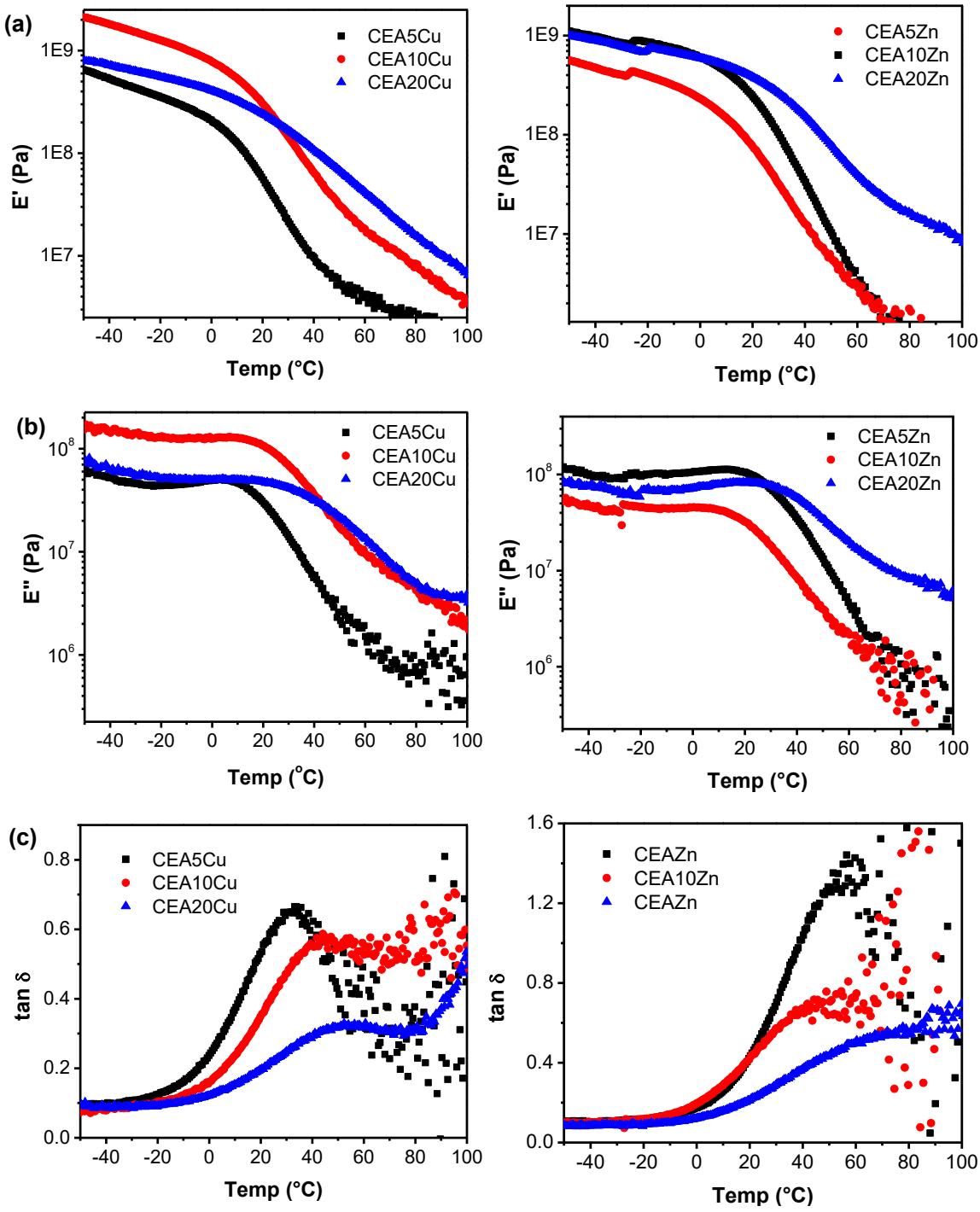

Figure 3.4. DMA spectra of metal-ligand coordinated copolymers with a metal-to-acid ratio of 1:2, (a) storage modulus, (b) loss modulus, and (c) tan delta.

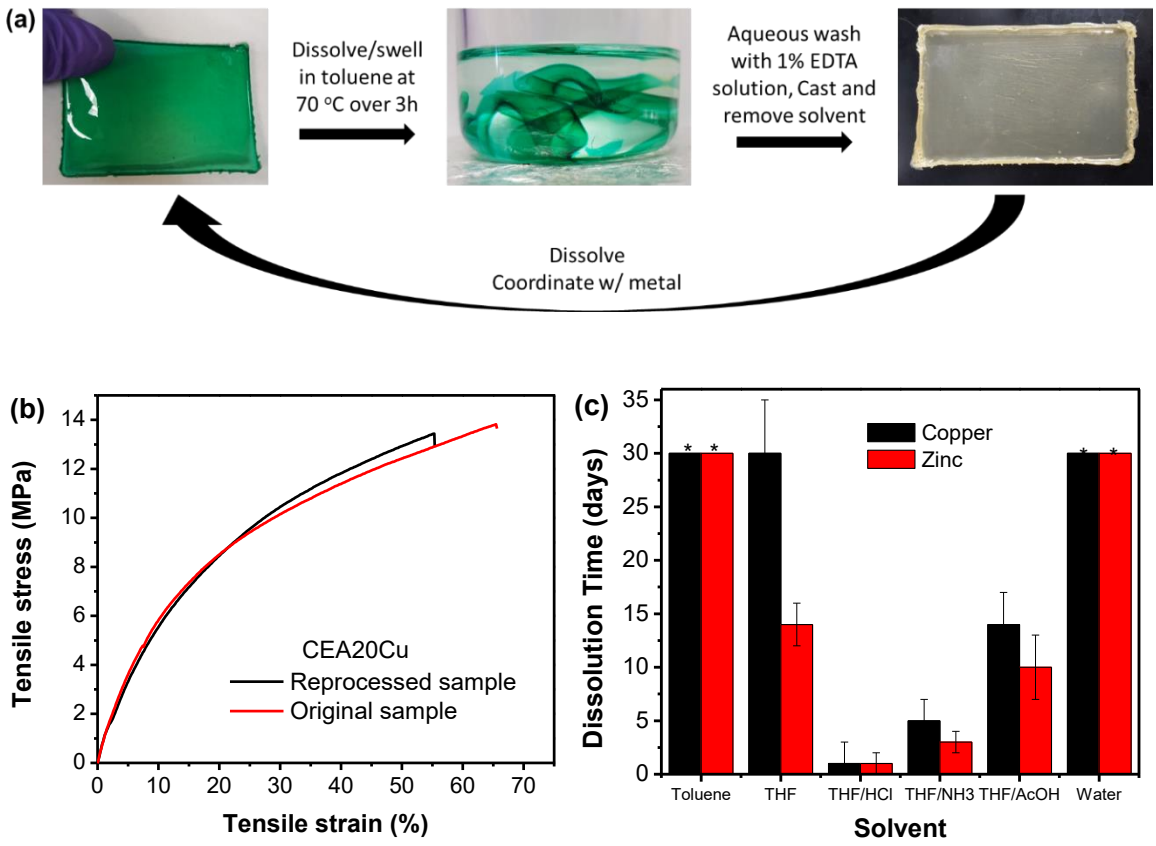

Figure 3.5. (a) Reprocessing of copolymers by dissolving polymer, removing metal using EDTA, and reprocessing into new samples. (b) Tensile curve of reprocessed sample after complete salt-removal and repeated complexation. (c) Dissolution of copper and zinc coordinated copolymers in a variety of solvents. Films noted with an asterisk did not dissolve after 30 days.

Due to the dynamic non-covalent interactions of metal-ligand coordination, the copolymers should remain processable. The ability to be reprocessed and remolded into new samples is a hallmark trait of thermoplastics and an important attribute to many industrially relevant polymeric materials. As the metal-ligand coordination in our two systems is very different in coordination strength, we expected to see differences in their reprocessability. Overall, copper films took longer to dissolve and only dissolved in coordinating solvents, particularly when heated or in presence of other ligands (HCl, NH_3)

(**Figure 3.5**). Zinc films, on the other hand, dissolved much faster into solvents. Once dissolved, films with either metal could be directly recast into films with similar properties. It was also possible to dissolve films, extract the metal using EDTA, and reprocess them into new samples; either as plain copolymer films or samples featuring varying metals or ratios (**Figure 3.5a**). The ability to remain reprocessable with good mechanical properties and the capacity to recycle the metal-ligand coordination show promise for tailoring this approach to desirable applications and helping mitigate market dependence on current petroleum-sourced thermoplastics.

Stimuli-Responsive Properties of Copolymers

With the presence of physical crosslinking, it was expected that these copolymers may exhibit stimuli-responsive behavior. The reversible nature of the metal-ligand coordination would allow the breakage and reformation the metal-acid bond under thermal (increased temperature) or chemical (solvent) stress. Before testing stimuli-responsive properties, DMA was used to determine bond lability.

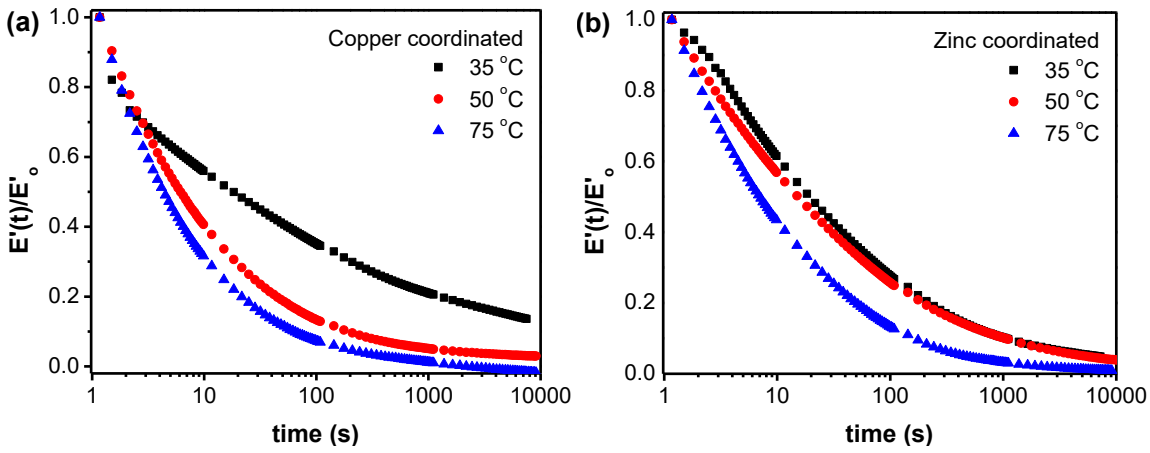

Figure 3.6. Stress relaxation experiments of (A) CEA20Cu and (B) CEA20Zn at varying temperatures.

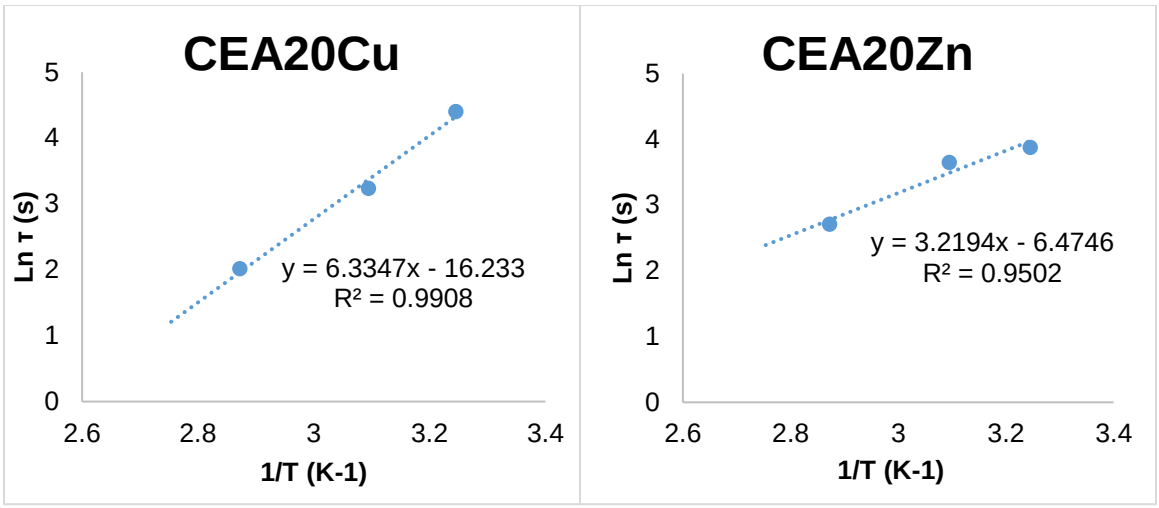

Figure 3.7. Stress relaxation time (τ) vs. 1/T for (a) CEA20Cu and (b) CEA20Zn. Follows an Arrhenius law: $1/\tau = 1/\tau_o \; e^{(-E_a/RT)}$, where τ_o is constant (s), E_a is activation energy (J/mol), R is the ideal gas constant (8.314472 J/mol*K), and T is temperature (K). Activation energy is determined from the slope E_a/R.55 For copper this is 52.7 kJ/mol, while for zinc this is 26.8 kJ/mol.

Stress relaxation studies were performed in a tension mode, utilizing thermally induced polymer plasticity to track the ability of a sample to recover over time (**Figure 4**). Both samples were observed with a similar initial rate of relaxation due to the presence of dynamic coordinated crosslinks. **CEA20Zn** was able to undergo full stress relaxation at all three temperature, whereas **CEA20Cu** could not undergo full relaxation until starting at 50 ^{o}C. The recovery time at a range of temperature follows a Maxwell behavior and can be plotted using an Arrhenius relationship to determine activation energy – i.e., the energy required to break and reform the dynamic bonds (**Figure S9**). As expected by its difficulty reaching full relaxation at lower temperature, copper-coordinated films were stronger and required more energy to break the bond (~56 kJ/mol) than zinc-containing films (~26 kJ/mol) (**Figure 4**). Films with higher metal-ligand coordination density also took longer to fully stress relax, as more dynamic bonds needed to be broken and reformed in these samples (**Figure S10**). Unfortunately, due to the viscoelastic nature of the copolymers,

similar tension-based stress relaxation studies could not be performed on the copolymers for comparison.

Self-healing studies were performed on metal-coordinated copolymers. As discussed previously, the zinc bonds are significantly more labile than copper and are therefore expected to show better self-healing behavior, which was confirmed as zinc films displayed a complete self-healing in 2-5 hours at 70 °C. Optical microscopy was used to confirm that self-healing occurred, while tensile testing revealed no mechanical loss (**Figure 3.8**).

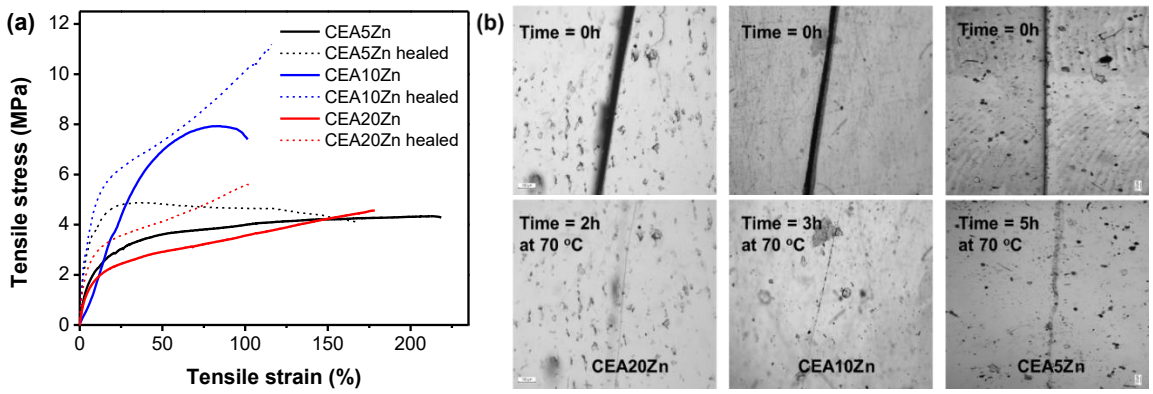

Figure 3.8. (a) Stress-strain curves of CEA5Zn, CEA10Zn, and CEA20Zn films before-cut and after-healed at 70 °C for 5 h. (b) Optical microscopy images of these films comparing cut film samples and self-healed film surfaces.

Films did see an increase in stiffness and strength, which is attributed to minor thermal crosslinking of the soybean chains. Films with higher metal-ligand density (**CEA20Zn**) were able to recover faster than those with lower density (**CEA10Zn** and **CEA5Zn**), as more bonds are present at the breakage site to allow for the reformation of necessary metal-ligand coordination. However, no self-healing was evident for copper films, even at elevated temperatures up to 120 °C where a rubbery plateau was reached. Due to the pseudo-covalent nature of the copper complex, the lack of self-healing is not surprising.[74] Copper-acetate bonds are likely too strong to break and reform on a reasonable time scale

to fully heal the materials. Additionally, the unit cell of the copper-acetate complex is significantly smaller than its zinc counterpart and needs closer proximity to ligands to reform, potentially limiting healing on a macroscale deformation such as ours.

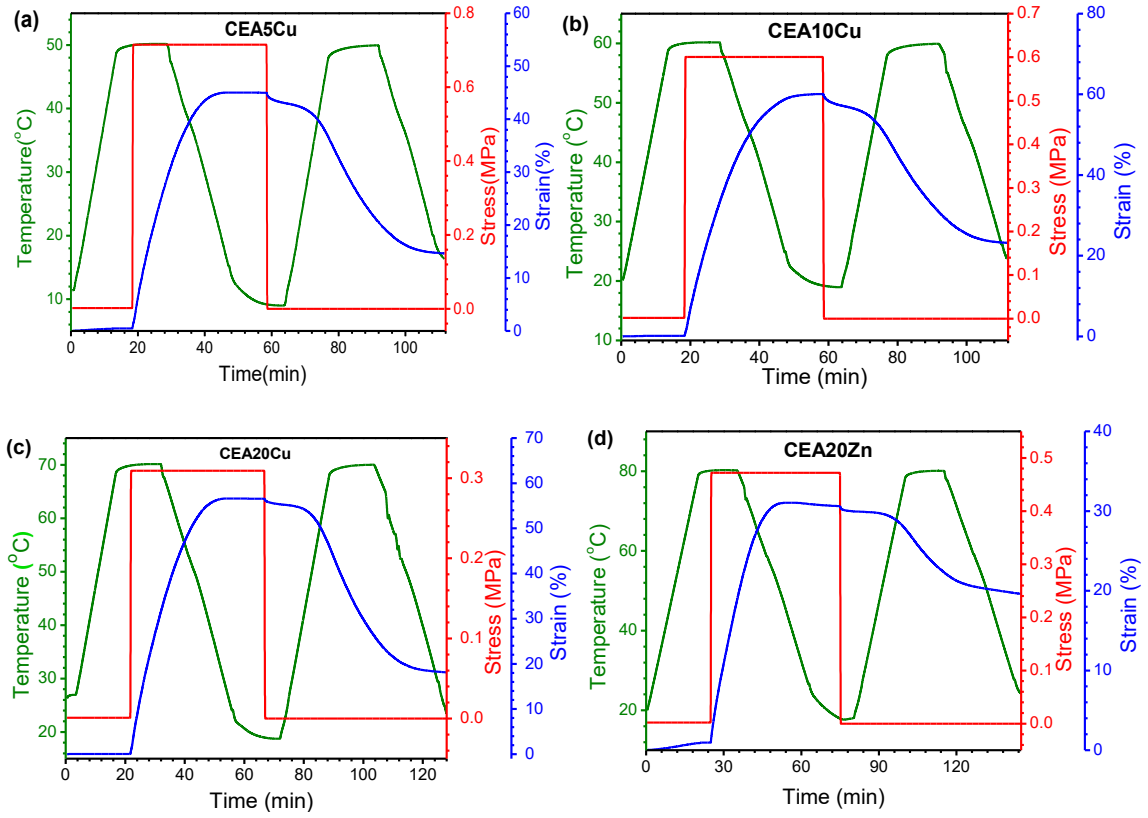

Figure 3.9. Dual (stress- and temperature-) programmed shape memory testing of (a) CEA5Cu, (b) CEA10Cu, (c) CEA20Cu, and (d) CEA20Zn.

Shape memory behavior was also studied. Thermal-responsive shape memory uses two networks, a permanent network and a dynamic network.[75-77] The permanent network relies on strong (typically covalent) bonds to switch back from the temporary to permanent shape. The temporary network relies on dynamic interactions, such as supramolecular interactions, in combination with other responses such as glass transition or crystallization temperature for thermal response.[78, 79] As confirmed from the self-healing studies, the

copper-ligand coordination is strong and could serve as a permanent network, while glass transition could be used to tune the temporary shape. As zinc coordination is much weaker especially when heated, we expected that zinc films would not display good shape memory. To test the shape memory behavior of metal-coordinated copolymers, we used dual-programmed (temperature and stress) DMA (**Figure 3.9**). All samples have good shape fixity (>95%). However, these samples showed poor shape recovery (~65% for all copper films, regardless of compositions, and 35% for **CEA20Zn**).

3.5 Conclusions

In summary, we developed a facile strategy that utilizes metal-ligand coordination to overcome poor chain entanglement and obtain mechanically enhanced biobased copolymers. In this system, the metal-ligand coordination behaves as crosslinking junctions, achieving remarkable improvement in thermomechanical properties. Copper-coordinated copolymers were observed with a marked increase in tensile strength and stiffness by increasing the metal-ligand density, significantly stronger than their zinc counterparts and consistent with the stronger bonding strength as confirmed by DMA studies. This stronger bond prevented self-healing properties of the copper films. Conversely, the zinc-carboxylate bonds were determined to be much weaker, which facilitated self-healing of the polymeric films. Overall, through the control of metal-ligand density, ligand availability, and coordination strength, thermomechanical properties and resultant stimuli-responsive properties can be tuned. This strategy is facile and could be customized to other biomass polymers.

3.6 References

1. Dodds, D. R.; Gross, R. A. Chemistry. Chemicals from Biomass. *Science* **2007,** 318, 1250-1251.
2. Ragauskas, A. J.; Williams, C. K.; Davison, B. H.; Britovsek, G.; Cairney, J.; Eckert, C. A.; Frederick, W. J., Jr.; Hallett, J. P.; Leak, D. J.; Liotta, C. L.; Mielenz, J. R.; Murphy, R.; Templer, R.; Tschaplinski, T. The Path Forward for Biofuels and Biomaterials. *Science* **2006,** 311, 484-489.
3. Schneiderman, D. K.; Hillmyer, M. A. 50th Anniversary Perspective: There Is a Great Future in Sustainable Polymers. *Macromolecules* **2017,** 50, 3733-3750.
4. Wang, Z.; Yuan, L.; Tang, C. Sustainable Elastomers from Renewable Biomass. *Acc. Chem. Res.* **2017,** 50, 1762-1773.
5. Yao, K. J.; Tang, C. B. Controlled Polymerization of Next-Generation Renewable Monomers and Beyond. *Macromolecules* **2013,** 46, 1689-1712.
6. Lambert, S.; Wagner, M. Environmental Performance of Bio-Based and Biodegradable Plastics: The Road Ahead. *Chem. Soc. Rev.* **2017,** 46, 6855-6871.
7. Biermann, U.; Bornscheuer, U.; Meier, M. A.; Metzger, J. O.; Schafer, H. J. Oils and Fats as Renewable Raw Materials in Chemistry. *Angew. Chem. Int. Ed.* **2011,** 50, 3854-3871.
8. Gandini, A.; Lacerda, T. M.; Carvalho, A. J.; Trovatti, E. Progress of Polymers from Renewable Resources: Furans, Vegetable Oils, and Polysaccharides. *Chem. Rev.* **2016,** 116, 1637-1669.
9. Lligadas, G.; Ronda, J. C.; Galia, M.; Cadiz, V. Renewable Polymeric Materials from Vegetable Oils: A Perspective. *Mater. Today* **2013,** 16, 337-343.
10. Montero de Espinosa, L.; Meier, M. A. R. Plant Oils: The Perfect Renewable Resource for Polymer Science?! *Eur. Polym. J.* **2011,** 47, 837-852.
11. Can, E.; Wool, R. P.; Küsefoğlu, S. Soybean- and Castor-Oil-Based Thermosetting Polymers: Mechanical Properties. *J. Appl. Polym. Sci.* **2006,** 102, 1497-1504.

12. Andjelkovic, D. D.; Valverde, M.; Henna, P.; Li, F.; Larock, R. C. Novel Thermosets Prepared by Cationic Copolymerization of Various Vegetable Oils—Synthesis and Their Structure–Property Relationships. *Polymer* **2005,** 46, 9674–9685.

13. Luo, Q.; Liu, M.; Xu, Y.; Ionescu, M.; Petrović, Z. S. Thermosetting Allyl Resins Derived from Soybean Oil. *Macromolecules* **2011,** 44, 7149-7157.

14. Yuan, L.; Zhang, Y.; Wang, Z.; Han, Y.; Tang, C. Plant Oil and Lignin-Derived Elastomers Via Thermal Azide-Alkyne Cycloaddition Click Chemistry. *ACS Sustainable Chem. Eng.* **2018,** 10.1021/acssuschemeng.8b05617.

15. Wang, Z.; Yuan, L.; Ganewatta, M. S.; Lamm, M. E.; Rahman, M. A.; Wang, J.; Liu, S.; Tang, C. Plant Oil-Derived Epoxy Polymers toward Sustainable Biobased Thermosets. *Macromol. Rapid Commun.* **2017,** 38, 1700009.

16. Xu, S. C.; Lamm, M. E.; Rahman, M. A.; Zhang, X. Z.; Zhu, T. Y.; Zhao, Z. D.; Tang, C. B. Renewable Atom-Efficient Polyesters and Thermosetting Resins Derived from High Oleic Soybean Oil. *Green Chem.* **2018,** 20, 1106-1113.

17. Tarnavchyk, I.; Popadyuk, A.; Popadyuk, N.; Voronov, A. Synthesis and Free Radical Copolymerization of a Vinyl Monomer from Soybean Oil. *ACS Sustainable Chem. Eng.* **2015,** 3, 1618-1622.

18. Chernykh, A.; Alam, S.; Jayasooriya, A.; Bahr, J.; Chisholm, B. J. Living Carbocationic Polymerization of a Vinyl Ether Monomer Derived from Soybean Oil, 2-(Vinyloxy)Ethyl Soyate. *Green Chem.* **2013,** 15, 1834-1838.

19. Yuan, L.; Wang, Z. K.; Trenor, N. M.; Tang, C. B. Amidation of Triglycerides by Amino Alcohols and Their Impact on Plant Oil-Derived Polymers. *Polym. Chem.* **2016,** 7, 2790-2798.

20. Yuan, L.; Wang, Z. K.; Trenor, N. M.; Tang, C. B. Robust Amidation Transformation of Plant Oils into Fatty Derivatives for Sustainable Monomers and Polymers. *Macromolecules* **2015,** 48, 1320-1328.

21. Ding, W.; Wang, S.; Yao, K.; Ganewatta, M. S.; Tang, C.; Robertson, M. L. Physical Behavior of Triblock Copolymer Thermoplastic Elastomers Containing Sustainable

Rosin-Derived Polymethacrylate End Blocks. *ACS Sustainable Chem. Eng.* **2017,** 5, 11470-11480.

22. Ganewatta, M. S.; Ding, W.; Rahman, M. A.; Yuan, L.; Wang, Z.; Hamidi, N.; Robertson, M. L.; Tang, C. Biobased Plastics and Elastomers from Renewable Rosin Via "Living" Ring-Opening Metathesis Polymerization. *Macromolecules* **2016,** 49, 7155-7164.

23. Wang, S.; Kesava, S. V.; Gomez, E. D.; Robertson, M. L. Sustainable Thermoplastic Elastomers Derived from Fatty Acids. *Macromolecules* **2013,** 46, 7202−7212.

24. Shin, J.; Lee, Y.; Tolman, W. B.; Hillmyer, M. A. Thermoplastic Elastomers Derived from Menthide and Tulipalin A. *Biomacromolecules* **2012,** 13, 3833-3840.

25. Rahman, M. A.; Lokupitiya, H. N.; Ganewatta, M. S.; Yuan, L.; Stefik, M.; Tang, C. Designing Block Copolymer Architectures toward Tough Bioplastics from Natural Rosin. *Macromolecules* **2017,** 50, 2069-2077.

26. Wang, Z.; Yuan, L.; Trenor, N. M.; Vlaminck, L.; Billiet, S.; Sarkar, A.; Prez, F. E. D.; Stefik, M.; Tang, C. Sustainable Thermoplastic Elastomers Derived from Plant Oil and Their "Click-Coupling" Via Tad Chemistry. *Green Chem.* **2015,** 17, 3806–3818.

27. Yuan, L.; Wang, Z.; Ganewatta, M. S.; Rahman, M. A.; Lamm, M. E.; Tang, C. A Biomass Approach to Mendable Bio-Elastomers. *Soft Matter* **2017,** 13, 1306-1313.

28. Song, L. Z.; Wang, Z. K.; Lamm, M. E.; Yuan, L.; Tang, C. B. Supramolecular Polymer Nanocomposites Derived from Plant Oils and Cellulose Nanocrystals. *Macromolecules* **2017,** 50, 7475-7483.

29. Brunsveld, L.; Folmer, B. J. B.; Meijer, E. W.; Sijbesma, R. P. Supramolecular Polymers. *Chem. Rev.* **2001,** 101, 4071-4097.

30. Yang, L.; Tan, X.; Wang, Z.; Zhang, X. Supramolecular Polymers: Historical Development, Preparation, Characterization, and Functions. *Chem. Rev.* **2015,** 115, 7196−7239.

31. Binder, W. H.; Bernstorff, S.; Kluger, C.; Petraru, L.; Kunz, M. J. Tunable Materials from Hydrogen-Bonded Pseudo Block Copolymers. *Adv. Mater.* **2005,** 17, 2824-2828.

32. Noro, A.; Nagata, Y.; Takano, A.; Matsushita, Y. Diblock-Type Supramacromolecule Via Biocomplementary Hydrogen Bonding. *Biomacromolecules* **2006,** 7, 1696-1699.

33. Sontjens, S. H. M.; Renken, R. A. E.; Gemert, G. M. L. v.; Engels, T. A. P.; Bosman, A. W.; Janssen, H. M.; Govaert, L. E.; Baaijens, F. P. T. Thermoplastic Elastomers Based on Strong and Well-Defined Hydrogen-Bonding Interactions. *Macromolecules* **2008,** 41, 5703-5708.

34. Razgoniaev, A. O.; Mikhailov, K. I.; Obrezkov, F. A.; Butaeva, E. V.; Ostrowski, A. D. Supramolecular Elastomers: Switchable Mechanical Properties and Tuning Photohealing with Changes in Supramolecular Interactions. *J. Polym. Sci., Part A: Polym. Chem.* **2018,** 56, 1003-1011.

35. Sautaux, J.; Montero de Espinosa, L.; Balog, S.; Weder, C. Multistimuli, Multiresponsive Fully Supramolecular Orthogonally Bound Polymer Networks. *Macromolecules* **2018,** 51, 5867-5874.

36. Freitas, L. L. d. L.; Stadler, R. Thermoplastic Elastomers by Hydrogen Bonding. 3. Interrelations between Molecular Parameters and Rheological Properties. *Macromolecules* **1987,** 20, 2478-2485.

37. Enke, M.; Bode, S.; Vitz, J.; Schacher, F. H.; Harrington, M. J.; Hager, M. D.; Schubert, U. S. Self-Healing Response in Supramolecular Polymers Based on Reversible Zinc–Histidine Interactions. *Polymer* **2015,** 69, 274-282.

38. Enke, M.; Bose, R. K.; Bode, S.; Vitz, J.; Schacher, F. H.; Garcia, S. J.; van der Zwaag, S.; Hager, M. D.; Schubert, U. S. A Metal Salt Dependent Self-Healing Response in Supramolecular Block Copolymers. *Macromolecules* **2016,** 49, 8418-8429.

39. Liu, J.; Tan, C. S.; Yu, Z.; Lan, Y.; Abell, C.; Scherman, O. A. Biomimetic Supramolecular Polymer Networks Exhibiting Both Toughness and Self-Recovery. *Adv. Mater.* **2017,** 29, 1604951.

40. Tang, Z.; Huang, J.; Guo, B.; Zhang, L.; Liu, F. Bioinspired Engineering of Sacrificial Metal–Ligand Bonds into Elastomers with Supramechanical Performance and Adaptive Recovery. *Macromolecules* **2016,** 49, 1781-1789.

41. Whittell, G. R.; Hager, M. D.; Schubert, U. S.; Manners, I. Functional Soft Materials from Metallopolymers and Metallosupramolecular Polymers. *Nat Mater* **2011,** 10, 176-88.

42. Yang, Y.; Urban, M. W. Self-Healing Polymeric Materials. *Chem. Soc. Rev.* **2013,** 42, 7446-7467.

43. Jiang, Z. C.; Xiao, Y. Y.; Kang, Y.; Pan, M.; Li, B. J.; Zhang, S. Shape Memory Polymers Based on Supramolecular Interactions. *ACS Appl. Mater. Interfaces* **2017,** 9, 20276-20293.

44. Mozhdehi, D.; Ayala, S.; Cromwell, O. R.; Guan, Z. Self-Healing Multiphase Polymers Via Dynamic Metal-Ligand Interactions. *J. Am. Chem. Soc.* **2014,** 136, 16128-31.

45. Zhang, X.; Tang, Z.; Guo, B.; Zhang, L. Enabling Design of Advanced Elastomer with Bioinspired Metal-Oxygen Coordination. *ACS Appl. Mater. Interfaces* **2016,** 8, 32520-32527.

46. Rowan, S. J.; Cantrill, S. J.; Cousins, G. R. L.; Sanders, J. K. M.; Stoddart, J. F. Dynamic Covalent Chemistry. *Angew. Chem. Int. Ed.* **2002,** 41, 898-952.

47. Maeda, T.; Otsuka, H.; Takahara, A. Dynamic Covalent Polymers: Reorganizable Polymers with Dynamic Covalent Bonds. *Prog. Polym. Sci.* **2009,** 34, 581-604.

48. Zhang, Z. P.; Rong, M. Z.; Zhang, M. Q. Polymer Engineering Based on Reversible Covalent Chemistry: A Promising Innovative Pathway Towards New Materials and New Functionalities. *Prog. Polym. Sci.* **2018,** 80, 39-93.

49. Denissen, W.; Winne, J. M.; Du Prez, F. E. Vitrimers: Permanent Organic Networks with Glass-Like Fluidity. *Chem. Sci.* **2016,** 7, 30-38.

50. Brutman, J. P.; Delgado, P. A.; Hillmyer, M. A. Polylactide Vitrimers. *ACS Macro Lett.* **2014,** 3, 607-610.

51. Zhao, S.; Abu-Omar, M. M. Recyclable and Malleable Epoxy Thermoset Bearing Aromatic Imine Bonds. *Macromolecules* **2018,** 51, 9816-9824.

52. Song, F.; Li, Z.; Jia, P.; Zhang, M.; Bo, C.; Feng, G.; Hu, L.; Zhou, Y. Tunable "Soft and Stiff", Self-Healing, Recyclable, Thermadapt Shape Memory Biomass Polymers Based on Multiple Hydrogen Bonds and Dynamic Imine Bonds. *Journal of Materials Chemistry A* **2019,** 7, 13400-13410.

53. Rao, Y.-L.; Feig, V.; Gu, X.; Nathan Wang, G.-J.; Bao, Z. The Effects of Counter Anions on the Dynamic Mechanical Response in Polymer Networks Crosslinked by Metal–Ligand Coordination. *J. Polym. Sci., Part A: Polym. Chem.* **2017,** 55, 3110-3116.

54. Mozhdehi, D.; Neal, J. A.; Grindy, S. C.; Cordeau, Y.; Ayala, S.; Holten-Andersen, N.; Guan, Z. Tuning Dynamic Mechanical Response in Metallopolymer Networks through Simultaneous Control of Structural and Temporal Properties of the Networks. *Macromolecules* **2016,** 49, 6310-6321.

55. Wei, P.; Yan, X.; Huang, F. Supramolecular Polymers Constructed by Orthogonal Self-Assembly Based on Host-Guest and Metal-Ligand Interactions. *Chem. Soc. Rev.* **2015,** 44, 815-32.

56. Grindy, S. C.; Learsch, R.; Mozhdehi, D.; Cheng, J.; Barrett, D. G.; Guan, Z.; Messersmith, P. B.; Holten-Andersen, N. Control of Hierarchical Polymer Mechanics with Bioinspired Metal-Coordination Dynamics. *Nat Mater* **2015,** 14, 1210-6.

57. Yang, S. K.; Ambade, A. V.; Weck, M. Main-Chain Supramolecular Block Copolymers. *Chem. Soc. Rev.* **2011,** 40, 129-37.

58. Rowan, S. J.; Beck, J. B. Metal–Ligand Induced Supramolecular Polymerization: A Route to Responsive Materials. *Faraday Discuss.* **2005,** 128, 43-53.

59. Pollino, J. M.; Weck, M. Non-Covalent Side-Chain Polymers: Design Principles, Functionalization Strategies, and Perspectives. *Chem. Soc. Rev.* **2005,** 34, 193-207.

60. Fox, J. D.; Rowan, S. J. Supramolecular Polymerizations and Main-Chain Supramolecular Polymers. *Macromolecules* **2009,** 42, 6823-6835.

61. Wang, F.; Zhang, J.; Ding, X.; Dong, S.; Liu, M.; Zheng, B.; Li, S.; Wu, L.; Yu, Y.; Gibson, H. W.; Huang, F. Metal Coordination Mediated Reversible Conversion

between Linear and Cross-Linked Supramolecular Polymers. *Angew. Chem. Int. Ed.* **2010,** 49, 1090-1094.

62. Lewis, R. W.; Malic, N.; Saito, K.; Evans, R. A.; Cameron, N. R. Ultra-High Molecular Weight Linear Coordination Polymers with Terpyridine Ligands. *Chem Sci* **2019,** 10, 6174-6183.
63. Gustafson, R. L.; Lirio, J. A. Binding of Divalent Metal Ions by Cross-Linked Polyacrylic Acid. *The Journal of Physical Chemistry* **1968,** 72, 1502-1505.
64. Irving, H.; Williams, R. J. P. 637. The Stability of Transition-Metal Complexes. *J. Chem. Soc.* **1953,** 10.1039/JR9530003192, 3192-3210.
65. Leussing, D. L. The Estimation of the Stabilities of Bivalent Transition Metal Complexes and Deviations from the Irving-Williams Order. *Talanta* **1960,** 4, 264-267.
66. Johnson, D. A.; Nelson, P. G. Factors Determining the Ligand Field Stabilization Energies of the Hexaaqua 2+ Complexes of the First Transition Series and the Irving-Williams Order. *Inorg. Chem.* **1995,** 34, 5666-5671.
67. Grindy, S. C.; Holten-Andersen, N. Bio-Inspired Metal-Coordinate Hydrogels with Programmable Viscoelastic Material Functions Controlled by Longwave Uv Light. *Soft Matter* **2017,** 13, 4057-4065.
68. Auletta, J. T.; LeDonne, G. J.; Gronborg, K. C.; Ladd, C. D.; Liu, H.; Clark, W. W.; Meyer, T. Y. Stimuli-Responsive Iron-Cross-Linked Hydrogels That Undergo Redox-Driven Switching between Hard and Soft States. *Macromolecules* **2015,** 48, 1736-1747.
69. Jackson, A. C.; Beyer, F. L.; Price, S. C.; Rinderspacher, B. C.; Lambeth, R. H. Role of Metal–Ligand Bond Strength and Phase Separation on the Mechanical Properties of Metallopolymer Films. *Macromolecules* **2013,** 46, 5416-5422.
70. Seguel, G. V.; Rivas, B. L.; Novas, C. Polymeric Ligand-Metal Acetate Interactions: Spectroscopic Study and Semi-Empirical Calculations. *J. Chil. Chem. Soc.* **2005,** 50.

71. Xu, Y.; Yuan, L.; Wang, Z.; Wilbon, P. A.; Wang, C.; Chu, F.; Tang, C. Lignin and Soy Oil-Derived Polymeric Biocomposites by “Grafting from” Raft Polymerization. *Green Chem.* **2016,** 18, 4974-4981.

72. van Nierkerk, J. N.; Schoening, F. R. L. A New Type of Copper Complex as Found in the Crystal Structure of Cupric Acetate, $Cu_2(Ch_3coo)_4*2h_2o$. *Acta Crystallogr.* **1953,** 6, 277-232.

73. van Nierkerk, J. N.; Schoening, F. R. L.; Talbot, J. H. The Crystal Structure of Zinc Acetate Dihydrate, $Zn(Ch_3coo)_2*H_2o$. *Acta Crystallogr.* **1953,** 6, 720-723.

74. Vidavsky, Y.; Bae, S.; Silberstein, M. N. Modulating Metallopolymer Mechanical Properties by Controlling Metal Ligand Crosslinking. *J. Polym. Sci., Part A: Polym. Chem.* **2018,** 56, 1117-1122.

75. Xie, T. Recent Advances in Polymer Shape Memory. *Polymer* **2011,** 52, 4985-5000.

76. Ratna, D.; Karger-Kocsis, J. Recent Advances in Shape Memory Polymers and Composites: A Review. *J. Mater. Sci.* **2008,** 43, 254-269.

77. Hu, J.; Zhu, Y.; Huang, H.; Lu, J. Recent Advances in Shape–Memory Polymers: Structure, Mechanism, Functionality, Modeling and Applications. *Prog. Polym. Sci.* **2012,** 37, 1720-1763.

78. Wang, Z.; Zhang, Y.; Yuan, L.; Hayat, J.; Trenor, N. M.; Lamm, M. E.; Vlaminck, L.; Billiet, S.; Du Prez, F. E.; Wang, Z.; Tang, C. Biomass Approach toward Robust, Sustainable, Multiple-Shape-Memory Materials. *ACS Macro Lett.* **2016,** 5, 602-606.

79. Lamm, M. E.; Wang, Z.; Zhou, J.; Yuan, L.; Zhang, X.; Tang, C. Sustainable Epoxy Resins Derived from Plant Oils with Thermo- and Chemo-Responsive Shape Memory Behavior. *Polymer* **2018,** 144, 121-127.

80. M. Lamm, L. Song, Z. Wang, B. Lamm, L. Fu and C. Tang, *Polym. Chem*., **2019**, Accepted Manuscript , DOI: 10.1039/C9PY01479A

CHAPTER 4

PLANT OIL-DERIVED COPOLYMERS WITH REMARKABLE POST-POLYMERIZATION INDUCED MECHANICAL ENHANCEMENT FOR HIGH PERFORMANCE COATING APPLICATIONS

Lamm, M.; Li, P.; Hankinson, S.; Zhu, T.; Tang, C., Plant Oil-Derived Copolymers with Remarkable Post-Polymerization Induced Mechanical Enhancement for High Performance Coating Applications. *Polymer*, **2019**, *174*, 170-177. Adapted with permission from Elsevier.

4.1 Abstract

Polymer coatings have been heavily utilized in many industrial and civil applications where a protective thermoset material with enhanced properties such as chemical and physical resistance, thermal stability, and tailorable mechanical properties is desired. Plant oils are a class of promising biomass toward sustainable polymers, but have yet to be fully harnessed in tailorable thermoset coatings due to the challenging functionalization and extensive crosslinking processes required to achieve desirable thermomechanical properties. In this work, we demonstrated that soybean methacrylate (SBMA) from high oleic soybean oil (HOSO) can be utilized to produce bio-based acrylic thermoset copolymers through an industrially viable semi-batch emulsion polymerization process with various commonly used co-monomers such as methyl methacrylate, styrene, and butyl acrylate. A wide range of monomer feed ratios with SBMA from 0 to 50 wt% was easily achieved with minimal modifications allowing for good tunability of thermal and mechanical properties in the prepared latexes. More importantly, a simple and effective auto-oxidative crosslinking of the latex films provided extreme mechanical enhancements making these thermosets good candidates in ultra-strong, ultra-tough, and high T_g coating applications.

4.2 Introduction

Thermoset polymers have been widely used as high performance coatings in many industrial applications due to their thermal stability, chemical and mechanical resistance, facile processing, and tailorable mechanical properties. Chemically and mechanically resistant thermoset polymers are frequently used as specialized coatings on substrates for heavy duty work such as laboratory benches, automotive parts, and construction materials.

Resins, including epoxy and phenol, are widely used as durable coating materials due to their low cost and facile crosslinking chemistry.[1, 2] Unfortunately, the curing agents, solvents, and additives in thermoset resin materials often pose health hazards, such as known carcinogenic formaldehyde or suspected endocrine disruptor bisphenol A.[3] Extensive efforts have been focused on replacing these hazardous components with benign bio-derived alternatives.[4-11] On the other hand, acrylate-based thermoset systems present an alternative with better tailorable properties, owing to their greater structural diversity and safer options for post-polymerization functionalization.[12] Acrylate monomers of various structures and chemical compositions can be copolymerized with a variety of co-monomers including styrenes, vinyl ethers, and other (meth)acrylates.[13] Higher molecular weight and better chemical composition control can be achieved in comparison to the epoxy and phenolic resin-based systems as the initial polymerization and subsequent crosslinking occur in two separate steps. Furthermore, crosslinking in these systems can be conveniently achieved by utilizing light and/or heat without the need to use toxic catalysts or other additives.[14-16] However, these acrylate-based materials have relied primarily on petrochemicals raising large environmental and sustainability concerns.

In searching for new approaches to preparing more robust and environmentally benign, high performance coatings from plant oils, we realized that utilizing free radical emulsion polymerization to obtain higher molecular weight acrylate polymers with preserved functional groups for facile post-polymerization modification could provide a convenient access to desirable mechanical properties. Biomass encompasses a variety of structures that have shown promise in range of polymer applications including coatings for biomaterials and adhesives.[17-24] Plant oils have shown great potential as biomass resources to replace

petrochemicals in polymer materials.[25-29] Owing to their versatility in structures, various functionalization can be easily carried out to produce a range of materials from thermoplastics to thermosets.[18, 30-35] Fatty acid-derived acrylate polymers have also shown facile crosslinking via UV exposure or simple auto-oxidation, resulting in high performance coatings useful in pressure sensitive adhesives.[36-38] To our knowledge, no prior reported work has focused on utilizing plant oil acrylates to obtain stiff, tough, high T_g performance coatings competitive with current epoxy and phenolic resins. The robust free radical emulsion polymerization process allows for an easy preparation of higher molecular weight polymers and thus better mechanic properties, and hence has been heavily utilized in industry to produce acrylic coatings with optimal properties.[39-41] In addition, various types of co-monomers can be easily incorporated to prepare copolymers in the emulsion polymerization process offering a convenient tuning of the physical and mechanical properties. More importantly, the resulting waterborne polymers can be used directly without the need for removing harmful organic solvents, making them the most sought-after high volume materials in applications pursuing high environmental and health standards. Therefore, increasing amount of attention has centered on the more efficient and effective incorporation of sustainable and bio-based materials in high volume polymers to reduce the carbon footprint.[42-45]

Unfortunately, due to their strong hydrophobicity and unique inherent reactivity, bio-based acrylic monomers from plant oils, and other hydrophobic biomass sources, have been largely ignored in emulsion-based free radical polymerization until recently.[45-53] Voronov and co-workers recently developed a series of bio-based vinylic monomers from various plant oil sources (including olive oil, soybean oil, sunflower oil and linseed oil), and

adopted *them* to prepare waterborne latexes in a miniemulsion polymerization process.[54-56] Their later work also highlighted the potential of plant oil-based monomers to produce latex polymers with high bio-based content (up to ~ 60 wt%) via a more feasible batch process indicating the practicality of utilizing plant oils to produce waterborne latex polymers.[57] Recent success in adapting hydrophobic acrylate monomers (such as methacrylated methyl oleate) in conventional batch emulsion polymerization process has aspired us to examine the possibility and potential of high oleic soybean (HOSO)-based monomers in a more industrially relevant semi-batch emulsion polymerization process.[58-60] Additionally, the host-guest chemistry of high water soluble cyclodextrin has been adopted to tackle the hydrophobicity problem of plant oil derived monomers.[61, 62] It is worthwhile to note that *ab initio* emulsion polymerization has achieved great success on incorporation of hydrophobic monomers, though the process is less appealing in scaling.[63, 64]

Herein we report a study on the semi-batch emulsion copolymerization of a soybean methacrylate monomer (SBMA) with various co-monomers to prepare waterborne latex polymers with tunable compositions and thermomechanical properties. The bio-based acrylic monomer, SBMA, can be readily prepared in a highly efficient and scalable two-step process from HOSO (**Scheme 1**).[33, 34, 65] The homopolymer of SBMA (PSBMA) has a unique soft and tacky nature and can serve as a renewable replacement for other low T_g acrylic polymers such as butyl acrylate polymers in current acrylic coatings. The pendant unsaturated fatty side chain in soybean methacrylate (SBMA) can be used for post-polymerization oxidative crosslinking to further improve the properties and performance of bio-based latex polymers, without the need for further functionalization.[66, 67] In this

work, we also demonstrate that a simple oxidative curing of the prepared bio-based latex films can lead to remarkable enhancement in mechanical properties, resulting in ultra-strong, ultra-tough thermoset materials competitive with high performance coatings.

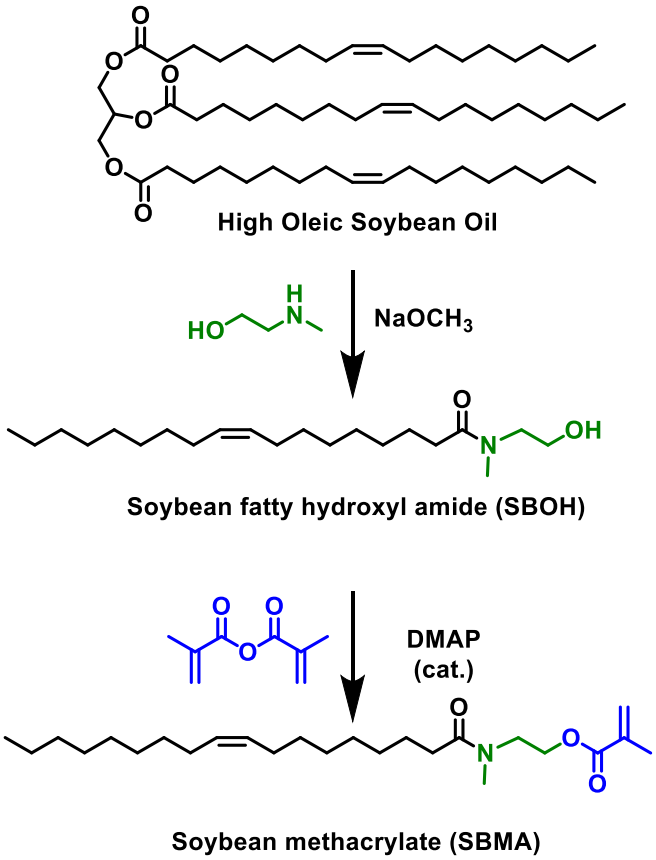

Figure 4.1. Synthesis of soybean methacrylate (SBMA) starting with high oleic soybean oil via a fatty amide alcohol intermediate.

4.3 Experimental

Materials

Plenish™ high oleic soybean oil (HOSO) was provided by DuPont Pioneer. E-Sperse® 100 was provided by Ethox Chemicals. Azobisisobutyronitrile (AIBN, 98%, Aldrich) was recrystallized twice from methanol. Monomers were passed through basic alumina to

remove inhibitors in reactivity studies and were used as received in emulsion polymerization studies. All other reagents were purchased from commercial resources and used as received unless otherwise mentioned. Soybean methacrylate (SBMA) was prepared in 3 kg-batch according to our previously reported procedures. (**Scheme 1** and **Figure S1**).[33, 34] Solution polymers used for reactivity ratio determination were synthesized using free radical polymerization in a previously reported procedure.[33, 34, 68]

Characterization

^{1}H NMR spectra were recorded on a Bruker Avance III HD 300 spectrometer using $CDCl_3$ as solvent with tetramethylsilane (TMS) as reference. Zetasizer nano instrument, equipped with an 830 nm wavelength laser, was used to determine the particle size for all emulsion polymers. Solid content was determined by drying ~1 g of latex on an aluminum pan at 55 ^{o}C overnight, using the equation 1 below. W_i is the initial mass of latex used and W_f is the final mass of dried latex.

(1) $$solid\ content\ = \frac{W_f}{W_i} \times 100$$

The glass transition temperature (T_g) of polymers was tested through differential scanning calorimetry (DSC) conducted on a DSC 2000 instrument (TA Instruments). Samples were first heated from -70 ^{o}C to 200 ^{o}C at a rate of 10 ^{o}C/min. After cooling down to -70 ^{o}C at the same rate, the data was collected from the second heating scan. About 8 mg of each sample was used for the DSC test, under nitrogen gas at a flow rate of 50 mL/min. Tensile stress-strain testing was carried out on an Instron 5543 A testing instrument. Dog-bone shaped specimens were cut from the cast film with a length of 20 mm and width of 5.0 mm. The thickness was measured prior to each measurement. Testing

was done at room temperature with a crosshead speed of 20 mm/min. Five replicate samples were used to obtain an average value for each.

Synthesis of Emulsion copolymers of SBMA with methyl methacrylate (MMA), styrene (S), and butyl acrylate (BA)

A pre-emulsion was prepared by mixing 40 mL of DI water, 60 g (in total) of monomers, and 4.8 g of E-Sperse® 100 (8 wt% of total monomer feed), and homogenized. The reactor charge was prepared by mixing ~10 % v/v of the above pre-emulsion and 50 mL of DI water, and placed in a cylinder reactor vessel (with overhead mechanical stirring). The reactor charge was heated till the internal temperature of the reactor charge reached 80 ^{o}C. The initial catalyst solution, 0.1 g of ammonium persulfate (APS) in 1 mL of DI water, was injected. The reaction was kept at 80-85 ^{o}C for 20 minutes to allow micelle formation. The remaining pre-emulsion was slowly pumped in over 3 hrs *concurrently* with the delay catalyst solution, 0.18 g of APS (0.3 wt% of total monomer feed) in 30 mL of DI water. After pumping finished, the emulsion was stirred for 30 minutes. Finishing catalyst, ammonium persulfate (0.1 g in 1 mL DI water) was added and stirred for 15 minutes. The mixture was then cooled to 65 ^{o}C. Once cooled, redox catalysts were added in the following order; iron (II) sulfate (0.1 g in 1 mL DI water), ammonium persulfate (0.1 g in 1 mL DI water), and sodium bisulfite (0.1 g in 1 mL DI water). After stirring for 30 minutes, the emulsion was cooled to room temperature and filtered through fine mesh to remove any particulates.

Preparation of Copolymer Films

Emulsion copolymer latexes (6mL each respectively, MMA20-50, S20-50, and BA20-50) were poured into Teflon molds. The latex films were obtained by drying at 55 ^{o}C over 48 h and then at 75 ^{o}C for 24 h under vacuum. Samples were cut for tensile testing.

Preparation of Crosslinked Films

The crosslinked latex films were obtained by placing the above films in the oven under air at 125 ^{o}C for 16 h. After cooling to room temperature, the crosslinked films were cut for tensile testing and Soxhlet extraction.

Model Study of Auto-Oxidative Plant Oil Curing using small molecule analogs

High oleic soybean oil and oleic acid (2 mL of each) were placed in two different respective aluminum pans. Pans were placed in an oven at 125 ^{o}C for 16 h.

Soxhlet Extraction

Solvent extraction of latex and crosslinked films were carried out by Soxhlet extraction using tetrahydrofuran (THF) as the solvent for 36 h. A 500 mL round bottom flask filled with 300 mL THF was connected to a Soxhlet extractor. All samples were vacuum dried, weighed, packed in filter papers, and inserted into the extractor. The extracted samples were dried at 40 ^{o}C under vacuum for 36 h and weighed. Procedure was repeated twice to obtain an average. The sol contents of all films were calculated according to the following previously reported equation 2,

(2) $$\text{Crosslinked content (\%)} = 100 - \left(\frac{W_i - W_f}{W_i}\ x\ 100\right)$$

where W_i is the sample weight before extraction and W_f is the sample weight after extraction and vacuum dry.[16]

4.4 Results and Discussion

Reactivity Ratios of Copolymers

Soybean methacrylate (SBMA) was copolymerized with three different monomers to determine structural incorporation and practicality. As no previous copolymers had been studied using SBMA and our selected copolymers, we chose to confirm the copolymerization feasibility and copolymer composition prior to moving forward with emulsion polymerization testing. All reactivity ratios were determined for our copolymers with styrene, methyl methacrylate, and butyl acrylate. All copolymers were synthesized via solution polymerization in toluene.

Table 4.1. Reactivity ratios for all copolymers containing soybean methacrylate (SBMA), determined using the Fineman Ross method.

Copolymerization	r_1 **(SBMA)**	r_2 **(co-monomer)**
Methyl methacrylate	0.375 (± 0.03)	0.896 (± 0.07)
Styrene	1.083 (± 0.1)	1.051 (± 0.17)
Butyl acrylate	1.013 (± 0.02)	0.963 (± 0.05)

Using the Fineman-Ross method for reactivity ratio determination, seven copolymers of SBMA with styrene (S), methyl methacrylate (MMA), and butyl acrylate (BA), respectively, were synthesized. The results were graphed according to an established procedure using the monomer molar feed ratios and the in-polymer fraction ratios (**Figure**

4.2) measured by ^{1}H NMR.[1] Reactivity ratios (r_1 and r_2) (**Table 4.1**) suggest well behaved free-radical copolymerization of SBMA with these monomers to provide random copolymers. These reactivity ratios of SBMA with comonomers also help explain the high conversion and low coagulation present in our emulsion polymerization system. As our latex copolymers are likely random copolymers, like their solution cohorts, the monomer starvation throughout our polymerization, due to the semi-batch process, and reactivity ratios indicate that any monomer present should quickly and easily incorporate into the growing polymer, resulting in good control of the polymerization.

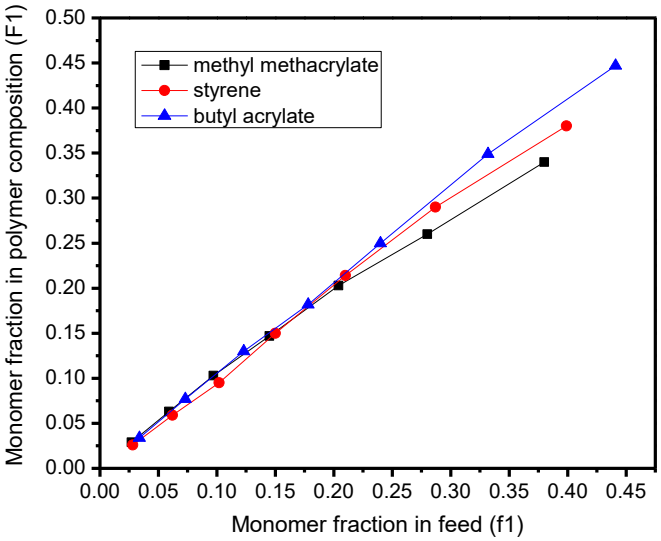

Figure 4.2. Fineman Ross plots used to determine reactivity ratios of SBMA copolymers. Monomer content in feed versus polymer composition.

Synthesis of Latex Polymers

Latex copolymers of varying wt. % of soybean methacrylate (SBMA) with three common co-monomers, i.e., styrene (S), methyl methacrylate (MMA), and butyl acrylate (BA) were prepared via emulsion polymerization. A semi-batch process that starves the

reaction of both monomer and initiator was chosen, allowing for more manageable exotherms and better control of the polymerization.[69] E-Sperse® 100 was selected over the commonly used sodium lauryl sulfate (SLS) as the surfactant to prepare a stable pre-emulsion of SBMA with other monomers. E-Sperse® 100 was found to have overall better performance in the surfactant screening test showing little to no emulsion breakdown in 72 hours. The pre-emulsion mixture was also homogenized to further insure its good stability during the delayed pumping stage.

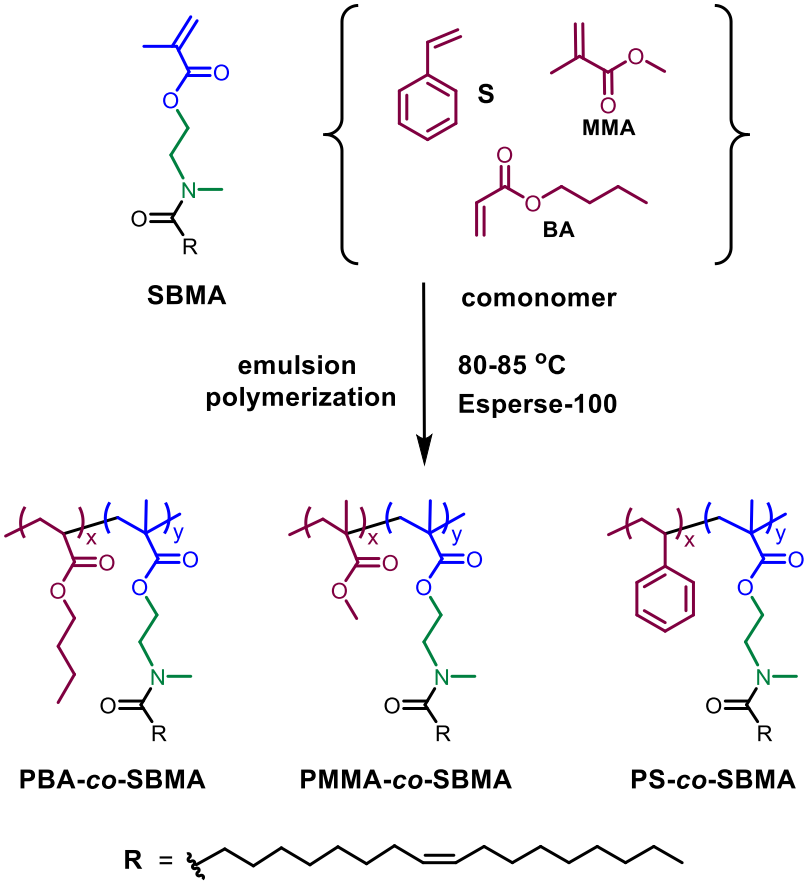

Figure 4.3. Synthesis of copolymers by free-radical emulsion polymerization using soybean methacrylate (SBMA) and a variety of co-monomers including methyl methacrylate (MMA), styrene (S), and butyl acrylate (BA). Copolymers contain between 10-50 wt% SBMA.

To start each polymerization, a small fraction of pre-emulsion was diluted with additional water, homogenized, and heated to 80 ^{o}C before the initial catalyst (ammonium persulfate, AP) was added. This initialization step was easily identified by the onset of a blueish color in the solution due to the micellar formation. Next, the reaction propagation was maintained at 80 to 85 ^{o}C and starved by slow addition of remaining pre-emulsion mixture and delay catalyst (AP) solution. In the finishing step, a chase catalyst (AP) was added at the reaction temperature before the reaction mixture was cooled down to 65 ^{o}C. Afterwards a redox finishing catalyst (AP, iron (II) sulfate, and sodium bisulfite) was added to push the complete consumption of residual monomers and achieve a high conversion.[70] Each type of catalyst serves a unique role in our polymerization. The delay catalyst is added into the starved reaction to initiate any monomers in situ and propagate the reaction. The chase catalyst serves to initiate any residual monomers and allows for movement into the larger growing polymer particles. The finishing catalyst works uniquely at a lower temperature to ensure all monomers in the liquid phase and can be brought into particles and incorporated into the final polymers in order to achieve high conversion. Detailed procedure is provided in the Methods section in the SI.

The prepared latexes were characterized using a variety of methods, and results were provided in **Table 4.2**. All polymers are named using their co-monomers followed by the weight percentage of SBMA. For example, MMA10 is referred to the copolymer of poly(methyl methacrylate-*co*-soybean methacrylate) (PMMA-*co*-SBMA) with 10 wt% SBMA. Auto-oxidative crosslinked samples are denoted with a "C" in the end. For example, S40C is referred to the crosslinked copolymer of poly(styrene-*co*-SBMA) (PS-*co*-SBMA) with 40 wt% SBMA.

Table 4.2. Characterization of latex copolymers containing soybean methacrylate (SBMA).

Copolymer	Molar Ratio in Feed (X/SBMA)[a]	Molar Ratio in Polymer (X/SBMA)[b]	Conv. (%) (X/SBMA)	Particle size (nm)	Solid content (%)[c]	T_g (°C)[d]
MMA10	1.0/0.028	1.0/0.025	99/99	97.0 (± 21)	33	87
MMA20	1.0/0.055	1.0/0.05	98/99	66.1 (± 17)	35	79
MMA30	1.0/0.11	1.0/0.13	98/99	52.8 (± 15)	33	74
MMA40	1.0/0.2	1.0/0.18	97/99	49.3 (± 13)	29	54
MMA50	1.0/0.26	1.0/0.23	96/98	45.8 (± 14)	30	42
S10	1.0/0.029	1.0/0.035	99/99	102.8 (± 24)	29	75
S20	1.0/0.064	1.0/0.07	97/99	77.0 (± 19)	34	72
S30	1.0/0.11	1.0/0.11	96/99	68.4 (± 18)	31	61
S40	1.0/0.26	1.0/0.3	95/99	66.2 (± 16)	27	50
S50	1.0/0.32	1.0/0.37	95/98	62.8 (± 15)	29	40
BA10	1.0/0.036	1.0/0.045	99/99	78.8 (± 16)	28	-47
BA20	1.0/0.081	1.0/0.12	99/99	77.5 (± 17)	30	-40
BA30	1.0/0.14	1.0/0.19	99/99	67.6 (± 18)	28	-32
BA40	1.0/0.32	1.0/0.38	97/99	64.2 (± 17)	25	-29
BA50	1.0/0.46	1.0/0.52	97/98	50.5 (± 15)	31	-20

[a] X = comonomer. [b] molar ratio in polymer was determined using ^{1}H NMR. [c]The number-average particle size determined using DLS. [d]T_g of dried latex determined using DSC (2nd heating cycle).

Overall, SBMA showed good incorporation with a variety of co-monomers. Little to no coagulation was observed with these polymerizations, likely due to the robust semi-batch process (good heat dissipation and controlled reaction rate) together with the excellent cross-reactivity between SBMA with co-monomers (**Figure 4.1** and **Table 4.1**). As a result, molar ratios in monomer feed and in the final polymers were in good consistency. High conversions (>95%) for both SBMA and co-monomers were confirmed using ^{1}H NMR. Slight decrease in co-monomer conversion (styrene, methyl methacrylate, and butyl acrylate) was observed with higher SBMA content in all copolymerizations. All latexes have a relatively small particle size (below 100 nm), likely due to the relatively high surfactant content (3 wt% overall) in the current recipes. Particle size was also found to decrease with increasing SBMA content regardless of comonomer composition, which was speculated to result from the surfactant like structure of our SBMA monomer. Solid contents of all latexes was consistent and in line with the expected ~30%, reaffirming the high level of conversion achieved in our emulsion polymerizations.

Glass transition temperatures (T_g) of the latex copolymers were found to follow a predicted trend consistent with those calculated from the Fox equation. Unfortunately, due to the SBMA and surfactant content, the observed T_g's are very broad. Styrene and methyl methacrylate copolymer latexes showed decreases in T_g with increasing SMBA content. This is well expected considering the T_g of homopolymer PSBMA is around -6 ^{o}C. Increasing SBMA fraction would result in a drastic decrease in T_g of the copolymers with MMA or S (Note that the homopolymers of PMMA and PS have their T_g's of 105-120 ^{o}C and 100 ^{o}C, respectively). Alternatively, an increase of SBMA content in the butyl acrylate

copolymers should cause an increase in T_g (Note that the homopolymer PBA has a T_g of -54 ^oC).

Molecular weight data is not readily available for these copolymers due to solubility issues. All copolymers are only fully soluble in dichloromethane and chloroform. However, they are sparingly soluble in the operable solvents (tetrahydrofuran and dimethylformamide) with our GPC systems. Despite repeated attempts, the copolymer samples could not be fully dissolved leaving significant an amount of residue when passing through 0.2 micron filter. Therefore, data was not collected considering the partially soluble samples may likely interfere with GPC measurements and produce inaccurate molecular weight information.

Mechanical Properties of Latex Copolymers

Latex copolymers of soybean methacrylate with styrene and methyl methacrylate, respectively, were capable of forming free-standing films when the SBMA content was 20-50 wt% but, became too brittle as the SBMA content dropped to 10 wt%. Conversely, all latex copolymers of SBMA and butyl acrylate were too soft to form free-standing films. The tensile curves are shown in **Figure 4.4**. Complete mechanical data is summarized in **Table 4.3**.

Elasticity of the copolymer film was found to increase with the increasing soy monomer content in the latex copolymers. The elasticity enhancement was dramatic on latex films made with styrene copolymers (S20-S50). For example, the tensile strain increased from 36.5% for S40, to 359% for S50 when SBMA content increased from 40 to 50 wt%. Generally, styrene copolymer films were tougher than methyl methacrylate copolymer

films of the similar level of SBMA content. For example, the toughness of copolymer latex films nearly doubled from MMA40 to MMA50 but quadrupled from S40 to S50.

Table 4.3. Tensile properties of latex copolymers containing soybean methacrylate.

Copolymer	Stress at break (MPa)	Strain at break (%)	Toughness (MJ/m^3)	Young's Modulus (MPa)
MMA20	28.6 (± 0.4)	4.1 (± 0.2)	0.55 (± 0.02)	928.4 (± 10.2)
MMA30	9.7 (± 0.3)	19.8 (± 0.4)	1.91 (± 0.2)	379.5 (± 6.6)
MMA40	9.9 (± 0.4)	29.6 (± 0.4)	2.75 (± 0.3)	355.3 (± 5.6)
MMA50	11.0 (± 0.2)	56.4 (± 2.1)	5.98 (± 0.6)	240.0 (± 3.2)
S20	29.1 (± 0.3)	3.8 (± 0.3)	0.38 (± 0.01)	1300.7 (± 12.1)
S30	38.8 (± 0.5)	5.7 (± 0.8)	0.99 (± 0.03)	532.1 (± 7.8)
S40	9.7 (± 0.4)	36.5 (± 0.8)	3.63 (± 0.3)	361.2 (± 4.4)
S50	9.7 (± 0.6)	359.0 (± 7.2)	12.8 (± 0.9)	5.4 (± 0.5)

Higher soy content in general resulted in longer elongation and decreased stress at break. It is most notable that increasing SBMA content caused decreases in stiffness but sizable increases in toughness. This trend was observed in both copolymers of styrene and methyl methacrylate respectively. For instance, MMA20 showed a toughness of only 0.55 MJ/m^3 and Young's modulus of 928.4 MPa. In comparison, MMA50 demonstrated a toughness of 5.98 MJ/m^3, a nearly ten-fold increase, and Young's modulus of 240.0 MPa, about three quarters loss. Similarly, S50 showed a toughness of 12.8 MJ/m^3, a nearly ten times increase compared with S20 (0.38 MJ/m^3), and a Young's modulus of 5.4 MPa, a decimating loss in comparison to S20 (1300.7 MPa). This observed trend is likely due to the long fatty

chain of soybean monomer acting as a plasticizer in the copolymers prepared with stiffer co-monomers such as styrene and methyl methacrylate. Similar toughness enhancement has been observed in earlier works of incorporating plant oil-based monomers into polymer systems and has been considered a promising attribute in coating applications.[206, 207]

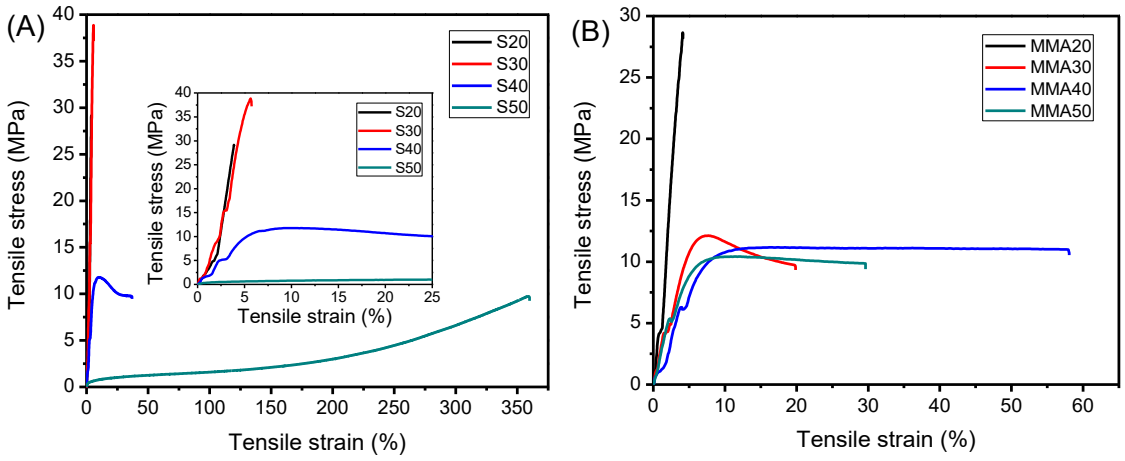

Figure 4.4. Tensile curves of (A) PS-*co*-SBMA, inset magnifies graph to show tensile strain between 0-25 %, and (B) PMMA-*co*-SBMA copolymers.

Auto-oxidative Crosslinking

Plant oils possess crosslinkable alkene functional groups on their fatty chains. Our HOSO-derived SBMA has one alkene group per fatty chain on average, comprised of a variety of saturated, monounsaturated, and polyunsaturated fatty acids. These alkene groups when exposed to atmospheric oxygen at elevated temperatures can undergo auto-oxidation and form crosslinked structures in polymer.[71, 72] This oxidative crosslinking process can be accelerated by the addition of metal salts, or enzymes.[73, 74] High crosslinking is important in thermosets for high performance coating applications as they dictate many of the necessary thermomechanical and chemical resistance properties.[1] A model study

using our soybean oil and oleic acid was used to confirm our crosslinking strategy was viable and robust.

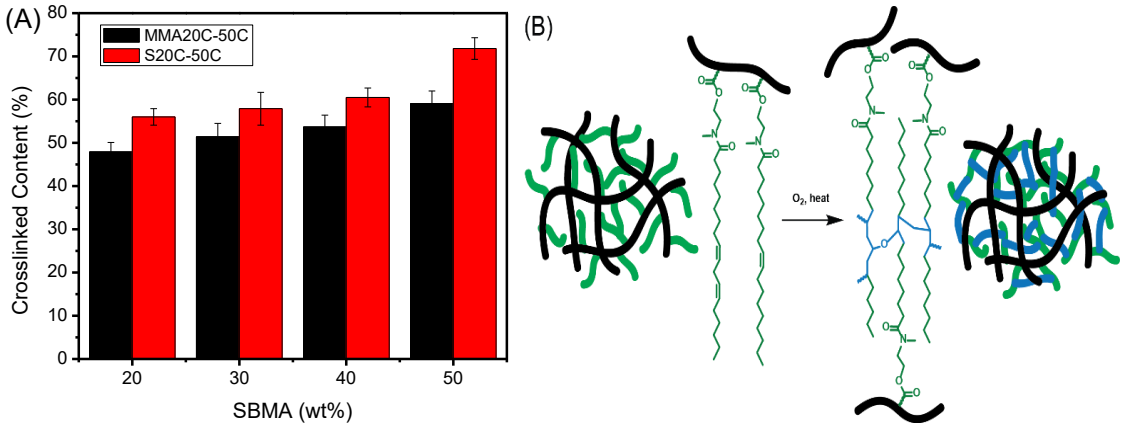

Figure 4.5. (A) Crosslinked content of copolymers as determined by Soxhlet extraction of crosslinked films (MMA20C-50C and S20C-50C). (B) A schematic presentation of the auto-oxidative crosslinking process involving the oleic amide chains.

Our bio-based latex copolymers contained 10-50 wt% SBMA and were able to achieve high levels of crosslinking without the need for catalysts. Dried latex films were placed in an open oven at 125 ^{o}C and allowed to crosslink over 16 h. Soxhlet extraction was carried out to help examine the level of crosslinking present in the films. The crosslinked content can be estimated by weight percentage of the non-soluble content of the films after exhaustive extraction. Details of extraction procedure are provided in the SI. Both non-crosslinked copolymers samples (MMA10-50 and S10-50) and crosslinked samples (MMA10C-50C and S10C-50C) were examined for comparison purposes (**Figure 4.5**). Butyl acrylate copolymers were not examined with Soxhlet extraction. The low T_g of these samples made it too difficult to extract and accurately weigh both initial residual sample without sample loss due to their tacky nature. All non-crosslinked samples (MMA10-50 and S10-50) were found to fully dissolve upon exhaustive extraction. In contrast, all

crosslinked films were found to have a significant amount of non-soluble content upon exhaustive extraction (**Figure 4.5**). All thermally processed latex films had a high level of crosslinking at >50%. Furthermore, crosslinked latex films showed a qualitative correlation between SBMA content and crosslinked content, where higher SBMA content resulted in higher crosslinked content. Interestingly, all styrene copolymers were found to achieve higher levels of crosslinking than methyl methacrylate films. For example, the styrene copolymer with 50 wt% of SBMA was found to reach a crosslinked content around 73% (S50C) whereas the counterpart methyl methacrylate copolymer was found to have a crosslinked content of around 60% (MMA50C).

Curing Model Study

Due to its lack of conjugated unsaturated and doubly allylic units, oleic acid (oleate) derived materials are harder to undergo auto-oxidative crosslinking. However, our high oleic soybean oil (HOSO) contains a greater fraction of oleate chains together with a small fractions of conjugated linoleic and linolenic acid chains. These conjugated fatty acids allow for initiation of the crosslinking reaction, which can further propagate through the oleic acid chains. To test this hypothesis, our HOSO was crosslinked at 125 ^{o}C for 16 h, the same conditions used on our latex films. Separately, oleic acid was also crosslinked to determine if the lack of conjugated fatty acids could still initiate crosslinking. It is worth mentioning that our oleic acid is ~90% and contains around ~8% linoleic acid chains, which can serve to initiate the reaction. Additionally, our HOSO is comprised of ~10% linoleic and linolenic acid chains which contain the necessary conjugation to initiate crosslinking and ~20% saturated fatty acids which do not participate in crosslinking.

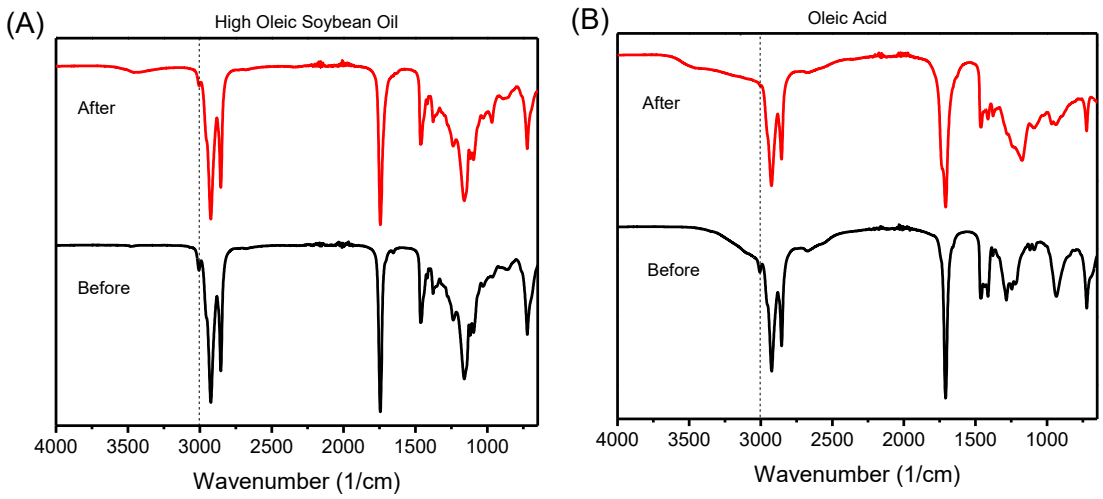

Figure 4.6. FTIR spectrum of (A) HOSO) and (B) oleic acid, before and after curing.

After crosslinking, conversion was determined by NMR, with oleic acid reaching higher conversion of 75% while HOSO only reached ~65%. Due to the fatty acid composition of these samples, these results are expected. Both samples were also monitored using FTIR (**Figure 4.6**). A marked decreased in the C=C-H stretch around 3000 cm^{-1} was observed for both samples in consistent with the crosslinking confirmed by decreasing alkene content on NMR. Thus the model curing study using small molecule analogs found overall good crosslinking under the operation condition (16 h @ 125 ^{o}C) suggesting that the SBMA content should react favorably in the crosslinking process within the latex films.

Mechanical Properties of Crosslinked Latexes

All crosslinked latex films were found to have dramatically enhanced mechanical properties (**Figure 4.7**). The most remarkable increase in properties was seen in the crosslinked methyl methacrylate copolymer MMA20C and styrene copolymer S20C, which were found to reach a tensile strength of 122.5 and 131.3 MPa respectively. This corresponds to a four-folded enhancement than non-crosslinked samples. In general,

copolymer films with higher soy content were found to increase in elasticity but decrease in strength upon crosslinking. Both crosslinked copolymer films made with methyl methacrylate (MMA10-40C) and styrene (S10-40C), respectively, showed an overall increase in strength, toughness, and stiffness, but marked decrease in elasticity (**Table 4.4**).

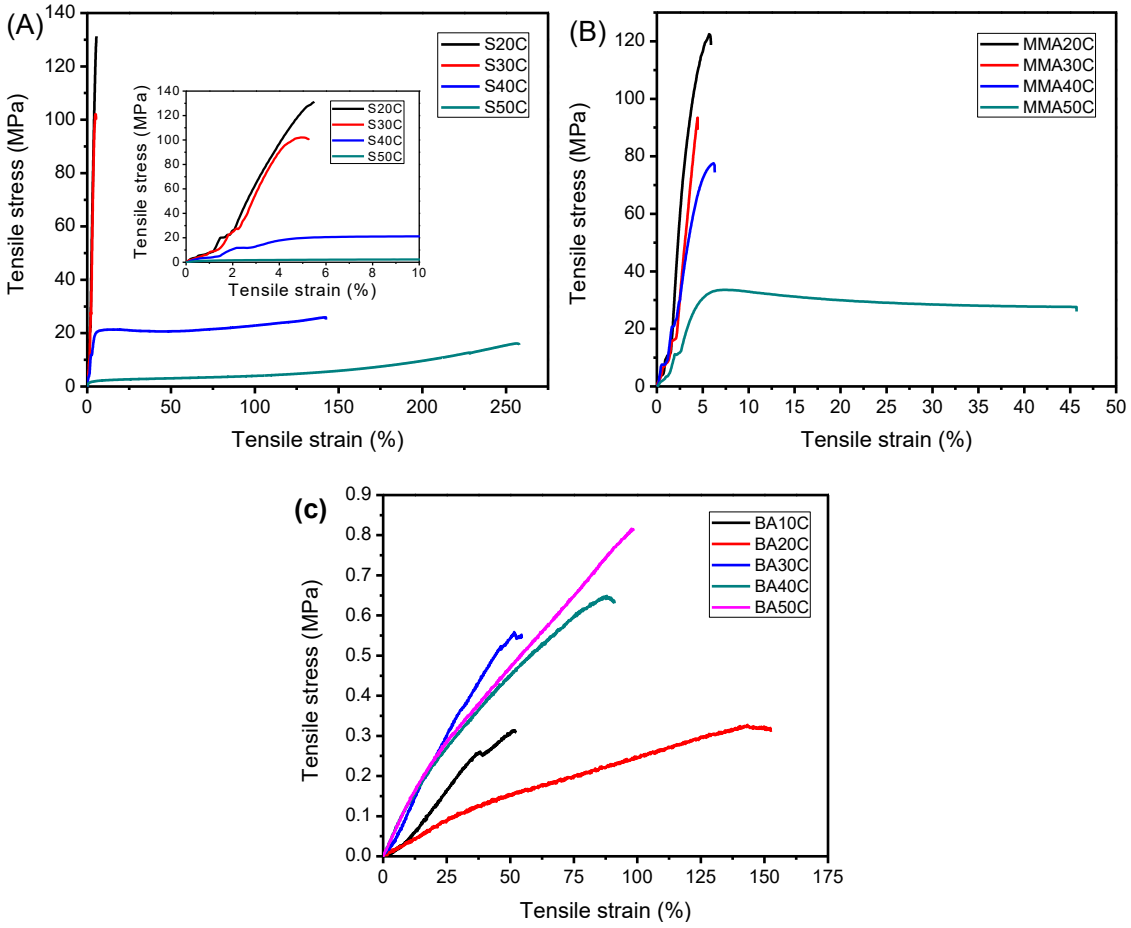

Figure 4.7. Tensile curves of (A) PS-*co*-SBMA (S20C-S50C), inset magnifies graph showing tensile strain between 0-10 %, (B) PMMA-*co*-SBMA (MMA20C-MMA50C), and (c) PBA-*co*-SBMA (BA10C-50C) crosslinked copolymers.

All crosslinked butyl acrylate copolymer films, despite being quite soft, were able to form free-standing films, showing a marked improvement over their viscoelastic non-crosslinked counterparts (**Figure 4.7**). All butyl acrylate copolymers showed increasing

stress at break with increasing soy content (**Table 4.4**). For example, crosslinked butyl acrylate copolymer with 50 wt% of SBMA (BA50C) showed almost doubled stress (0.81 MPa) at break in comparison to the crosslinked counterpart (0.31 MPa) with 10 wt% of SBMA (BA10C). A similar trend was observed with toughness, which increased from 0.08 MJ/m^3 for BA10C to 0.45 MJ/m^3 for BA50C, a significant increase.

Impressive increases in the Young's modulus of the latex films were also observed upon crosslinking. For example, crosslinked methyl methacrylate copolymer MMA20C were found to have a drastically higher Young's modulus (5.04 GPa) in comparison with uncrosslinked counterpart (928.4 MPa). Similar enhancements were also readily observable with crosslinked films of MMA30C, S20C, and S30C all showing a much higher modulus of ~3 GPa than their non-crosslinked counterparts (less than 1 GPa).

Furthermore, crosslinked copolymer films often showed improved toughness than non-crosslinked counterparts. For example, styrene copolymer with 40 wt% of SBMA was found to have an over 10-fold increase in toughness upon crosslinking (31.08 MJ/m^3 for S50C *versus* 0.38 MJ/m^3 for S50). However, the crosslinking-induced toughness enhancement appeared to be highly influenced by the copolymer compositions and fluctuate from case to case. For example, crosslinked copolymers MMA40C and S50C were found to have very marginal improvements in toughness than their non-crosslinked counterparts. Further studies are currently carried out in our laboratory to examine the relationship between the toughness and copolymer composition and structure.

Table 4.4. Tensile properties of crosslinked latex copolymers containing soybean methacrylate (SBMA).

Copolymer	Stress at break (MPa)	Strain at break (%)	Toughness (MJ/m^3)	Young's Modulus (MPa)
MMA20C	122.5 (± 0.4)	5.7 (± 0.2)	3.87 (± 0.03)	5041.3 (± 7.2)
MMA30C	93.5 (± 0.3)	4.4 (± 0.4)	1.52 (± 0.01)	3553.9 (± 4.1)
MMA40C	77.6 (± 0.4)	6.2 (± 0.4)	2.69 (± 0.03)	2103.3 (± 2.3)
MMA50C	27.7 (± 0.2)	45.5 (± 2.1)	12.79 (± 0.4)	1065.6 (± 3.1)
S20C	131.3 (± 0.3)	5.5 (± 0.3)	3.23 (± 0.01)	3240.9 (± 9.1)
S30C	102.1 (± 0.5)	4.9 (± 0.8)	2.56 (± 0.02)	3370.4 (± 5.4)
S40C	25.9 (± 0.4)	141.9 (± 0.8)	31.08 (± 0.9)	468.0 (± 2.1)
S50C	16.1 (± 0.6)	256.6 (± 7.2)	25.64 (± 0.2)	10.1 (± 0.3)
BA10C	0.31 (± 0.05)	51.8 (± 1.1)	0.08 (± 0.02)	0.73 (± 0.1)
BA20C	0.32 (± 0.03)	150.6 (± 2.3)	0.30 (± 0.09)	0.60 (± 0.1)
BA30C	0.55 (± 0.1)	51.7 (± 0.5)	0.17 (± 0.03)	1.15 (± 0.05)
BA40C	0.64 (± 0.04)	89.7 (± 0.6)	0.36 (± 0.06)	1.40 (± 0.2)
BA50C	0.81(± 0.06)	98.1 (± 0.9)	0.45 (± 0.06)	1.08 (± 0.1)

Admittedly, minor deviations in property trends were observed for some crosslinked samples such as S30C and BA20C. This was speculated to associate with the population density, distribution, and fatty chain conformation of the SBMA units on the polymer particle surface. Due to the higher molecular weight of SBMA versus co-monomers, copolymers with lower wt% of SBMA will have very low molar percentage of SBMA. For

example, copolymers BA20 and BA30 only have approximately 6% to 10% molar percentage of SBMA. The low molar percentage of SBMA will translate to a very sparse population of SBMA on the particle surface, which likely may cause long SBMA chain to fold or bend back onto the surface. This in turn would increase the difficulty for the oleic fatty chain from different polymer particles to meet each other during the curing reaction. Furthermore, the complex nature of biomass source might have increased the chance of random deviations in low SBMA samples. For example, the auto-oxidation process might have to start from the small fraction of linoleic and linolenic chains (~10% in our HOSO) which are much more reactive toward oxygen. The oleic fatty chains by themselves are much harder to undergo auto-oxidative crosslinking process. The presence of small fraction of unreactive saturated fatty chain (~20% in our HOSO) also have impacts on the crosslinking reaction. Unfortunately, it is extremely difficult to experimentally monitor and measure the SBMA chain location and availability. We have carried out model curing studies on the small molecule analogs to confirm the effectiveness of our auto-oxidative crosslinking procedure. However, due to the complexities discussed above, we have to refrain from investigating the level of crosslinking present in these samples and accept the possibility of potential random deviation. Future work should focus on utilizing computational modeling to assist in determining and mitigating this issue. Nevertheless, the ultra-high strength, impressive stiffness, and toughness achieved by simple crosslinking of these films indicates potential as acrylic thermoset replacement for current high performance, high T_g coating materials like epoxy and phenolic resins.

4.5 Conclusions

Soybean methacrylate (SBMA) was copolymerized with a variety of co-monomers including styrene, methyl methacrylate, and butyl acrylate using an industrially relevant, safer semi-batch emulsion polymerization method. All polymerizations showed good control with near complete incorporation of monomers and predictable properties. Tensile tests on the corresponding polymer films revealed that high soy content improved elasticity and toughness, while low soy content boosted stiffness and strength. Such tunable thermomechanical properties present a useful attribute towards a range of high performance coating applications. Crosslinking of copolymer latex films via easy auto-oxidation provided thermomechanically enhanced materials with a high degree of crosslinking. Incorporation of plant oil derived methacrylate monomers into polymer latexes has demonstrated good potentials as a cheaper, simpler, and effective strategy to prepare heavy usage, high T_g performance acrylic coatings with tunable thermomechanical properties. The remarkable enhancement in thermomechanical property also points to great promise for plant oil-based methacrylates in developing further high performing sustainable materials in the future.

4.6 References

1. Mcgrail, P. T.; Street, A. C. Structure-Property Relationships in High-Performance Thermoset-Thermoplastic Blends. Makromol. Chem., Macromol. Symp. 1992, 64, 75-84.
2. Jin, F. L.; Li, X.; Park, S. J. Synthesis and Application of Epoxy Resins: A Review. J. Ind. Eng. Chem. 2015, 29, 1-11.

3. Mashouf Roudsari, G.; Mohanty, A. K.; Misra, M. Study of the Curing Kinetics of Epoxy Resins with Biobased Hardener and Epoxidized Soybean Oil. ACS Sustainable Chem. Eng. 2014, 2, 2111-2116.

4. Faye, I.; Decostanzi, M.; Ecochard, Y.; Caillol, S. Eugenol Bio-Based Epoxy Thermosets: From Cloves to Applied Materials. Green Chem. 2017, 19, 5236-5242.

5. Scarica, C.; Suriano, R.; Levi, M.; Turri, S.; Griffini, G. Lignin Functionalized with Succinic Anhydride as Building Block for Biobased Thermosetting Polyester Coatings. ACS Sustainable Chem. Eng. 2018, 6, 3392-3401.

6. Zhao, S.; Huang, X. N.; Whelton, A. J.; Abu-Omar, M. M. Renewable Epoxy Thermosets from Fully Lignin-Derived Triphenols. ACS Sustainable Chem. Eng. 2018, 6, 7600-7608.

7. Jiang, Y.; Ding, D. C.; Zhao, S.; Zhu, H. Y.; Kenttamaa, H. I.; Abu-Omar, M. M. Renewable Thermoset Polymers Based on Lignin and Carbohydrate Derived Monomers. Green Chem. 2018, 20, 1131-1138.

8. Park, S. J.; Jin, F. L.; Lee, J. R. Synthesis and Thermal Properties of Epoxidized Vegetable Oil. Macromol. Rapid Commun. 2004, 25, 724-727.

9. Wang, Z.; Yuan, L.; Ganewatta, M. S.; Lamm, M. E.; Rahman, M. A.; Wang, J.; Liu, S.; Tang, C. Plant Oil-Derived Epoxy Polymers toward Sustainable Biobased Thermosets. Macromol. Rapid Commun. 2017, 38, 1700009.

10. Jian, X.-Y.; An, X.-P.; Li, Y.-D.; Chen, J.-H.; Wang, M.; Zeng, J.-B. All Plant Oil Derived Epoxy Thermosets with Excellent Comprehensive Properties. Macromolecules 2017, 50, 5729-5738.

11. Pan, X.; Sengupta, P.; Webster, D. C. High Biobased Content Epoxy-Anhydride Thermosets from Epoxidized Sucrose Esters of Fatty Acids. Biomacromolecules 2011, 12, 2416-28.

12. Sadler, J. M.; Nguyen, A. P. T.; Toulan, F. R.; Szabo, J. P.; Palmese, G. R.; Scheck, C.; Lutgen, S.; La Scala, J. J. Isosorbide-Methacrylate as a Bio-Based Low Viscosity Resin for High Performance Thermosetting Applications. J. Mater. Chem. A 2013, 1, 12579-12586.

13. Penzel, E., Polyacrylates. In Ullmann's Encyclopedia of Industrial Chemistry, Wiley-VCH Verlag GmbH & Co. KGaA: Weinheim, 2005; 10.1002/14356007.a21_157.

14. Nobel, M. L.; Mendes, E.; Picken, S. J. Acrylic-Based Nanocomposite Resins for Coating Applications. J. Appl. Polym. Sci. 2007, 104, 2146-2156.

15. Montemor, M. F. Functional and Smart Coatings for Corrosion Protection: A Review of Recent Advances. Surf. Coat. Technol. 2014, 258, 17-37.

16. Decker, C. Photoinitiated Crosslinking Polymerisation. Prog. Polym. Sci. 1996, 21, 593-650.

17. Pramudya, I.; Kim, C.; Chung, H. Synthesis and Adhesion Control of Glucose-Based Bioadhesive Via Strain-Promoted Azide–Alkyne Cycloaddition. Polym. Chem. 2018, 9, 3638-3650.

18. Wang, Z.; Yuan, L.; Tang, C. Sustainable Elastomers from Renewable Biomass. Acc. Chem. Res. 2017, 50, 1762-1773.

19. Emerson, J. A.; Garabedian, N. T.; Burris, D. L.; Furst, E. M.; Epps, T. H. Exploiting Feedstock Diversity to Tune the Chemical and Tribological Properties of Lignin-Inspired Polymer Coatings. ACS Sustainable Chem. Eng. 2018, 6, 6856-6866.

20. Sainz, M. F.; Souto, J. A.; Regentova, D.; Johansson, M. K. G.; Timhagen, S. T.; Irvine, D. J.; Buijsen, P.; Koning, C. E.; Stockman, R. A.; Howdle, S. M. A Facile and Green Route to Terpene Derived Acrylate and Methacrylate Monomers and Simple Free Radical Polymerisation to Yield New Renewable Polymers and Coatings. Polym. Chem. 2016, 7, 2882-2887.

21. Li, A.; Li, K. Pressure-Sensitive Adhesives Based on Epoxidized Soybean Oil and Dicarboxylic Acids. ACS Sustainable Chem. Eng. 2014, 2, 2090-2096.

22. Nasiri, M.; Reineke, T. M. Sustainable Glucose-Based Block Copolymers Exhibit Elastomeric and Adhesive Behavior. Polym. Chem. 2016, 7, 5233-5240.

23. Bunker, S. P.; Wool, R. P. Synthesis and Characterization of Monomers and Polymers for Adhesives from Methyl Oleate. Journal of Polymer Science Part a-Polymer Chemistry 2002, 40, 451-458.

24. Ahn, K. B.; Kraft, S.; Wang, D.; Sun, X. S. Thermally Stable, Transparent, Pressure-Sensitive Adhesives from Epoxidized and Dihydroxyl Soybean Oil. Biomacromolecules 2011, 12, 1839-1843.

25. Biermann, U.; Bornscheuer, U.; Meier, M. A.; Metzger, J. O.; Schafer, H. J. Oils and Fats as Renewable Raw Materials in Chemistry. Angew. Chem. Int. Ed. 2011, 50, 3854-3871.

26. Gandini, A.; Lacerda, T. M.; Carvalho, A. J.; Trovatti, E. Progress of Polymers from Renewable Resources: Furans, Vegetable Oils, and Polysaccharides. Chem. Rev. 2016, 116, 1637-1669.

27. Miao, S.; Wang, P.; Su, Z.; Zhang, S. Vegetable-Oil-Based Polymers as Future Polymeric Biomaterials. Acta Biomater. 2014, 10, 1692-1704.

28. Zhang, C. Q.; Garrison, T. F.; Madbouly, S. A.; Kessler, M. R. Recent Advances in Vegetable Oil-Based Polymers and Their Composites. Prog. Polym. Sci. 2017, 71, 91-143.

29. Lligadas, G.; Ronda, J. C.; Galia, M.; Cadiz, V. Renewable Polymeric Materials from Vegetable Oils: A Perspective. Mater. Today 2013, 16, 337-343.

30. Bunker, S.; Staller, C.; Willenbacher, N.; Wool, R. Miniemulsion Polymerization of Acrylated Methyl Oleate for Pressure Sensitive Adhesives. Int. J. Adhes. Adhes. 2003, 23, 29-38.

31. Mosiewicki, M.; Aranguren, M. I.; Borrajo, J. Mechanical Properties of Linseed Oil Monoglyceride Maleate/Styrene Copolymers. J. Appl. Polym. Sci. 2005, 97, 825-836.

32. Tarnavchyk, I.; Popadyuk, A.; Popadyuk, N.; Voronov, A. Synthesis and Free Radical Copolymerization of a Vinyl Monomer from Soybean Oil. ACS Sustainable Chem. Eng. 2015, 3, 1618-1622.

33. Yuan, L.; Wang, Z. K.; Trenor, N. M.; Tang, C. B. Amidation of Triglycerides by Amino Alcohols and Their Impact on Plant Oil-Derived Polymers. Polym. Chem. 2016, 7, 2790-2798.

34. Yuan, L.; Wang, Z. K.; Trenor, N. M.; Tang, C. B. Robust Amidation Transformation of Plant Oils into Fatty Derivatives for Sustainable Monomers and Polymers. Macromolecules 2015, 48, 1320-1328.

35. Chernykh, A.; Alam, S.; Jayasooriya, A.; Bahr, J.; Chisholm, B. J. Living Carbocationic Polymerization of a Vinyl Ether Monomer Derived from Soybean Oil, 2-(Vinyloxy)Ethyl Soyate. Green Chem. 2013, 15, 1834-1838.

36. de Espinosa, L. M.; Ronda, J. C.; Galià, M.; Cádiz, V. A New Route to Acrylate Oils: Crosslinking and Properties of Acrylate Triglycerides from High Oleic Sunflower Oil. J. Polym. Sci., Part A: Polym. Chem. 2009, 47, 1159-1167.

37. Wu, Q.; Hu, Y.; Tang, J.; Zhang, J.; Wang, C.; Shang, Q.; Feng, G.; Liu, C.; Zhou, Y.; Lei, W. High-Performance Soybean-Oil-Based Epoxy Acrylate Resins: "Green" Synthesis and Application in Uv-Curable Coatings. ACS Sustainable Chem. Eng. 2018, 6, 8340-8349.

38. Ahn, B. K.; Kraft, S.; Wang, D.; Sun, X. S. Thermally Stable, Transparent, Pressure-Sensitive Adhesives from Epoxidized and Dihydroxyl Soybean Oil. Biomacromolecules 2011, 12, 1839-1843.

39. Qun, W.; Shoukuan, F.; Tongyin, Y. Emulsion Polymerization. Prog. Polym. Sci. 1994, 19, 703-753.

40. Eliseeva, V. I.; Ivanchev, S. S.; Kuchanov, S. I.; Lebedev, A. V., Emulsion Polymerization and Its Applications in Industry. Springer: USA: New York City, 2012; p 195-213.

41. Asua, J. M. Emulsion Polymerization: From Fundamental Mechanisms to Process Developments. J. Polym. Sci., Part A: Polym. Chem. 2004, 42, 1025-1041.

42. Ragauskas, A. J.; Williams, C. K.; Davison, B. H.; Britovsek, G.; Cairney, J.; Eckert, C. A.; Frederick, W. J., Jr.; Hallett, J. P.; Leak, D. J.; Liotta, C. L.; Mielenz, J. R.; Murphy, R.; Templer, R.; Tschaplinski, T. The Path Forward for Biofuels and Biomaterials. Science 2006, 311, 484-489.

43. Dodds, D. R.; Gross, R. A. Chemistry. Chemicals from Biomass. Science 2007, 318, 1250-1251.

44. Yao, K. J.; Tang, C. B. Controlled Polymerization of Next-Generation Renewable Monomers and Beyond. Macromolecules 2013, 46, 1689-1712.

45. Sahu, P.; Bhowmick, A. K. Sustainable Self-Healing Elastomers with Thermoreversible Network Derived from Biomass Via Emulsion Polymerization. J. Polym. Sci., Part A: Polym. Chem. 2019, 57, 738-751.

46. Booth, G.; Delatte, D. E.; Thames, S. F. Incorporation of Drying Oils into Emulsion Polymers for Use in Low-Voc Architectural Coatings. Ind. Crops Prod. 2007, 25, 257-265.

47. Chern, C. S. Emulsion Polymerization Mechanisms and Kinetics. Prog. Polym. Sci. 2006, 31, 443-486.

48. Molina-Gutiérrez, S.; Ladmiral, V.; Bongiovanni, R.; Caillol, S.; Lacroix-Desmazes, P. Radical Polymerization of Biobased Monomers in Aqueous Dispersed Media. Green Chem. 2018, 10.1039/C8GC02277A.

49. Wang, J.; Lu, C.; Liu, Y.; Wang, C.; Chu, F. Preparation and Characterization of Natural Rosin Stabilized Nanoparticles Via Miniemulsion Polymerization and Their Pressure-Sensitive Adhesive Applications. Ind. Crops Prod. 2018, 124, 244-253.

50. Moreno, M.; Goikoetxea, M.; Barandiaran, M. J. Biobased-Waterborne Homopolymers from Oleic Acid Derivatives. J. Polym. Sci., Part A: Polym. Chem. 2012, 50, 4628-4637.

51. Moreno, M.; Miranda, J. I.; Goikoetxea, M.; Barandiaran, M. J. Sustainable Polymer Latexes Based on Linoleic Acid for Coatings Applications. Prog. Org. Coat. 2014, 77, 1709-1714.

52. Moreno, M.; Goikoetxea, M.; de la Cal, J. C.; Barandiaran, M. J. From Fatty Acid and Lactone Biobased Monomers toward Fully Renewable Polymer Latexes. J. Polym. Sci., Part A: Polym. Chem. 2014, 52, 3543-3549.

53. Boscán, F.; Paulis, M.; Barandiaran, M. J. Towards the Production of High Performance Lauryl Methacrylate Based Polymers through Emulsion Polymerization. Eur. Polym. J. 2017, 93, 44-52.

54. Demchuk, Z.; Kohut, A.; Voronov, S.; Voronov, A. Versatile Platform for Controlling Properties of Plant Oil-Based Latex Polymer Networks. ACS Sustainable Chem. Eng. 2018, 6, 2780-2786.

55. Demchuk, Z.; Shevchuk, O.; Tarnavchyk, I.; Kirianchuk, V.; Lorenson, M.; Kohut, A.; Voronov, S.; Voronov, A. Free-Radical Copolymerization Behavior of Plant-Oil-Based Vinyl Monomers and Their Feasibility in Latex Synthesis. ACS Omega 2016, 1, 1374-1382.

56. Demchuk, Z.; Kirianchuk, V.; Kingsley, K.; Voronov, S.; Voronov, A. Plasticizing and Hydrophobizing Effect of Plant Oil Based Acrylic Monomers in Latex Copolymers with Styrene and Methyl Methacrylate. Int. J. Theor. Appl. Nanotechnol. 2018, 6, 29-37.

57. Kingsley, K.; Shevchuk, O.; Demchuk, Z.; Voronov, S.; Voronov, A. The Features of Emulsion Copolymerization for Plant Oil-Based Vinyl Monomers and Styrene. Ind. Crops Prod. 2017, 109, 274-280.

58. Jensen, A. T.; Couto de Oliveira, A. C.; Goncalves, S. B.; Gambetta, R.; Machado, F. Evaluation of the Emulsion Copolymerization of Vinyl Pivalate and Methacrylated Methyl Oleate. J. Appl. Polym. Sci. 2016, 133, 44129.

59. Jensen, A. T.; Sayer, C.; Araujo, P. H. H.; Machado, F. Emulsion Copolymerization of Styrene and Acrylated Methyl Oleate. Eur. J. Lipid Sci. Technol. 2014, 116, 37-43.

60. Bunker, S. P.; Wool, R. P. Synthesis and Characterization of Monomers and Polymers for Adhesives from Methyl Oleate. J. Polym. Sci., Part A: Polym. Chem. 2002, 40, 451-458.

61. Kohut, A.; Demchuk, Z.; Kingsley, K.; Voronov, S.; Voronov, A. Dual Role of Methyl-B-Cyclodextrin in the Emulsion Polymerization of Highly Hydrophobic Plant Oil-Based Monomers with Various Unsaturations. Eur. Polym. J. 2018, 108, 322-328.

62. Leyrer, R. J.; Mächtle, W. Emulsion Polymerization of Hydrophobic Monomers Like Stearyl Acrylate with Cyclodextrin as a Phase Transfer Agent. Macromol. Chem. Phys. 2000, 201, 1235-1243.

63. Ferguson, C. J.; Hughes, R. J.; Pham, B. T. T.; Hawkett, B. S.; Gilbert, R. G.; Serelis, A. K.; Such, C. H. Effective Ab Initio Emulsion Polymerization under Raft Control. Macromolecules 2002, 35, 9243-9245.

64. Crosbie, D.; Stubbs, J.; Sundberg, D. Catalytic Emulsion Polymerization of Olefins: Ab-Initio Polymerization of a Family of Norbornene-Derived Monomers. Macromolecules 2008, 41, 2445-2450.

65. Wang, Z.; Yuan, L.; Trenor, N. M.; Vlaminck, L.; Billiet, S.; Sarkar, A.; Du Prez, F. E.; Stefik, M.; Tang, C. Sustainable Thermoplastic Elastomers Derived from Plant Oil and Their "Click-Coupling" Via Tad Chemistry. Green Chem. 2015, 17, 3806-3818.

66. Song, L. Z.; Wang, Z. K.; Lamm, M. E.; Yuan, L.; Tang, C. B. Supramolecular Polymer Nanocomposites Derived from Plant Oils and Cellulose Nanocrystals. Macromolecules 2017, 50, 7475-7483.

67. Yuan, L.; Wang, Z.; Ganewatta, M. S.; Rahman, M. A.; Lamm, M. E.; Tang, C. A Biomass Approach to Mendable Bio-Elastomers. Soft Matter 2017, 13, 1306-1313.

68. Lamm, M. E.; Wang, Z.; Zhou, J.; Yuan, L.; Zhang, X.; Tang, C. Sustainable Epoxy Resins Derived from Plant Oils with Thermo- and Chemo-Responsive Shape Memory Behavior. Polymer 2018, 144, 121-127.

69. Asua, J. M. Challenges for Industrialization of Miniemulsion Polymerization. Prog. Polym. Sci. 2014, 39, 1797-1826.

70. Bacon, R. G. R. The Initiation of Polymerisation Processes by Redox Catalysts. Quarterly Reviews 1955, 9, 287-310.

71. Juita; Dlugogorski, B. Z.; Kennedy, E. M.; Mackie, J. C. Low Temperature Oxidation of Linseed Oil: A Review. Fire Sci. Rev. 2012, 1, 3.

72. Soucek, M. D.; Khattab, T.; Wu, J. Review of Autoxidation and Driers. Prog. Org. Coat. 2012, 73, 435-454.

73. Greimel, K. J.; Perz, V.; Koren, K.; Feola, R.; Temel, A.; Sohar, C.; Acero, E. H.; Klimant, I.; Guebitz, G. M. Banning Toxic Heavy-Metal Catalysts from Paints: Enzymatic Cross-Linking of Alkyd Resins. Green Chem. 2013, 15, 381-388.

74. Oyman, Z. O.; Ming, W.; van der Linde, R. Oxidation of Drying Oils Containing Non-Conjugated and Conjugated Double Bonds Catalyzed by a Cobalt Catalyst. Prog. Org. Coat. 2005, 54, 198-204.

CHAPTER 5

SUSTAINABLE EPOXY RESINS DERIVED FROM PLANT OILS WITH THERMO- AND CHEMO-RESPONSIVE SHAPE MEMORY BEHAVIOR

Lamm, M.; Wang, Z.; Zhou, J.; Yuan, L.; Zhang, X.; Tang, C., Sustainable epoxy resins derived from plant oils with thermo- and chemo-responsive shape memory behavior *Polymer*, **2018**, *144*, 121-127.

5.1 Abstract

Shape-memory epoxy resins were synthesized using plant oils and cellulose nanocrystals (CNCs). Epoxidized soybean homopolymers (PESBMA) were grafted from CNCs using surface-initiated atom transfer radical polymerization (SI-ATRP). The polymer grafted CNCs were combined with P(ESBMA-*co*-SBMA) copolymer and cured using anhydride to prepare epoxy resins. Controlling weight fractions of CNCs and ratios of epoxide to anhydride provided tunability over mechanical and thermal properties. The grafted polymer nanocomposites were also compared to simple blends to confirm better properties of the grafted system. Thermo- and chemo-responsive shape memory properties were obtained for these materials.

5.2 Introduction

Shape memory polymers (SMPs) are a class of smart materials that can change functions upon exposure to external stimuli, such as temperature, pH, solvation, or electricity.[1-4] Most of these materials utilize petroleum-based chemicals for their components. Recent advances have focused on making sustainable SMPs from renewable resources for a variety of applications, including biomedical uses.[5-11] SMPs typically involve two separate networks: a permanent network and a temporary or switchable network. The permanent network is needed to maintain a permanent shape while the switchable network is responsible for allowing induction of a temporary shape resulting from a stimulus. In general, the easiest and most widely used switchable SMPs are thermo-responsive, in which the switching temperature, often the glass transition temperature (T_g) of the temporary network polymers, is just above room temperature.

The two networks in a SMP serve different functions and therefore require distinct chemistries. Specifically, the first, permanent network serves to control and return the material to the primary permanent shape. This can be achieved using covalent bonding. The second network, the temporary or switchable network, utilizes dynamic interactions such as hydrogen bonding or other exploitable properties such as crystallization. Many systems have utilized nanocrystals or nanomaterials to achieve the response, such as graphene oxide, magnetite, silica, and polymers like polylactic acid (PLA) and polycaprolactone (PCL), which help strengthen the permanent network and provide a switchable network through crystallinity.[12-22]

Cellulose, specifically cellulose nanocrystals (CNCs), possesses crystallinity and high mechanical strength, and shows potential for the preparation of entirely biobased shape memory polymers.[23-31] Similarly, plant oil based polymer materials have shown promise in the preparation of shape memory polymers.[32-34] Our group successfully synthesized SMPs using CNCs and soybean oil, where the permanent network was achieved through triazolinedione (TAD) crosslinking chemistry.[5] However, a more economical and industry-benign approach is epoxy curing chemistry.[35] We recently demonstrated the preparation of biobased epoxy resins from soybean polymers.[36,37] Herein we present thermo- and chemo-responsive shape memory composites using supramolecular soybean epoxy resins with CNCs, utilizing epoxy curing to form a permanent network while hydrogen-bonding and T_g induced a dynamic network. The response of hydrogen bonding and T_g allows thermal and chemical triggers. CNCs were grafted with soybean polymers via surface-initiated atom transfer radical polymerization (SI-ATRP).

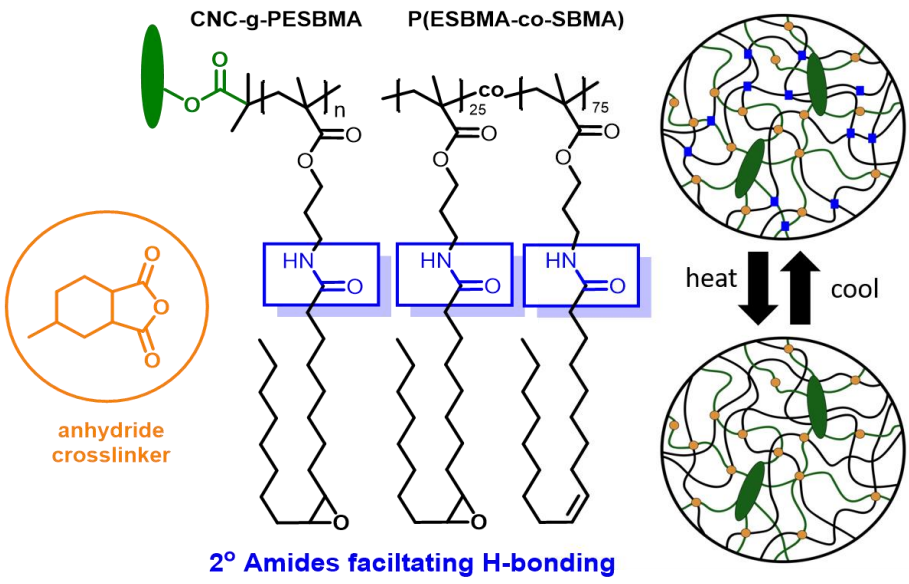

Figure 5.1. Shape memory polymers using soybean oil polymers and cellulose nanocrystals containing epoxy-curing networks and supramolecular hydrogen-bonding networks.

5.3 Experimental

Materials

Plenish high oleic soybean oil (HOSO) was provided by DuPont Pioneer. Cellulose nanocrystals were provided by CelluForce (Canada). Azobisisobutyronitrile (AIBN, 98%, Aldrich) was recrystallized twice from methanol. Monomers were run through basic alumina to remove inhibitors. All other reagents were from commercial resources and used as received unless otherwise mentioned. Soybean methacrylate (SBMA) and epoxidized soybean methacrylate (ESBMA) were prepared according to our previous work (Scheme S1).[26, 36, 38-42] Bromoisobutyryl bromide-coated cellulose nanocrystal as initiators (CNC-Br) were synthesized according to literature.[5, 43]

Characterization

300 MHz ^{1}H NMR spectra were recorded on a Bruker Avance III HD 300 spectrometer using $CDCl_3$ as solvent with tetramethylsilane (TMS) as an internal reference. Molecular weight and molecular weight distribution of polymers were determined by gel permeation chromatography (GPC) on a Waters system equipped with a 515 HPLC pump, a 2410 refractive index detector, and three Styragel columns (HR1, HR3, HR5E in the effective molecular weight range of 100-5,000 g/mol, 500-30,000 g/mol, and 5,000-500,000 g/mol, respectively) with HPLC grade tetrahydrofuran (THF) as the eluent at 30 ^oC and a flow rate of 1.0 mL/min. THF and polymer solutions were filtered through microfilters with an average pore size of 0.2 μm. The columns were calibrated against polystyrene standards. GPC samples were prepared by dissolving the sample in THF with a concentration of 5.0 mg/mL and passing through microfilters with average pore size of 0.2 μm. Fourier transform infrared spectrometry (FTIR) spectra were taken on a PerkinElmer spectrum 100 FTIR spectrometer. Zetasizer nano instrument, equipped with an 830 nm wavelength laser, was used to determine the hydrodynamic radius (R_h) of CNCs and CNC-g-PSBMA. X-ray photoelectron spectroscopy (XPS) measurements were carried out on a Thermo-VG Scientific ESCALAB 250 X-ray photoelectron spectrometer. The glass transition temperature (T_g) of polymers was tested through differential scanning calorimetry (DSC) conducted on a DSC 2000 instrument (TA Instruments). Samples were first heated from −70 to +200 °C at a rate of 10 °C/min. After cooling down to −70 °C at the same rate, the data was collected from the second heating scan. About 8 mg of each sample was used for the DSC test with nitrogen gas at a flow rate of 50 mL/min. Dynamic thermomechanical analysis (DMA) was performed by using a Q800 DMA (TA Instruments). The DMA

spectra were scanned with a frequency of 10 Hz and a heating rate of 3 ^{o}C/min. All the shape memory tests were carried out in a stress controlled thin film tension mode. Thermogravimetric analysis (TGA) was conducted on a Q5000 TGA system (TA Instruments), ramping from 25 to 600 °C with a rate of 10 °C/min. About 10 mg of sample was used per test. Tensile stress−strain testing was carried out with an Instron 5543A testing instrument. The films were prepared by dissolving 1 g of polymers in 15 mL of solvent. The solution of polymers was poured in a PTFE mold. After the evaporation of solvent over 72 h, the film was put under vacuum for 4 h at room temperature followed by 4 h at 60 °C. Dog-bone shaped specimens were cut from the cast film with a length of 20 mm and width of 5.0 mm. The thickness was measured prior to each measurement. Testing was done at room temperature with a crosshead speed of 20 mm/min. Five replicate samples were used to obtain an average value for each.

Synthesis of CNC-g-PESBMA by SI-ATRP

CNC-Br (104 mg, 0.0466 mmol of Br), ESBMA (3.00 g, 7.13 mmol), tris[2-(dimethylamino)ethyl]amine (Me_6TREN) (23 mg, 0.1 mmol), THF (1.0 mL) and dimethylformamide (DMF) (1.0 mL) were introduced to a 10 mL Schlenk flask. The solution was degassed by three freeze−pump−thaw cycles and sealed. Cu(I)Br (14.4 mg, 0.1 mmol) was added during the last cycle. The flask was sealed under nitrogen and placed into an oil bath set at 90 °C. After 36-72 h, the polymerization was stopped by opening the flask and exposing the reactive mixture to air. THF was added to the mixture, and the product was precipitated into cold methanol three times. The resulting polymer was dried under vacuum at 40 °C.

Synthesis of P(ESBMA-co-SBMA) Copolymer

ESBMA (3.00 g, 7.13 mmol), SBMA (9.00 g, 21.4 mmol), AIBN (46.9 mg, 0.285 mmol) and dry toluene (12 mL) were introduced to a 50 mL round bottom flask. The flask was sealed, purged with nitrogen for 20 minutes and placed into an oil bath at 75 °C. After 7 h, the polymerization was stopped by opening the flask and exposing the reactive mixture to air. THF was added to the mixture, and the product was precipitated into cold methanol three times. The resulting polymer was dried under vacuum at 40 °C.

Synthesis of Epoxy Resins

A typical procedure was as follows: CNC-*g*-PESBMA (0.5 g) was dispersed in 1 mL DMF. To this solution was added P(ESBMA-*co*-SBMA) (0.5 g), 4-methycyclohexan-1,2-dicarboxylic anhydride (39.2 mg, 0.675 mmole), 1,8-diazabicyclo [5.4.0] undec-7-ene (DBU) (10 mg), and 5 mL THF. The solutions were sonicated for 5 minutes, degassed, and poured into Teflon molds. Solvents were evaporated at room temperature over 72 hours. The films were then placed into an oven under vacuum for 24 hours and heated under vacuum at 50 ºC for 24 hours. Finally, the films were cured at 100 ºC for 24 hours.

5.4 Results & Discussion

Synthesis of Soybean Polymers and Epoxy Resins

SMPs were synthesized in multiple steps. First, CNC-Br as an initiator was synthesized using a procedure reported earlier.[43] This reaction involves the esterification of hydroxyl groups on CNCs using bromoisobutyryl bromide (BIBr). The initiator was characterized by FTIR and XPS, which allowed the determination of grafted bromine sites on the surface of CNC (**Figure 5.3** and **Table 5.1**). The CNC-Br was determined to have ~1.3 wt%

bromine from the bromoisobutyryl groups functionalized onto the surface (first reaction in **Figure 5.2**).

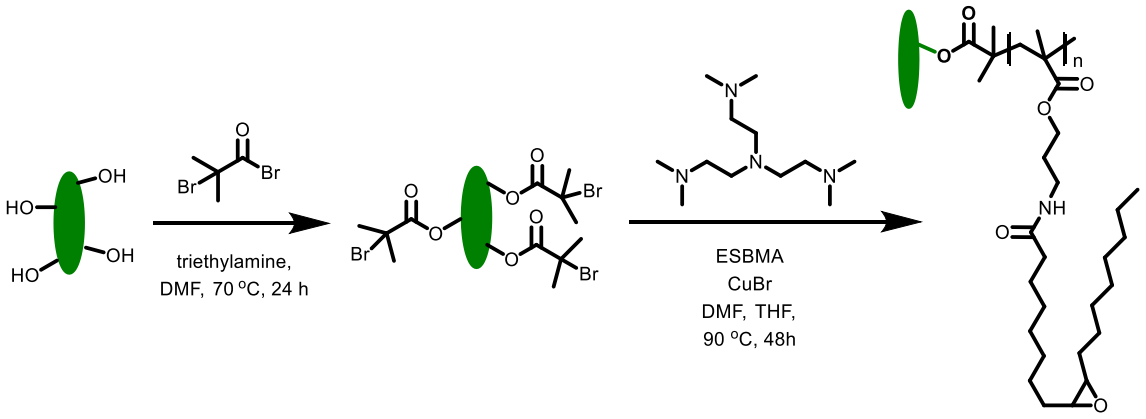

Figure 5.2. Synthesis of CNC-*g*-PESBMA by SI-ATRP using CNC-Br as initiator.

Epoxidized soybean methacrylate monomer (ESBMA) was prepared using a reported method.[42] Soybean oil was transformed into a fatty alcohol, which was subsequently epoxidized using 3-chloroperoxybenzoic acid (m-CPBA). The epoxidized soybean alcohol was reacted with methacrylic anhydride using a base catalyst to prepare the soybean epoxy monomer. CNC-*g*-PESBMA was subsequently synthesized by SI-ATRP, as shown in **Figure 5.2**. The final grafted polymer was characterized by ^{1}H NMR and XPS (**Figure 5.3** and **Table 5.1**). XPS data confirmed the presence of bromine and nitrogen respectively on grafted CNC initiators and polymers. The absence of bromine in CNC-*g*-PESBMA could be due to Br content below the detection limit, given the dramatic decrease of bromine after polymers were grafted.

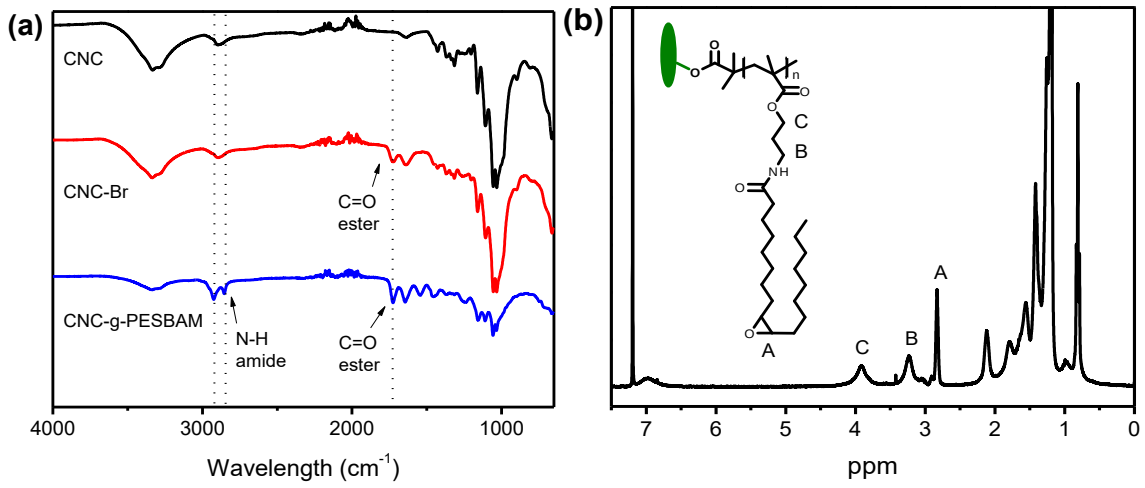

Figure 5.3. (a) FTIR spectra of CNC, CNC-Br, and CNC-*g*-PESBMA; (b) ^{1}H NMR spectrum of CNC-*g*-PESBMA.

Table 5.1. XPS data (atomic percentages) comparing the bare CNC, CNC-Br, and CNC-*g*-PESBMA.

	% O 1s	**% C 1s**	**% Br 3d**	**% N 1s**	**O/C**
Bare CNC	44.3	55.7	---	---	0.79
CNC-Br	40.8	57.9	1.3	---	0.70
CNC-g-PESBMA	28.1	67.3	---	4.6	0.42

The weight content of cellulose in the grafted polymer was determined to be 3.9 wt% using conversion and ratio of initiator to monomer via ^{1}H NMR. Higher amount of cellulose resulted in poor dispersion of the CNC-Br initiators in the polymerization solvent system likely due to a lack of solubility. The number average molecular weight (M_n = 49.5 KDa) was determined theoretically using ^{1}H NMR (to obtain conversion, $[M]_o/[I]_o$ = 150, M_o = 424 g/mol), and a T_g of 20 ^{o}C was determined by DSC. P(ESBMA-*co*-SBMA)

copolymers were synthesized using free radical polymerization. The P(ESBMA-*co*-SBMA) copolymer used for blending has a M_n of 40.7 KDa and a T_g of 13 ^{o}C. CNC-*g*-PESBMA grafted polymer was blended with P(ESBMA-*co*-SBMA) copolymers. The control of composition between ESBMA and SBMA allowed for control of mechanical properties for tailored materials. Subsequent crosslinking can form epoxy resins.

Mechanical Properties of Soy Polymers and Epoxy Resins

To prepare epoxy resins, P(ESBMA-co-SBMA) was dispersed in THF. The mixture was crosslinked by 4-methycyclohexan-1,2-dicarboxylic anhydride with DBU as a catalyst. Various ratios of epoxide to anhydride were used to optimize mechanical properties (**Figure 5.4a**). A ratio of epoxide to anhydride at 2:1 produced the strongest and toughest films, while lower ratios resulted in poor mechanical properties and higher ratios reduced toughness. With the ratio of epoxide to anhydride at 2:1, four samples were synthesized with weight fraction of CNCs in the range of 0 to 1.8 wt% using a combination of grafted and copolymer (**Figure 5.4b**). There was a marked decrease in toughness with introduction of CNCs. It is likely due to the increase in epoxide crosslinkers with increasing amount of CNC-*g*-PESBMA polymer. Grafted CNC composites were also compared with simple blends of CNCs and polymers (**Figure 5.4c**). The grafted materials showed a significant change in mechanical properties with a decrease in elasticity, likely due to an increase in crosslinking. In comparison, simple blends between epoxy polymer and cellulose lacked noticeable robustness. This is likely caused by the lack of good interactions between the CNC filler and polymer matrix in the blend.

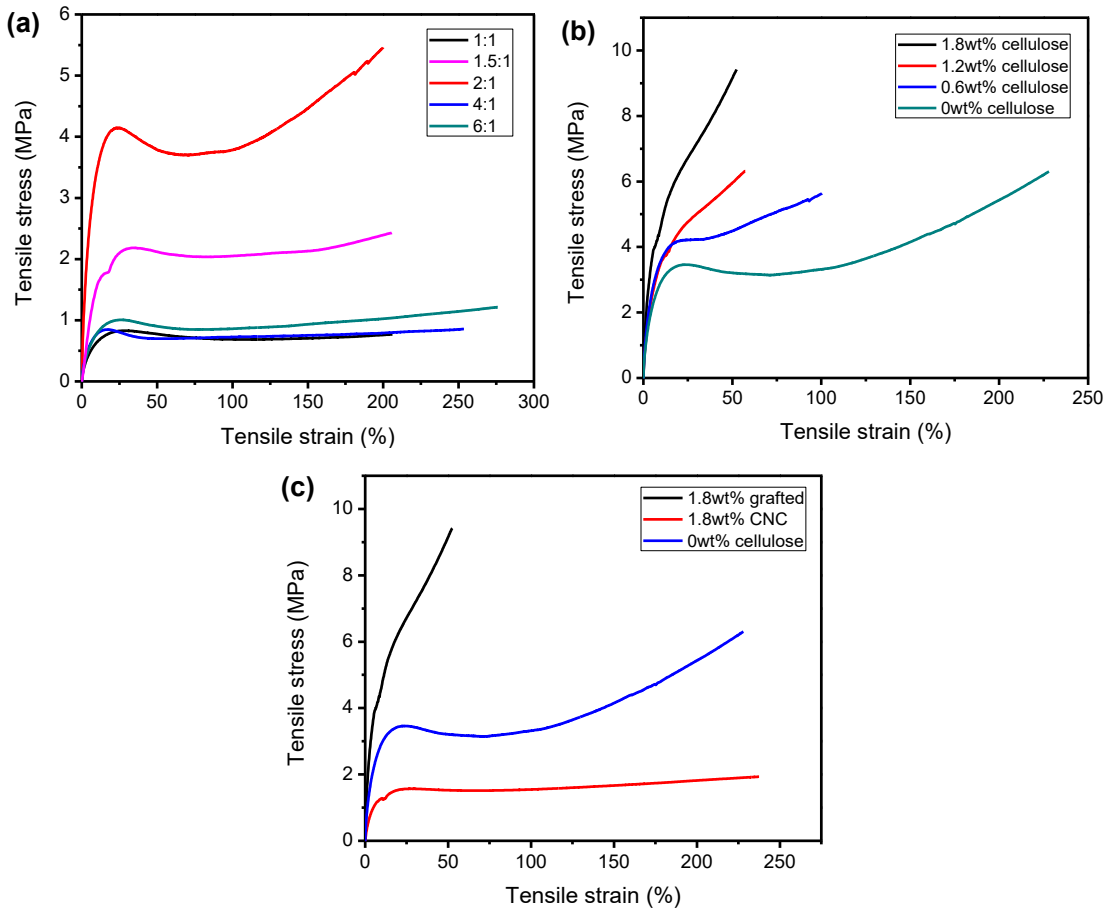

Figure 5.4. Tensile curves: (a) epoxy resins featuring various ratios of epoxide to anhydride of virgin polymer without cellulose; (b) epoxy resins featuring varying weight fractions of CNCs using a ratio of epoxide to anhydride of 2:1. (c) comparing the grafted polymer, free polymer, and a blended nanocomposite.

Dynamic mechanical analysis (DMA) was performed on the epoxy resins to help determine their mechanical behavior (**Figure 5.5**). Resins with three different fractions of CNCs (0.6 wt%, 1.2 wt%, and 1.8 wt%) displayed similar loss modulus and storage modulus above room temperature, with a clear plateau starting at 50 ^{o}C for the 0.6 wt% resins around 5000 MPa. The rubbery plateau for the 1.2 and 1.8 wt% resins begins later above 70 ^{o}C around 600 MPa. Unfortunately, the resins with 1.2 wt% and 1.8 wt% CNCs were quite brittle, with complete breakage of samples above 80 ^{o}C, which did not occur for the 0.6 wt% sample. Thus, the resin with 0.6 wt% CNC was chosen as the sample for the

remainder of testing, as it maintained desirable flexibility, did not break before reaching a complete rubbery plateau, and maintained a higher storage modulus at increased temperature.

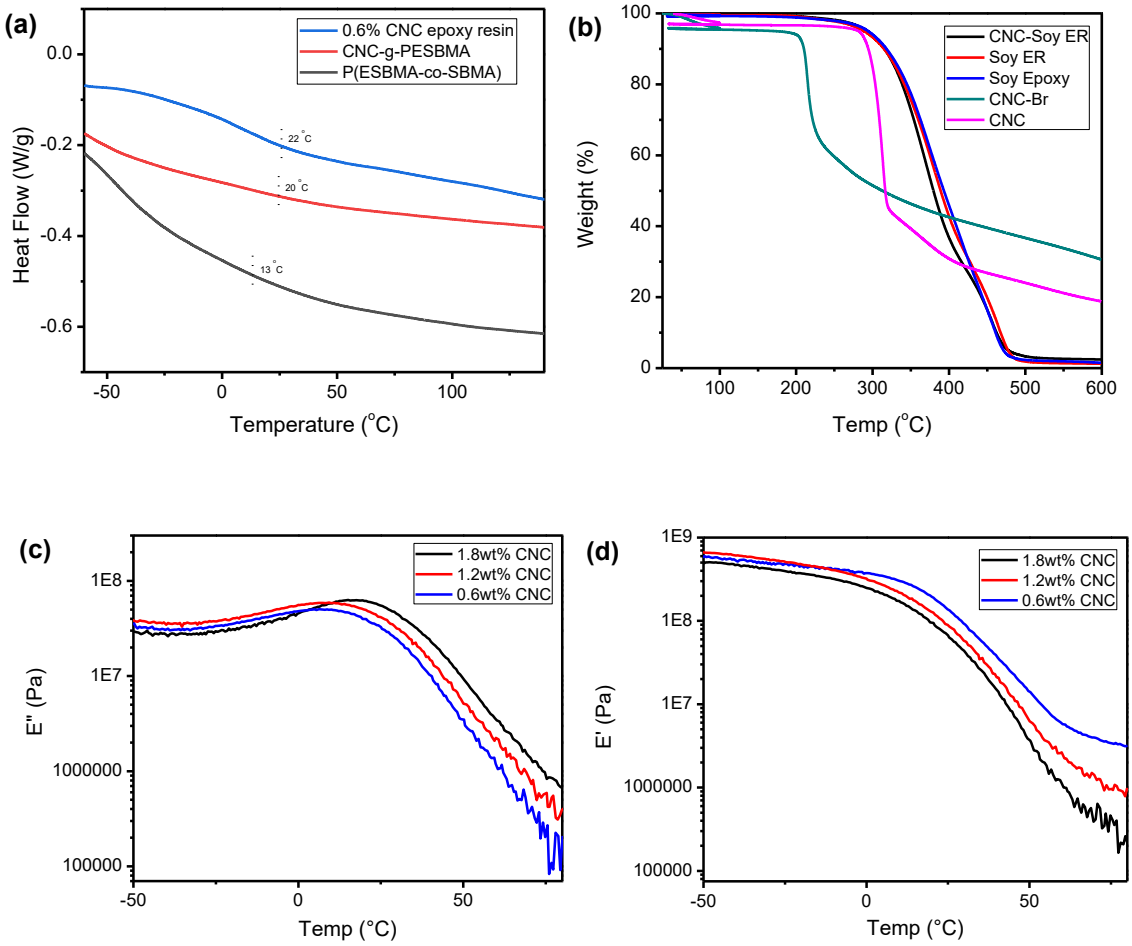

Figure 5.5. (a) DSC curves of 0.6wt% CNC epoxy resin, CNC-*g*-PESBMA, and P(ESBMA-*co*-SBMA) copolymer. (b) TGA data for the various materials. (c) Loss modulus and (d) Storage modulus of the epoxy resins containing various wt% of CNC.

Thermal Properties of Soy Polymers and Epoxy Resins

DSC and DMA were used to determine the T_g of polymers and corresponding epoxy resins. DSC provided comparison of T_g between virgin free copolymer, grafted polymer, and epoxy resin, whereas DMA allowed for a more sensitive measurement of T_g for the

epoxy resin (**Figure 5.5**). Incorporation of CNCs into soybean polymers resulted in a slightly higher T_g, where P(ESBMA-*co*-SBMA) has a T_g of 13 ^oC, versus 20 ^oC for CNC-*g*-PESBMA. The final epoxy resin containing 0.6 wt% cellulose has a T_g of 22 ^oC; however, DMA showed a T_g of 12 ^oC using the sigmoidal change in storage modulus. All polymers and epoxy resins showed high thermal stability, with 10 wt% loss at 315-318 ^oC. (**Table 5.2** and **Figure 5.5**).

Table 5.2. Thermal properties of grafted copolymer, free soybean copolymer and the epoxy resin. T_g was measured using DSC.

Samples	**Tg (^oC)**	**Temperature of 10% weight loss (T_{d10}, ^oC)**
P(ESBMA-co-SBMA)	13	318
CNC-g-PESBMA	20	315
0.6wt% CNC Epoxy Resin	22	315

Thermo- and Chemo-Responsive Shape Memory Properties

These epoxy resins were expected to exhibit shape memory properties. The polymer matrix is made up of two separate networks. The permanent network involves crosslinking due to epoxide curing. The switchable network involves hydrogen bonding between hydroxyl groups on cellulose and secondary amides on the soybean polymers. Once heated above the T_g, the polymer chains could significantly reduce hydrogen bonding network and enhance chain mobility, allowing deformation of polymers into a temporary shape. When polymers are cooled under stress, chains are locked with stressed conformation as the hydrogen bonding resumes. If polymers are heated again, the hydrogen bonding is again

disrupted, and the polymer films quickly return to the thermodynamically favored permanent shape.

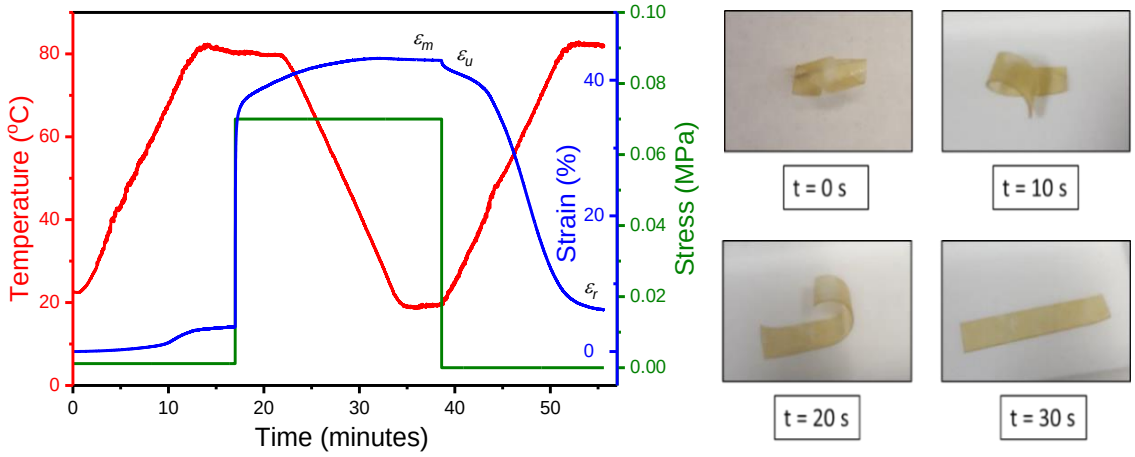

Figure 5.6. Dual (stress- and temperature-) programmed shape memory testing of epoxy resin with 0.6 wt% CNC; photos of films show time-dependent recovery.

As shown in **Figure 5.6**, stress- and temperature-programmed DMA was used to quantitatively analyze the shape memory properties of epoxy resins. The epoxy resin with 0.6 wt% CNC was heated to 80 °C and deformed under constant stress (0.07 MPa). A strain of 42 % was obtained within 5 min. Following deformation, the film was cooled to 20 °C under the same stress (0.07 MPa). After cooling, the stress was released and the strain was tracked as the sample was reheated to 80 °C. Shape fixity was used to determine how well the polymer holds the stimulated temporary shape after removal of stress. According to equation 1,

(1) $$R_f = \frac{\varepsilon_u}{\varepsilon_m} \times 100\%$$

where $\mathcal{E}_m$ is the strain after stretching and fixing for temporary shape and $\mathcal{E}_u$ is the strain after removal of stress, the shape fixity ratio was calculated to be 96.7 %. Shape recovery

was used to determine how well the polymer recovers back to the original permanent shape. According to equation 2,

(2) $$R_{r1} = \frac{\varepsilon_r}{\varepsilon_u} \times 100\%$$

where $\mathcal{E}_r$ is the strain after recovery from temporary shape, the shape recovery ratio was calculated to be 85.4 %.

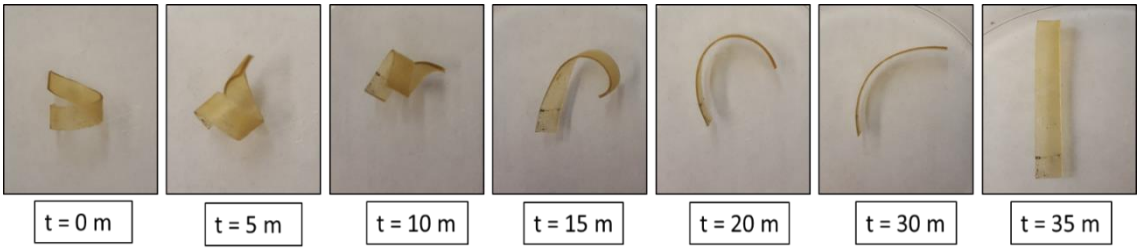

Figure 5.7. Time-dependent chemo-responsive shape memory testing in methanol at room temperature.

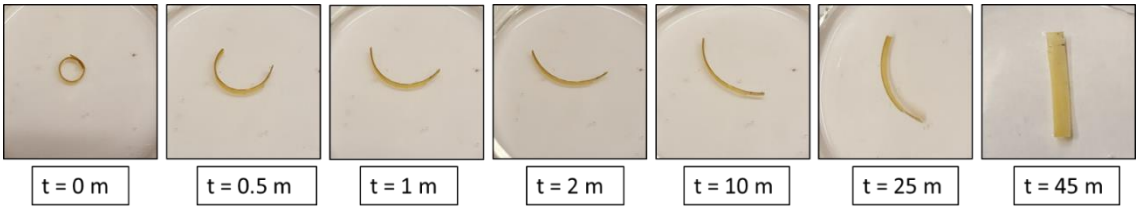

Figure 5.8. Time-dependent chemo-responsive shape memory testing in water at 40 ^{o}C.

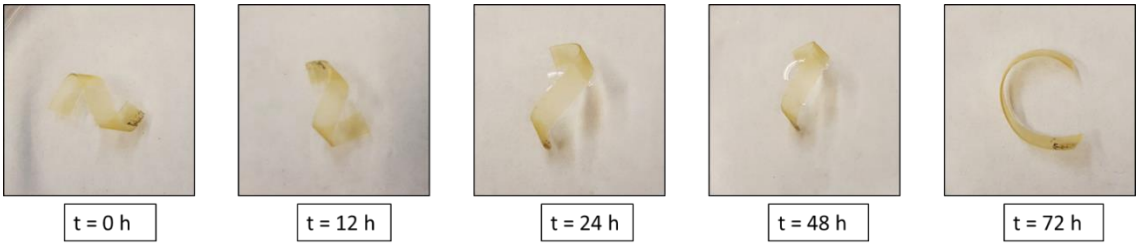

Figure 5.9. Time-dependent chemo-responsive shape memory. Samples are at room temperature and water submersed.

Beyond thermo-responsive properties, other stimuli to the disruption of hydrogen bonds can also serve to stimulate the shape memory response of these composite materials.[44] Chemo-responsive behaviors were tested using solvents that could disrupt H-bonding, such as water and methanol. Methanol can easily be absorbed into the polymer matrix and interrupt hydrogen bonding within the polymer, leading to a return to the permanent shape in 35 minutes (**Figure 5.7**). Water can also interrupt hydrogen bonds; however, water molecules exhibited slower diffusion into the polymer matrix than methanol, resulting in incomplete recovery while films were submersed at room temperature (**Figure 5.9**). When heated to 40 ^{o}C, a combination of thermo- and chemo-response can accelerate shape recovery in just 45 minutes in water (**Figure 5.8**).

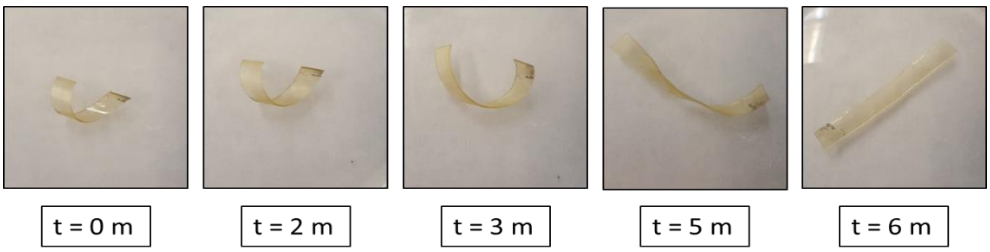

Figure 5.10. Time-dependent chemo-responsive shape memory. Samples are at room temperature and sealed in a container with THF vapor.

Although THF is an aprotic polar solvent that cannot hydrogen bond itself, its vapor easily penetrated into the polymer matrix and caused quick return to the original shape in 6 minutes (**Figure 5.10**). THF vapors serve to plasticize the polymer matrix, decreasing T_g and increasing flexibility and rubbery properties. When exposed to THF vapor, the polymer gained flexibility and caused faster recovery to the entropically favored original permanent shape.

5.5 Conclusions

Epoxy resins were synthesized using soybean oil and cellulose nanocrystals via SI-ATRP. The resulting materials showed both thermo- and chemo-responsive shape memory. All synthesized polymers can be easily characterized to determine mechanical and thermal properties. These results indicate high thermal stability and excellent strength of the final epoxy resins. Overall, such results for these sustainable epoxy resins demonstrate promising utilization as smart materials.

5.6 References

(1) Hu, J.; Zhu, Y.; Huang, H.; Lu, J. Recent advances in shape–memory polymers: Structure, mechanism, functionality, modeling and applications. Prog. Polym. Sci. 2012, 37, 1720-1763.

(2) Xie, T. Recent advances in polymer shape memory. Polymer 2011, 52, 4985-5000.

(3) Jiang, Z. C.; Xiao, Y. Y.; Kang, Y.; Pan, M.; Li, B. J.; Zhang, S. Shape Memory Polymers Based on Supramolecular Interactions. ACS Appl. Mater. Interfaces 2017, 9, 20276-20293.

(4) Montero de Espinosa, L.; Meesorn, W.; Moatsou, D.; Weder, C. Bioinspired Polymer Systems with Stimuli-Responsive Mechanical Properties. Chem. Rev. 2017, 12851–12892.

(5) Wang, Z.; Zhang, Y.; Yuan, L.; Hayat, J.; Trenor, N. M.; Lamm, M. E.; Vlaminck, L.; Billiet, S.; Du Prez, F. E.; Wang, Z.; Tang, C. Biomass Approach toward Robust, Sustainable, Multiple-Shape-Memory Materials. ACS Macro Lett. 2016, 5, 602-606.

(6) Chan, B. Q.; Low, Z. W.; Heng, S. J.; Chan, S. Y.; Owh, C.; Loh, X. J. Recent Advances in Shape Memory Soft Materials for Biomedical Applications. ACS Appl. Mater. Interfaces 2016, 8, 10070-10087.

(7) Pilate, F.; Toncheva, A.; Dubois, P.; Raquez, J.-M. Shape-memory polymers for multiple applications in the materials world. Eur. Polym. J. 2016, 80, 268-294.

(8) Santhosh Kumar, K. S.; Biju, R.; Reghunadhan Nair, C. P. Progress in shape memory epoxy resins. React. Funct. Polym. 2013, 73, 421-430.

(9) Yang, Y.; Urban, M. W. Self-healing polymeric materials. Chem. Soc. Rev. 2013, 42, 7446-7467.

(10) Zhou, J.; Sheiko, S. S. Reversible shape-shifting in polymeric materials. J. Polym. Sci., Part B: Polym. Phys. 2016, 54, 1365-1380.

(11) Ratna, D.; Karger-Kocsis, J. Recent advances in shape memory polymers and composites: a review. J. Mater. Sci. 2008, 43, 254-269.

(12) Lai, S. M.; Lan, Y. C. Shape memory properties of melt-blended polylactic acid (PLA)/thermoplastic polyurethane (TPU) bio-based blends. J. Polym. Res. 2013, 20, 140.

(13) Das, R.; Banerjee, S. L.; Kundu, P. P. Fabrication and characterization of in situ graphene oxide reinforced high-performance shape memory polymeric nanocomposites from vegetable oil. RSC Adv. 2016, 6, 27648-27658.

(14) Lashgari, S.; Karrabi, M.; Ghasemi, I.; Azizi, H.; Messori, M.; Paderni, K. Shape memory nanocomposite of poly(L-lactic acid)/graphene nanoplatelets triggered by infrared light and thermal heating. Express Polym. Lett. 2016, 10, 349-359.

(15) Liu, Y.; Zhao, J.; Zhao, L.; Li, W.; Zhang, H.; Yu, X.; Zhang, Z. High Performance Shape Memory Epoxy/Carbon Nanotube Nanocomposites. ACS Appl. Mater. Interfaces 2016, 8, 311-320.

(16) Montarnal, D.; Capelot, M.; Tournilhac, F.; Leibler, L. Silica-like malleable materials from permanent organic networks. Science 2011, 334, 965-968.

(17) Razzaq, M. Y.; Anhalt, M.; Frormann, L.; Weidenfeller, B. Mechanical spectroscopy of magnetite filled polyurethane shape memory polymers. Mater. Sci. Eng. A 2007, 471, 57-62.

(18) Alvarado-Tenorio, B.; Romo-Uribe, A.; Mather, P. T. Microstructure and Phase Behavior of POSS/PCL Shape Memory Nanocomposites. Macromolecules 2011, 44, 5682-5692.

(19) Lützen, H.; Gesing, T. M.; Kim, B. K.; Hartwig, A. Novel cationically polymerized epoxy/poly(ε-caprolactone) polymers showing a shape memory effect. Polymer 2012, 53, 6089-6095.

(20) Razzaq, M. Y.; Anhalt, M.; Frormann, L.; Weidenfeller, B. Thermal, electrical and magnetic studies of magnetite filled polyurethane shape memory polymers. Mater. Sci. Eng. A 2007, 444, 227-235.

(21) Tsujimoto, T.; Takayama, T.; Uyama, H. Biodegradable Shape Memory Polymeric Material from Epoxidized Soybean Oil and Polycaprolactone. Polymers 2015, 7, 2165-2174.

(22) Tsujimoto, T.; Uyama, H. Full Biobased Polymeric Material from Plant Oil and Poly(lactic acid) with a Shape Memory Property. ACS Sustainable Chem. Eng. 2014, 2, 2057-2062.

(23) Isikgor, F. H.; Becer, C. R. Lignocellulosic biomass: a sustainable platform for the production of bio-based chemicals and polymers. Polym. Chem. 2015, 6, 4497-4559.

(24) Mariano, M.; El Kissi, N.; Dufresne, A. Cellulose nanocrystals and related nanocomposites: Review of some properties and challenges. J. Polym. Sci., Part B: Polym. Phys. 2014, 52, 791-806.

(25) Meesorn, W.; Shirole, A.; Vanhecke, D.; de Espinosa, L. M.; Weder, C. A Simple and Versatile Strategy To Improve the Mechanical Properties of Polymer Nanocomposites with Cellulose Nanocrystals. Macromolecules 2017, 50, 2364-2374.

(26) Wang, Z.; Yuan, L.; Tang, C. Sustainable Elastomers from Renewable Biomass. Acc. Chem. Res. 2017, 50, 1762-1773.

(27) Eichhorn, S. J.; Dufresne, A.; Aranguren, M.; Marcovich, N. E.; Capadona, J. R.; Rowan, S. J.; Weder, C.; Thielemans, W.; Roman, M.; Renneckar, S.; Gindl, W.; Veigel, S.; Keckes, J.; Yano, H.; Abe, K.; Nogi, M.; Nakagaito, A. N.; Mangalam, A.; Simonsen, J.; Benight, A. S.; Bismarck, A.; Berglund, L. A.; Peijs, T. Review: current international research into cellulose nanofibres and nanocomposites. J. Mater. Sci. 2009, 45, 1-33.

(28) Song, L.; Wang, Z.; Lamm, M. E.; Yuan, L.; Tang, C. Supramolecular Polymer Nanocomposites Derived from Plant Oils and Cellulose Nanocrystals. Macromolecules 2017, 50, 7475-7483.

(29) Liu, Y.; Li, Y.; Yang, G.; Zheng, X.; Zhou, S. Multi-Stimulus-Responsive Shape-Memory Polymer Nanocomposite Network Cross-Linked by Cellulose Nanocrystals. ACS Appl. Mater. Interfaces 2015, 7, 4118-4126.

(30) Yu, J.; Liu, Y.; Liu, X.; Wang, C.; Wang, J.; Chu, F.; Tang, C. Integration of renewable cellulose and rosin towards sustainable copolymers by "grafting from" ATRP. Green Chem. 2014, 16, 1854-1864.

(31) Liu, Y.; Yao, K.; Chen, X.; Wang, J.; Wang, Z.; Ploehn, H. J.; Wang, C.; Chu, F.; Tang, C. Sustainable thermoplastic elastomers derived from renewable cellulose, rosin and fatty acids. Polym. Chem. 2014, 5, 3170-3181.

(32) Lligadas, G.; Ronda, J. C.; Galià, M.; Cádiz, V. Renewable polymeric materials from vegetable oils: a perspective. Mater. Today 2013, 16, 337-343.

(33) Miao, S.; Wang, P.; Su, Z.; Zhang, S. Vegetable-oil-based polymers as future polymeric biomaterials. Acta Biomater. 2014, 10, 1692-1704.

(34) Zhang, C.; Garrison, T. F.; Madbouly, S. A.; Kessler, M. R. Recent advances in vegetable oil-based polymers and their composites. Prog. Polym. Sci. 2017, 71, 91-143.

(35) Jin, F.-L.; Li, X.; Park, S.-J. Synthesis and application of epoxy resins: A review. J. Ind. Eng. Chem. 2015, 29, 1-11.

(36) Wang, Z.; Yuan, L.; Ganewatta, M. S.; Lamm, M. E.; Rahman, M. A.; Wang, J.; Liu, S.; Tang, C. Plant Oil-Derived Epoxy Polymers toward Sustainable Biobased Thermosets. Macromol. Rapid Commun. 2017.

(37) Xu, S.; Lamm, M.; Rahman, A.; Zhang, X.; Zhu, T.; Zhao, Z.; Tang, C. Renewable Atom-Efficient Polyesters and Thermosetting Resins Derived from High Oleic Soybean Oil. Green Chem. 2018, DOI: 10.1039/C1037GC03774K.

(38) Ganewatta, M. S.; Ding, W.; Rahman, M. A.; Yuan, L.; Wang, Z.; Hamidi, N.; Robertson, M. L.; Tang, C. Biobased Plastics and Elastomers from Renewable Rosin via “Living” Ring-Opening Metathesis Polymerization. Macromolecules 2016, 49, 7155-7164.

(39) Wang, Z.; Yuan, L.; Trenor, N. M.; Vlaminck, L.; Billiet, S.; Sarkar, A.; Prez, F. E. D.; Stefik, M.; Tang, C. Sustainable thermoplastic elastomers derived from plant oil and their “click-coupling” via TAD chemistry. Green Chem. 2015, 17, 3806–3818.

(40) Yuan, L.; Wang, Z.; Trenor, N. M.; Tang, C. Amidation of triglycerides by amino alcohols and their impact on plant oil-derived polymers. Polym. Chem. 2016, 7, 2790-2798.

(41) Yuan, L.; Wang, Z.; Trenor, N. M.; Tang, C. Robust Amidation Transformation of Plant Oils into Fatty Derivatives for Sustainable Monomers and Polymers. Macromolecules 2015, 48, 1320-1328.

(42) Xu, Y.; Yuan, L.; Wang, Z.; Wilbon, P. A.; Wang, C.; Chu, F.; Tang, C. Lignin and soy oil-derived polymeric biocomposites by “grafting from” RAFT polymerization. Green Chem. 2016, 18, 4974-4981.

(43) Morandi, G.; Heath, L.; Thielemans, W. Cellulose nanocrystals grafted with polystyrene chains through surface-initiated atom transfer radical polymerization (SI-ATRP). Langmuir 2009, 25, 8280-8286.

(44) Du, H.; Zhang, J. Solvent induced shape recovery of shape memory polymer based on chemically cross-linked poly(vinyl alcohol). Soft Matter 2010, 6, 3370-3376.

CHAPTER 6

SUMMARY AND OUTLOOK

Throughout this dissertation work, the use of macromolecular engineering to control polymer topologies and functionalities was discussed in depth. By carefully selecting monomers, and thus the subsequent supramolecular interactions, tailored materials were developed for a variety of applications, including acrylic coatings and epoxy resins. Additionally, the stimuli-responsive properties of these polymeric materials were considered.

In Chapters 2 and 3, supramolecular interactions such as hydrogen-bonding and metal-ligand coordination were used to mimic chain entanglement in plant oil-derived copolymers. Future research could pursue two directions, (1) utilizing additional dynamic bonding and (2) applying these facile strategies to other biomass-sourced monomers (**Figure 6.1**).

Dynamic bonding encompasses not only supramolecular interactions, but reversible covalent reactions. Depending on the dynamic bonding chosen, the resultant polymers could contain dynamic or covalent bonds, both of which can be used to tailor the strength and thus potential applications. Some strategies to explore are listed herein. First, the use of electrostatic interactions through monomer selection, such as pyridinium, sodium acrylate, or other charged monomers. Second, exploiting host-guest interactions by utilizing groups such as cucurbiturils and dendrimers, which can interact with and bind polar polymers. Finally, many reversible covalent reactions can be easily applied to biomass-derived polymers. These include disulfide bonds, Diels-Alder reactions, boronic esters, and a variety of aldehyde/ketone exchangeable reactions on the carbonyl group. Though it should be noted that due to the presence of covalent bonds in these reactions,

conditions necessary to force the reversible reaction might require the inclusion of catalysts, potentially limiting applications.

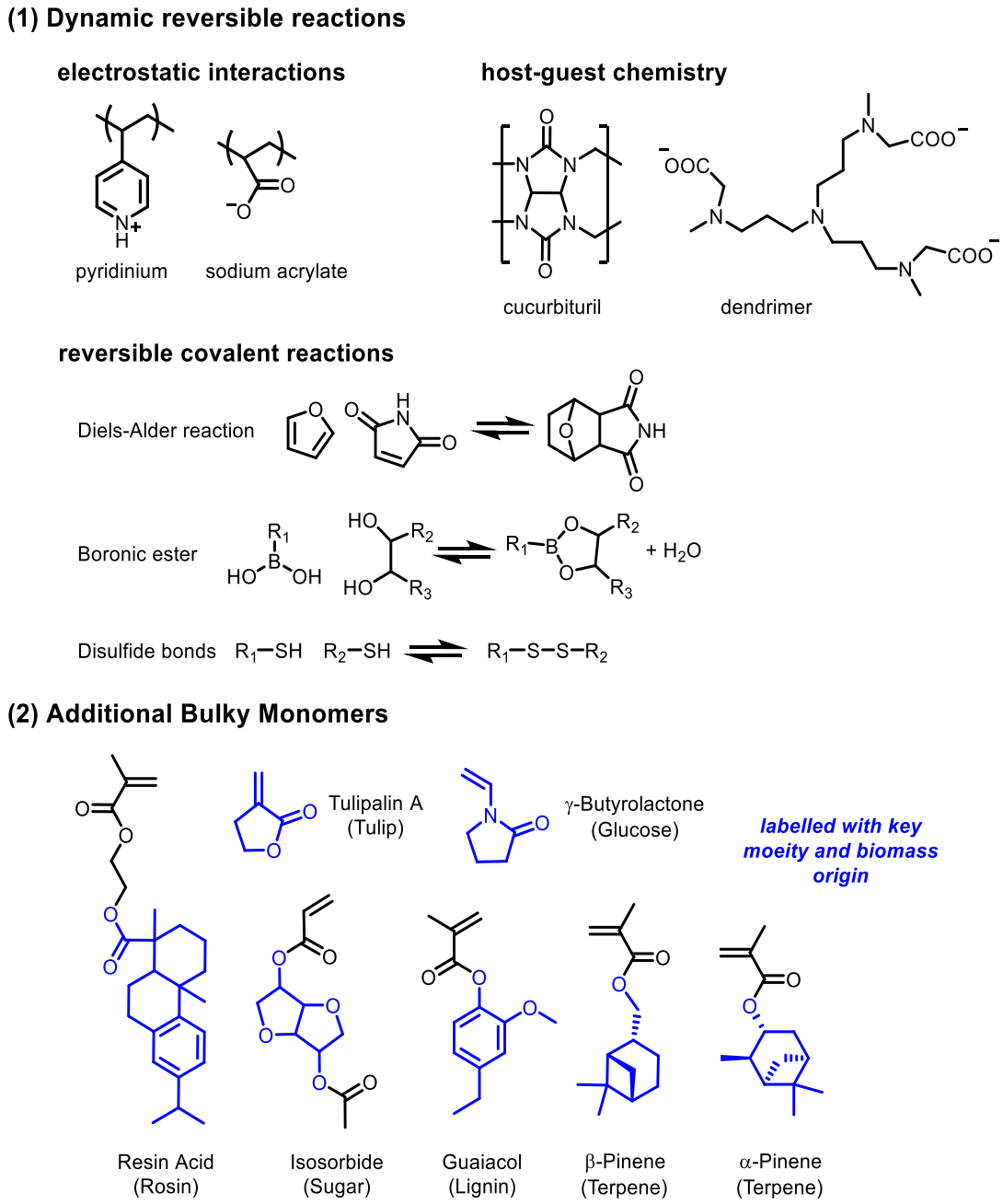

Figure 6.1. Chemistries for future research (a) using various dynamic reversible reactions and (b) by varying the biomass-derived monomer.

In Chapters 4 and 5, focus shifted to specific applications. Firstly, acrylic resins for polymeric coatings were synthesized using a biomass source (SBMA) to replace a petroleum analogue (butyl acrylate, BA). There are also biomass sources that can be used to substitute other widely used monomers, including using lignin-derived phenolics to replace styrene. Changing both monomers to biomass-derived sources would result in a much higher biomass content in the final materials, which is desirable for commercial applications. Additionally, studies need to be performed to optimize the emulsion polymerization reaction conditions. The surfactant loading and solid content both need to be adjusted to mimic industrial standards. Monomer substitution and reaction optimization could result in a final acrylic coating that is entirely biomass-derived with properties and procedures friendly for industrial practice.

In Chapter 5, epoxy resins were synthesized using a nanocomposite to enhance the thermomechanical properties and impart stimuli-response. Epoxy resins are a huge industry, but unfortunately rely on harmful chemicals, including bisphenol A (BPA), an epoxy precursor, which is a known reproductive toxin. Despite the promising stimuli-responsive properties in these materials, future work should focus on utilizing plant oils in epoxy resins. Due to their unique structure, plant oils can be used to replace both the epoxy pre-resin and anhydride-curing agent, allowing for a high bio content. Additionally, many of these plant oil chemicals are benign; therefore, they do not produce toxicity issues unlike some of their petroleum analogues.

APPENDIX A

PERMISSION TO REPRINT

SPRINGER NATURE

Title: Nanostructured functional materials prepared by atom transfer radical polymerization
Author: Krzysztof Matyjaszewski et al
Publication: Nature Chemistry
Publisher: Springer Nature
Date: Jun 22, 2009

Logged in as:
Meghan Lamm
Account #:
3001348923
LOGOUT

Order Completed

Thank you for your order.

This Agreement between Meghan Lamm ("You") and Springer Nature ("Springer Nature") consists of your license details and the terms and conditions provided by Springer Nature and Copyright Clearance Center.

Your confirmation email will contain your order number for future reference.

printable details

License Number	4666591279633
License date	Sep 12, 2019
Licensed Content Publisher	Springer Nature
Licensed Content Publication	Nature Chemistry
Licensed Content Title	Nanostructured functional materials prepared by atom transfer radical polymerization
Licensed Content Author	Krzysztof Matyjaszewski et al
Licensed Content Date	Jun 22, 2009
Type of Use	Thesis/Dissertation
Requestor type	academic/university or research institute
Format	print and electronic
Portion	figures/tables/illustrations
Number of figures/tables/illustrations	1
High-res required	no
Will you be translating?	no
Circulation/distribution	1 - 29
Author of this Springer Nature content	no
Title	MACROMOLECULAR ENGINEERING OF BIOMASS POLYMERS TOWARDS ENHANCED THERMOMECHANICAL PROPERTIES AND STIMULI-RESPONSIVE MATERIALS
Institution name	n/a
Expected presentation date	Dec 2019
Portions	FIGURE 2

Figure A.1. Permission to reprint Figure 1.3.

Title: Emulsion polymerization mechanisms and kinetics
Author: C.S. Chern
Publication: Progress in Polymer Science
Publisher: Elsevier
Date: May 2006

Order Completed

Thank you for your order.

This Agreement between Meghan Lamm ("You") and Elsevier ("Elsevier") consists of your license details and the terms and conditions provided by Elsevier and Copyright Clearance Center.

Your confirmation email will contain your order number for future reference.

printable details

License Number	4657210569827
License date	Aug 27, 2019
Licensed Content Publisher	Elsevier
Licensed Content Publication	Progress in Polymer Science
Licensed Content Title	Emulsion polymerization mechanisms and kinetics
Licensed Content Author	C.S. Chern
Licensed Content Date	May 1, 2006
Licensed Content Volume	31
Licensed Content Issue	5
Licensed Content Pages	44
Type of Use	reuse in a thesis/dissertation
Portion	figures/tables/illustrations
Number of figures/tables/illustrations	1
Format	both print and electronic
Are you the author of this Elsevier article?	No
Will you be translating?	No
Original figure numbers	Figure 1
Title of your thesis/dissertation	MACROMOLECULAR ENGINEERING OF BIOMASS POLYMERS TOWARDS ENHANCED THERMOMECHANICAL PROPERTIES AND STIMULI-RESPONSIVE MATERIALS
Expected completion date	Dec 2019
Estimated size (number of pages)	160

Figure A.2. Permission to reprint Figure 1.6.

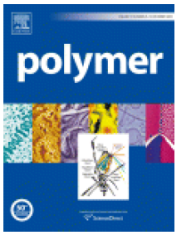

Title: A review of stimuli-responsive shape memory polymer composites
Author: Harper Meng,Guoqiang Li
Publication: Polymer
Publisher: Elsevier
Date: 19 April 2013

Order Completed

Thank you for your order.

This Agreement between Meghan Lamm ("You") and Elsevier ("Elsevier") consists of your license details and the terms and conditions provided by Elsevier and Copyright Clearance Center.

Your confirmation email will contain your order number for future reference.

printable details

License Number	4657651390320
License date	Aug 28, 2019
Licensed Content Publisher	Elsevier
Licensed Content Publication	Polymer
Licensed Content Title	A review of stimuli-responsive shape memory polymer composites
Licensed Content Author	Harper Meng,Guoqiang Li
Licensed Content Date	Apr 19, 2013
Licensed Content Volume	54
Licensed Content Issue	9
Licensed Content Pages	23
Type of Use	reuse in a thesis/dissertation
Portion	figures/tables/illustrations
Number of figures/tables/illustrations	1
Format	both print and electronic
Are you the author of this Elsevier article?	No
Will you be translating?	No
Original figure numbers	Figure 1
Title of your thesis/dissertation	MACROMOLECULAR ENGINEERING OF BIOMASS POLYMERS TOWARDS ENHANCED THERMOMECHANICAL PROPERTIES AND STIMULI-RESPONSIVE MATERIALS
Expected completion date	Dec 2019
Estimated size (number of pages)	160

Figure A.3. Permission to reprint Figure 1.8.

Copyright Clearance Center

Note: Copyright.com supplies permissions but not the copyrighted content itself.

1 PAYMENT 2 REVIEW 3 CONFIRMATION

Step 3: Order Confirmation

Thank you for your order! A confirmation for your order will be sent to your account email address. If you have questions about your order, you can call us 24 hrs/day, M-F at +1.855.239.3415 Toll Free, or write to us at info@copyright.com. This is not an invoice.

Confirmation Number: 11846055
Order Date: 08/28/2019

If you paid by credit card, your order will be finalized and your card will be charged within 24 hours. If you choose to be invoiced, you can change or cancel your order until the invoice is generated.

Payment Information

Meghan Lamm
mgradle@email.sc.edu
+1 (630) 618-8762
Payment Method: n/a

Order Details

Chemical Society reviews

Order detail ID:	71995249
Order License Id:	4657650339796
ISSN:	1460-4744
Publication Type:	e-Journal
Volume:	
Issue:	
Start page:	
Publisher:	ROYAL SOCIETY OF CHEMISTRY
Author/Editor:	Royal Society of Chemistry (Great Britain)

Permission Status: Granted
Permission type: Republish or display content
Type of use: Thesis/Dissertation

Requestor type	Academic institution
Format	Print, Electronic
Portion	chart/graph/table/figure
Number of charts/graphs/tables/figures	1
The requesting person/organization	Meghan Lamm
Title or numeric reference of the portion(s)	Figure 1
Title of the article or chapter the portion is from	Self-healing polymeric materials
Editor of portion(s)	N/A

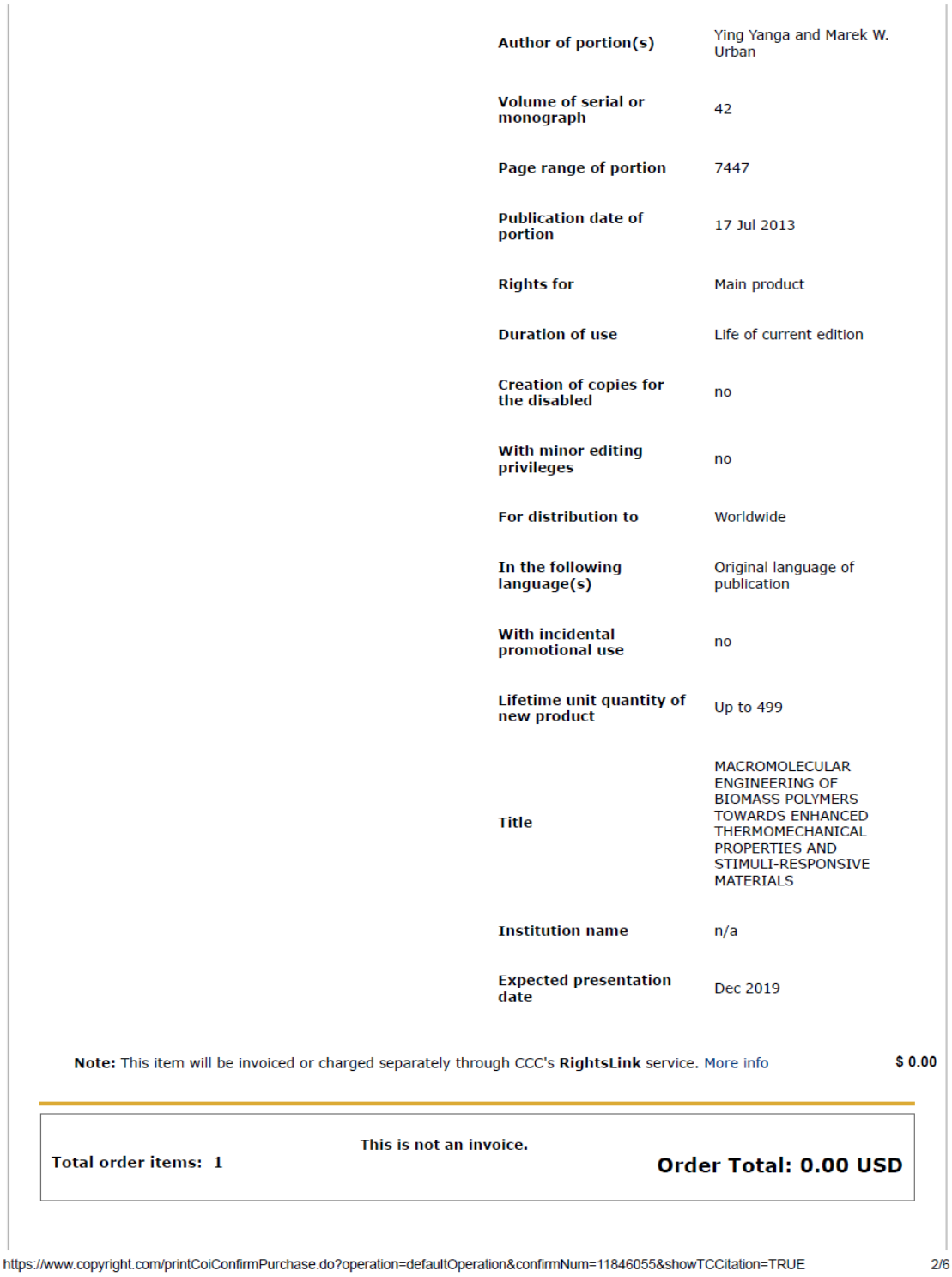

Author of portion(s)	Ying Yanga and Marek W. Urban
Volume of serial or monograph	42
Page range of portion	7447
Publication date of portion	17 Jul 2013
Rights for	Main product
Duration of use	Life of current edition
Creation of copies for the disabled	no
With minor editing privileges	no
For distribution to	Worldwide
In the following language(s)	Original language of publication
With incidental promotional use	no
Lifetime unit quantity of new product	Up to 499
Title	MACROMOLECULAR ENGINEERING OF BIOMASS POLYMERS TOWARDS ENHANCED THERMOMECHANICAL PROPERTIES AND STIMULI-RESPONSIVE MATERIALS
Institution name	n/a
Expected presentation date	Dec 2019

Note: This item will be invoiced or charged separately through CCC's **RightsLink** service. More info **$ 0.00**

This is not an invoice.

Total order items: 1 **Order Total: 0.00 USD**

Figure A.4. Permission to reprint Figure 1.9.

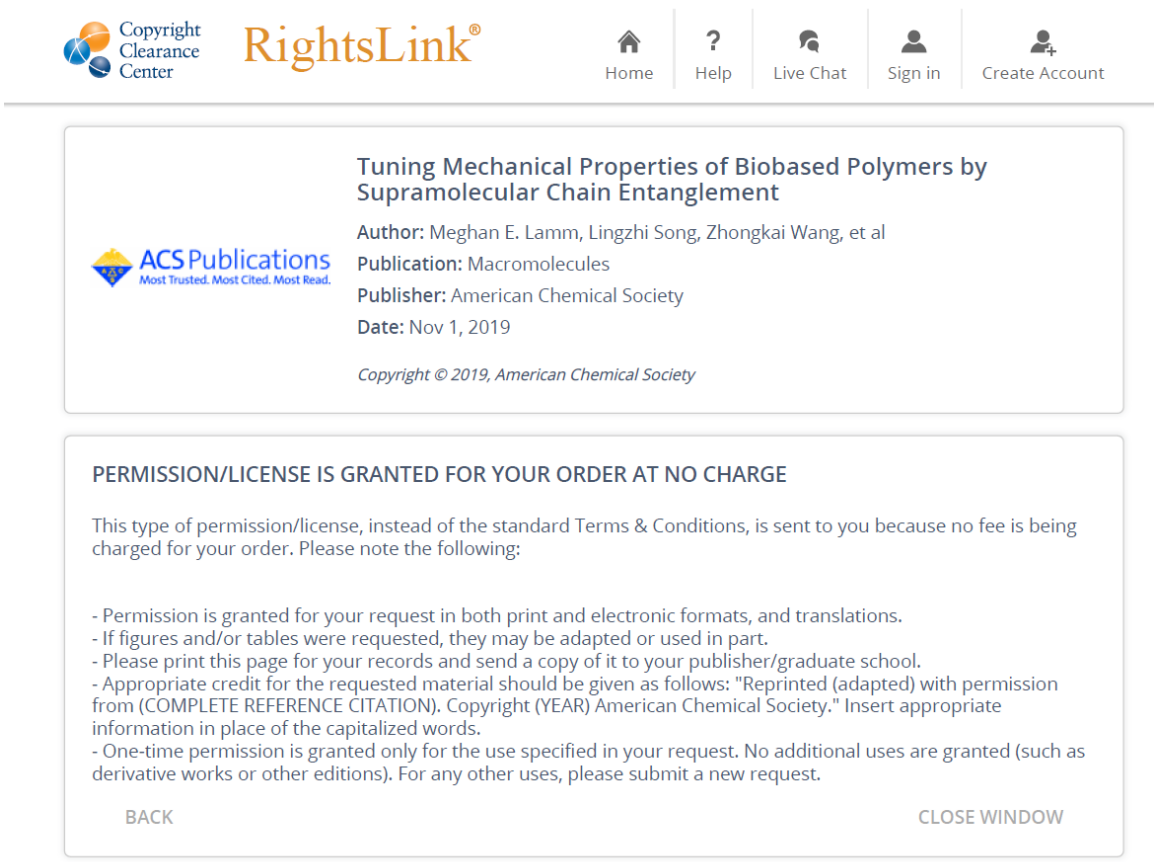

Figure A.5. Permission to reprint Chapter 2.

Rights retained by authors

When the author accepts the exclusive licence to publish for a journal article, he/she retains certain rights that may be exercised without reference to the Royal Society of Chemistry.

Reproduce/republish portions of the article (including the abstract).

Photocopy the article and distribute such photocopies and distribute copies of the PDF of the article for personal or professional use only (the Royal Society of Chemistry makes this PDF available to the corresponding author of the article upon publication. Any such copies should not be offered for sale. Persons who receive or access the PDF mentioned above must be notified that this may not be made available further or distributed.).

Adapt the article and reproduce adaptations of the article for any purpose other than the commercial exploitation of a work similar to the original.

Reproduce, perform, transmit and otherwise communicate the article to the public in spoken presentations (including those that are accompanied by visual material such as slides, overheads and computer projections).

The author(s) must submit a written request to the Royal Society of Chemistry for any use other than those specified above.

All cases of republication/reproduction must be accompanied by an acknowledgement (/journals-books-databases/journal-authors-reviewers/licences-copyright-permissions/#reuse-permission-requests) of first publication of the work by the Royal Society of Chemistry, the wording of which depends on the journal in which the article was published originally. The acknowledgement should also include a hyperlink to the article on the Royal Society of Chemistry website.

The author also has some rights concerning the deposition of the whole article.

Author reusing their own work published by the Royal Society of Chemistry

You do not need to request permission to reuse your own figures, diagrams, etc, that were originally published in a Royal Society of Chemistry publication. However, permission should be requested for use of the whole article or chapter except if reusing it in a thesis. If you are including an article or book chapter published by us in your thesis please ensure that your co-authors are aware of this.

Reuse of material that was published originally by the Royal Society of Chemistry must be accompanied by the appropriate acknowledgement of the publication. The form of the acknowledgement is dependent on the journal in which it was published originally, as detailed in 'Acknowledgements'.

Figure A.6. Permission to reprint Chapter 3.

Figure A.7. Permission to reprint Chapter 4.

Figure A.8. Permission to reprint Chapter 5.